

**CHARACTERIZATION OF SILICA CONTENT IN GOLD MINE DUST WITH RESPECT TO
PARTICLE SIZE**

by

Lauren G. Chubb

BS, MPH, University of Pittsburgh, 2010, 2013

Submitted to the Graduate Faculty of
the Graduate School of Public Health in partial fulfillment
of the requirements for the degree of
Doctor of Public Health

University of Pittsburgh

2016

UNIVERSITY OF PITTSBURGH
Graduate School of Public Health

This dissertation was presented

by

Lauren G. Chubb

It was defended on

April 11, 2016

and approved by

Aaron Barchowsky, PhD, Professor, Environmental and Occupational Health, Graduate
School of Public Health, University of Pittsburgh

Emanuele Cauda, PhD, Pittsburgh Mining Research Division, National Institute for
Occupational Safety and Health, Centers for Disease Control and Prevention

Steven Mischler, PhD, Adjunct Assistant Professor, Environmental and Occupational Health,
Graduate School of Public Health, University of Pittsburgh

Evelyn Talbott, DrPH, Professor, Epidemiology, Graduate School of Public Health, University
of Pittsburgh

Dissertation Advisor: Bruce Pitt, PhD, Professor and Chair, Environmental and
Occupational Health, Graduate School of Public Health, University of Pittsburgh

Copyright © by Lauren G. Chubb

2016

CHARACTERIZATION OF SILICA CONTENT IN GOLD MINE DUST WITH RESPECT TO PARTICLE SIZE

Lauren G. Chubb, DrPH

University of Pittsburgh, 2016

ABSTRACT

Globally, silicosis is responsible for thousands of deaths each year and is a major public health concern in industries like mining. Silicosis is caused by exposure to respirable crystalline silica, and while incidence of silicosis has declined in recent decades, its continued occurrence in young workers indicates that high crystalline silica exposures in the contemporary workforce persist despite monitoring efforts and regulatory enforcement.

Crystalline silica exposure is monitored in the mining industry via collection of respirable dust samples, from which both dust and crystalline silica concentrations are determined. Accurate quantification of crystalline silica is vital to assessing workers' exposure, and to limiting exposure through selection of appropriate engineering controls and personal protective equipment. To quantify crystalline silica in a sample, one of two analytic methods is used: X-ray diffraction and infrared spectroscopy. Previously, confounding effects of mineral composition and size distribution of dust were assumed to have only minor impact on the accuracy of both methods; however, as mining technologies evolve, so do the characteristics of the dust generated in mines, and such effects may no longer be negligible.

Evaluating the characteristics of mine dust with respect to particle size and crystalline silica content is imperative to understanding how crystalline silica analysis may be affected by these characteristics. To date, few studies have investigated particle size-related crystalline silica content in occupational dusts, and while some efforts have been made to characterize coal mine dusts, there has been no such effort to characterize metal/non-metal mine dusts. This study

undertakes detailed characterization of dusts from three gold mine operations, via analysis of size distribution using particle sizers and a cascade impactor; crystalline silica content by infrared and X-ray diffraction methods; and single-particle composition via scanning electron microscopy. Results indicate that the size distribution of crystalline silica within a particular dust is not equivalent to the dust's size distribution; the abundance of crystalline silica in a dust varies with particle size; the two methods of quantifying crystalline silica yield variable results depending on particle size; and, like crystalline silica, particle types of different elemental composition vary in abundance with respect to particle size.

TABLE OF CONTENTS

| | |
|--|------|
| ACKNOWLEDGEMENTS | xii |
| DEDICATION..... | xiii |
| NOMENCLATURE AND TERMS | xiv |
| 1.0 Introduction | 1 |
| 1.1 Regulation and Monitoring of Crystalline Silica Exposure | 8 |
| 1.2 Relevance of Particle Size to Dust Control and Exposure Assessment | 16 |
| 1.3 Particle Size Effects in Analytical Methods for the Quantification of Crystalline Silica | 22 |
| 1.3.1 Effect of Particle Size in IR Spectroscopy | 24 |
| 1.3.2 Effect of Particle Size in X-ray Diffraction Spectroscopy | 25 |
| 1.3.3 Significance of the Size Distribution of Calibration Material..... | 26 |
| 1.4 Mineral Interference in Analytical Methods for the Quantification of Crystalline Silica | 28 |
| 1.5 Previous Characterization of Occupational Dusts Containing Crystalline Silica..... | 31 |
| 1.6 Towards a More Accurate Quantification of Crystalline Silica | 33 |
| 1.7 Scope of Dissertation and Statement of Hypothesis | 37 |
| 2.0 Determination of the Size Distribution of Crystalline Silica in Gold Mine Dust | 39 |
| 2.1 Methods..... | 41 |
| 2.1.1 Characterization of Size Distribution: APS + SMPS | 42 |
| 2.1.2 Characterization of Size Distribution: Gravimetric Inversion..... | 43 |
| 2.1.3 Characterization of Particle Size-related Crystalline Silica Content | 44 |
| 2.1.4 Construction of a Crystalline Silica Size Distribution | 47 |

| | | |
|-------|---|----|
| 2.2 | Results | 47 |
| 2.2.1 | Size Distributions: APS + SMPS | 47 |
| 2.2.2 | Size Distributions (Total Dust, Crystalline Silica): Gravimetric Inversion..... | 49 |
| 2.2.3 | Characterization of Particle Size-related Crystalline Silica Content | 52 |
| 2.3 | Discussion | 54 |
| 3.0 | Comparison of Particle Size-related Analysis of Crystalline Silica by IR and XRD | |
| | Methods | 57 |
| 3.1 | Methods..... | 58 |
| 3.1.1 | Collection of Size-fractionated Samples..... | 58 |
| 3.1.2 | Comparison of IR and XRD Methods | 59 |
| 3.2 | Results | 59 |
| 3.3 | Discussion | 62 |
| 4.0 | Characterization of Particle Size-related Composition of Gold Mine Dust | 66 |
| 4.1 | Methods..... | 67 |
| 4.1.1 | Collection of Size-fractionated Samples for Single Particle Analysis | 68 |
| 4.1.2 | Size-fractionated Single Particle Analysis via SEM-EDS..... | 69 |
| 4.2 | Results | 70 |
| 4.3 | Discussion | 82 |
| 5.0 | Discussion and Conclusions | 86 |
| 5.1 | Implications of the Particle Size Distribution of Crystalline Silica..... | 86 |
| 5.2 | Implications of Particle Size-related Discrepancy in Crystalline Silica Analyses..... | 88 |
| 5.3 | Implications of Single-particle Analysis of Size-Fractionated Samples | 88 |

| | | |
|---|---|-----|
| 5.4 | Evaluation of Study Limitations and Strengths | 90 |
| 5.4.1 | Limitations | 90 |
| 5.4.2 | Strengths | 93 |
| 5.5 | Implications of the Overall Findings of This Study..... | 94 |
| APPENDIX A: SUMMARY OF SAMPLING CONDITIONS AND TIMES | | 98 |
| APPENDIX B: PARTICLE SIZE DISTRIBUTION OF A CRYSTALLINE SILICA REFERENCE MATERIAL..... | | 99 |
| APPENDIX C: EXAMPLES OF RULES FOR PARTICLE CLASSIFICATION BY EDS | | 100 |
| BIBLIOGRAPHY | | 101 |

LIST OF TABLES

| | |
|--|-----|
| Table 1 MOUDI stage cut-points | 44 |
| Table 2 MMD and GSD of the size distributions of total dust and total crystalline silica | 52 |
| Table 3 Proportional crystalline silica content (%) from IR and XRD data | 54 |
| Table 4 Crystalline silica composition (mass %) by IR and XRD | 60 |
| Table 5 Mass percent mineral composition of respirable dust | 70 |
| Table 6 Total particles analyzed by CCSEM | 71 |
| Table 7 Particle class relative abundance (% count and weight): Alaska | 73 |
| Table 8 Particle class relative abundance (% count and weight): Nevada | 74 |
| Table 9 Particle class relative abundance (% count and weight): South Africa | 75 |
| Table 10 Collection times of size-fractionated samples for crystalline silica analysis | 98 |
| Table 11 Collection times of size-fractionated samples for SEM-EDS analysis | 98 |
| Table 12 Particle classification rules for Nevada dust | 100 |

LIST OF FIGURES

| | |
|---|----|
| Figure 1 Distribution of age-adjusted silicosis mortality rates in the U.S., by county..... | 2 |
| Figure 2 IR spectrum of crystalline silica on PVC filter media..... | 11 |
| Figure 3 Scattering of X-rays..... | 13 |
| Figure 4 XRD diffractogram for crystalline silica | 14 |
| Figure 5 Arrangement of PVC filters and foil substrates on MOUDI stages | 45 |
| Figure 6 Particle number size distributions from merged SMPS-APS data..... | 48 |
| Figure 7 Particle mass size distributions: particles <32 μm | 50 |
| Figure 8 Particle mass size distributions: respirable fraction | 51 |
| Figure 9 Proportional crystalline silica content, by particle size | 53 |
| Figure 10 Ratio of IR to XRD quantification of crystalline silica, by particle size | 61 |
| Figure 11 Arrangement of TEM grids on MOUDI stage | 69 |
| Figure 12 SEM particle images and corresponding EDS spectra | 76 |
| Figure 13 Particle size-related trends in most abundant particle classes: Alaska | 77 |
| Figure 14 Particle size-related trends in most abundant particle classes: Nevada..... | 78 |
| Figure 15 Particle size-related trends in most abundant particle classes: South Africa..... | 79 |
| Figure 16 Particle size-related trends in silica, determined by EDS (count)..... | 80 |
| Figure 17 Particle size-related trends in silica, determined by EDS (weight) and IR/XRD | 81 |
| Figure 18 Particle mass size distribution of Min-U-Sil 5..... | 99 |

LIST OF EQUATIONS

| | |
|--|----|
| Equation 1 Dust standard for coal mines..... | 8 |
| Equation 2 Dust standard for metal/non-metal mines | 9 |
| Equation 3 Bragg's Law | 12 |
| Equation 4 Inhalable definition | 17 |
| Equation 5 Thoracic definition | 18 |
| Equation 6 Respirable definition..... | 18 |

ACKNOWLEDGEMENTS

I owe a deep debt of gratitude to all of my colleagues at the National Institute for Occupational Safety and Health, and particularly to the Aerosol and Toxic Substances team at the Pittsburgh Mining Research Division, without whose immense support this work would not have been possible. You have been exceptionally generous in sharing your time and expertise, and NIOSH has been a terrific place to learn and to grow over the past several years. Dr. Steve Mischler and Dr. Emanuele Cauda, especially, have been better teachers and mentors than I could have ever hoped to have. I am so grateful for all of the opportunities that NIOSH has afforded to me, and I am honored to work alongside such a dedicated and talented group of people.

I would like to thank each of my committee members, who have shown such enthusiasm for my research, and who have been a pleasure to work with; as well as Dr. Linda Pearce and Dr. Jim Peterson, who have been incredible advocates and mentors throughout my time at Pitt; and Dr. Courtney Roper and Dr. Leah Cambal, who have offered their invaluable scientific perspectives and their equally invaluable friendship. I would be remiss if I did not also thank MSHA (Pittsburgh) for their assistance with IR analysis, RJ Lee Group for analysis of XRD samples, Ms. Traci Lersch for her exceptional work and guidance with the electron microscopy portion of this research, and Dr. Teresa Barone, Dr. Art Miller, Mr. Joe Archer, and Mr. Shawn Vanderslice for their vital input on the methodologies of this work.

Finally, thank you to my parents and sister, who have been my biggest cheering squad; offered advice, support, and comedic relief at exactly the right moments; and pretended (sometimes even convincingly) to find my work as interesting as I do. I could not have done it without you.

DEDICATION

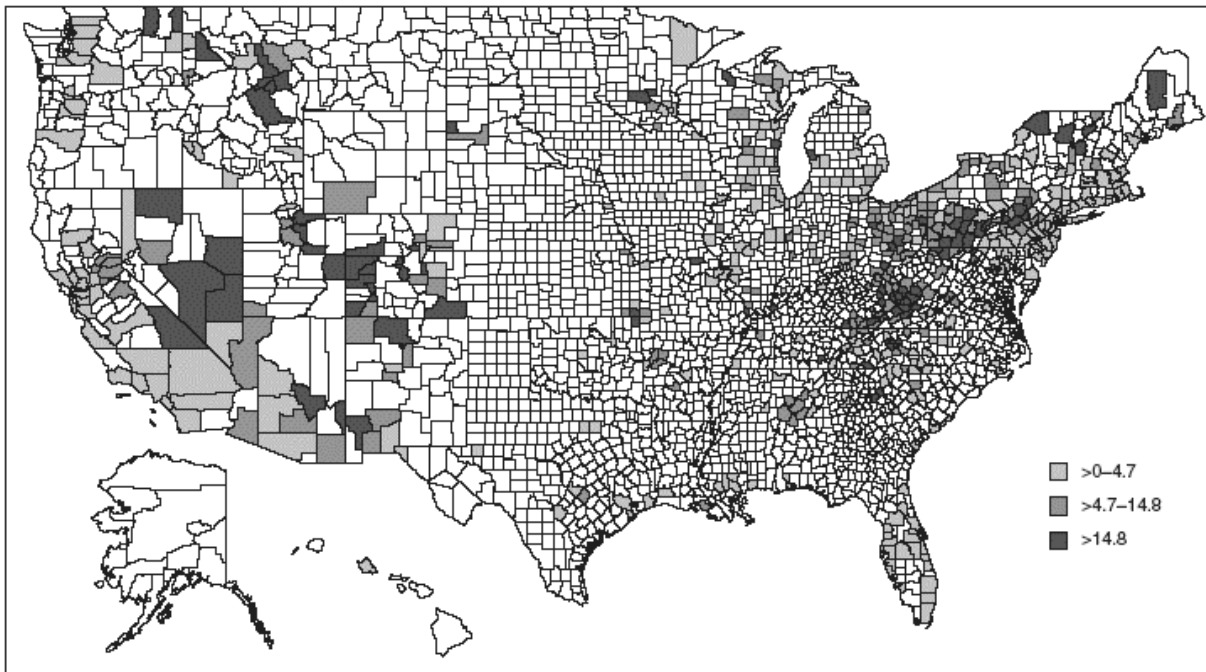
I dedicate this work to miners – past, present and future – whose work is so vital to our way of life, and whose health and safety should be guarded by the best protections that science can provide.

NOMENCLATURE AND TERMS

| | |
|--------------------|---|
| Crystalline silica | Forms of silicon dioxide (SiO_2) wherein molecules are arranged in a crystal lattice; used in this work to refer primarily to quartz |
| IR | Infrared spectroscopy |
| Metal/Non-metal | Term referring to non-coal types of mining operations; includes metal, stone, sand and gravel mines, etc. |
| Miner | A person working, in any capacity, at a mining operation |
| MMD | Mass Median Diameter |
| MOUDI | Microorifice Uniform Deposit Impactor |
| MSHA | Mine Safety and Health Administration |
| NIOSH | National Institute for Occupational Safety and Health |
| Polymorph | Any of several crystalline forms having the same chemical composition |
| SEM-EDS | Scanning Electron Microscopy with Energy Dispersive X-ray Spectroscopy |
| Size-fractionated | Samples of dust particles separated into narrow size bins, or ranges, based on particle aerodynamic diameter |
| XRD | X-ray Diffraction |

1.0 INTRODUCTION

In 2013, 46,300 deaths worldwide were attributed to silicosis (1). The many colloquial names – Miners’ Phthisis, Masons’ Disease, Black Lung, Potters’ Rot, Stonecutters’ Disease, Grinders’ Asthma – by which silicosis (and its related ailments) has been known throughout history points to its pervasiveness. From 1968 to 2002, silicosis was recorded as an underlying or contributing cause of death on a total of 16,300 death certificates in the United States (2), and between 2001 and 2010, silicosis was attributed as an underlying or contributing cause of death for 1,437 individuals in the United States (3), with 28 cases occurring in persons below the age of 44. Over the past several decades, annual silicosis deaths have declined; however, recent data has indicated not only a slowing of the decline in silicosis mortality, but also the emergence of silicosis deaths in younger workers (aged 15-44) (3-5). This trend indicates that although overall silicosis deaths have decreased, high level exposures to crystalline silica continue to occur in spite of monitoring and regulatory efforts, and that improvements to current protective measures are necessary to eliminate the occurrence of silicosis completely. Silicosis mortality within the U.S. is also geographically variable, with areas of Nevada, Pennsylvania, and West Virginia, for instance, showing particularly elevated rates of silicosis mortality (Figure 1).



* Per million persons aged ≥ 15 years. Rates were not calculated for counties with fewer than five deaths.

National Occupational Respiratory Mortality System, 1968-2002; image obtained from the Centers for Disease Control and Prevention's *Morbidity and Mortality Weekly Report* (2)

Figure 1 Distribution of age-adjusted silicosis mortality rates in the U.S., by county

Although improved industrial hygiene practices, particularly in developed countries such as the U.S., have led to an overall decline in silicosis, silicosis has recently begun to emerge in new groups of workers, such as in the oil and gas industry (particularly hydraulic fracturing) (6), as well as in the textiles industry (7). Concurrently, the disease remains strongly associated with particular occupations such as stonemasons, potters, construction workers, sand-blasters, foundry workers, and miners (8).

Silicosis, a chronic respiratory disease, is the primary outcome of concern for exposure to respirable crystalline silica. The Centers for Disease Control and Prevention estimates that, annually, 1.7 million people in the United States (8) are exposed to crystalline silica. Silicosis is characterized by the development of fibrotic nodules in the lungs (9). *Simple silicosis* typically becomes manifest after a long period of latency (two or more decades), at which point symptoms

such as shortness of breath and tightness in the chest may develop. As the disease progresses, lung function becomes progressively impaired, and can eventually result in respiratory failure and death. In cases of extreme exposure, disease progression may occur over just five to ten years (*accelerated silicosis*), or in just a few months to years (*acute silicosis*). Silicosis may occur and progress even years after exposure to crystalline silica has ended. While silicosis is incurable once it develops, it is also entirely preventable via prevention of exposure to crystalline silica.

Crystalline silica exposure is also associated with the development of lung cancer, and while there is a lack of consensus on the mechanism for the carcinogenicity of crystalline silica in the absence of silicosis (or if there is indeed a causal relationship between crystalline silica and lung cancer in the absence of silicosis) (10-12), the International Agency for Research on Cancer has classified crystalline silica as a Group 1 agent (carcinogenic to humans) (13). Exposure to crystalline silica also increases risk of tuberculosis (TB) and mycobacterial disease (14); this is of particular concern in countries such as South Africa, where prevalence of TB in miners is high (15). The relationship between crystalline silica exposure and TB is further complicated when an individual is immunocompromised, as with human immunodeficiency virus (HIV) (16-19). Crystalline silica exposure has also been implicated in other chronic conditions, such as renal disease (20) and connective tissue diseases such as rheumatoid arthritis, scleroderma, and antineutrophilic cytoplasmic antibody-positive vasculitis (21).

The mechanistic development of silicosis has been studied for decades, yet to this day a comprehensive understanding of the pathologic progression from crystalline silica exposure to disease has not been reached. What is apparent is that free radicals, which are either produced on the surface of crystalline silica or by the inflammatory processes that are initiated by the presence of crystalline silica particles in the lung, are strongly involved in the process (22). This has been verified by the presence, at autopsy, of stable free radicals in lung tissue of coal miners exposed to crystalline silica (23).

The mineral silica (chemical composition SiO_2) occurs as several crystalline polymorphs: quartz, cristobalite, and tridymite, keatite, coesite, stishovite, and moganite. Of these, only quartz, cristobalite, and tridymite are considered relevant to human exposure assessments, as other forms are rarely encountered. Quartz is the most abundant mineral in the earth's crust and is by far the most commonly encountered form of crystalline silica. Despite the abundance of naturally occurring crystalline silica, environmental exposures of appreciable magnitude are uncommon, as the crystalline silica encountered is generally in the form of solid rock, or as particles too large to contribute significantly to respiratory exposures. In occupational settings, however, where solid crystalline silica-containing rock is mechanically fractured and produces crystalline silica-containing dusts, exposures to respirable crystalline silica are a significant concern. The presence of crystalline silica in the respirable fraction of dust has been documented in various mining environments globally (24-27). In the U.S., crystalline silica can be found in the dust generated in coal mines, metal mines, and sand & gravel operations (28-30). In coal mines, the primary source of mineral dust, including crystalline silica dust, is the top strata above the coal seam that is being mined (31); in non-coal mining environments, crystalline silica is a component of the dust present in crushers and mills. As a result, silicosis is a significant occupational health hazard encountered in mining (8).

The causal relationship between exposure to crystalline silica and the development of silicosis has been recognized for decades and is well-accepted within the mining industry. Continued incidence of silicosis in young workers indicates that contemporary exposures to crystalline silica are sufficient to initiate the development of silicosis, but the underlying causes of these apparent overexposures are still subject to debate. Several scenarios, or a combination thereof, offer possible explanation for the ongoing incidence of silicosis:

- 1) **Crystalline silica exposure continues to occur above and beyond current regulatory limits.** One possibility is that there is a lack of adherence to standards, due either to insufficient efforts to control exposure, or to lack of knowledge of the occurrence of over-

exposures. It is ultimately in the best interest of the mine operator to protect employee health by preventing worker exposure to crystalline silica, as the occurrence of occupational injury and disease, including silicosis, leads to days away from work and loss of productivity. The more likely possibility is that limitations of laboratory methods for the analysis and quantification of crystalline silica (32) have resulted in “false negatives,” due to systematic underestimation of the quantity of crystalline silica in respirable dust samples, and the subsequent misclassification of worker exposure.

- 2) **Current crystalline silica regulations may not be sufficiently conservative to prevent the development of silicosis.** High variability in crystalline silica content of respirable dust has been implicated in the continued incidence of silicosis in coal miners (28), and a similar degree of variability in crystalline silica content is observed in metal/non-metal mines (30). Such variability makes it difficult to accurately predict crystalline silica concentrations in all areas of the mine, and overexposures can occur despite compliance with the dust standard. Alternatively, current exposure limits are based on mass-based measurement of crystalline silica, which assumes a dose-response relationship that is proportional to crystalline silica mass; however, while some toxicology studies have concluded that mass is indeed the relevant exposure metric (33), others have proposed that alternative metrics, such as surface area, would be more appropriate for exposure and dose determination (34, 35), though admittedly less convenient to measure.
- 3) **Evolution of mining practices and technologies has resulted in changes to the crystalline silica component of aerosolized dusts produced in mines, such that the crystalline silica component has become more potent in inducing biological damage leading to silicosis.** This could be due to higher exposure to freshly fractured crystalline silica (36), believed to be more potent in inducing reactive oxygen species (37); a shift in the size distribution of dusts towards particle sizes (either smaller or larger) which are more capable of inducing an inflammatory response (33, 34, 38, 39); or the increased presence

of co-toxicants, such as metallic contamination on the surface of crystalline silica particles (40, 41) or associated diesel particulate matter, which is present in most mining environments and has also been found to be carcinogenic (42).

These proposed explanations for the continued incidence of silicosis in the United States highlight the multifaceted nature of the problem, and suggest that a multidisciplinary approach will be required to fully eradicate and prevent future incidence of silicosis. Continued vigilance on the part of industry and government will be necessary to set regulatory limits for crystalline silica exposure that definitively protect the health of workers, and to ensure that regulations are followed and enforced with the utmost vigilance. However, in light of concerns outlined above, adherence to regulations – based on compliance monitoring – is not sufficient if monitoring efforts are not consistently accurate in quantifying the concentration of crystalline silica that workers are exposed to, nor is it sufficient if compliance monitoring does not make use of the most appropriate metrics for crystalline silica exposure.

Addressing these concerns requires contemplation of the theoretical limitations of quantitative methods with respect to real-world dusts encountered in mining environments. Aerosols of real mine dusts must be studied more extensively: the size distributions of numerous dusts must be characterized, as well as the size distributions of the crystalline silica component of each dust, and the size distribution of other mineral components. Such characterization is particularly needed for silicate and aluminosilicate minerals, molecules of which may have chemical bonds or crystalline structure similar to that of silica, leading to confounding analytical effects that may adversely affect the accurate quantification of crystalline silica. Exposure limits and vigilant monitoring will be inadequate in preventing silicosis if crystalline silica cannot be accurately quantified due to common attributes of mine dust.

Assessment and re-evaluation of regulations for respirable dust and crystalline silica in the mining industry are ongoing, as is research concerning the toxicological mechanisms governing how crystalline silica exposure progresses to the development of silicosis. If monitoring

strategies are not reliably accurate, or if they do not address all relevant factors of crystalline silica exposures, then even stringent regulations and strict compliance with regulatory limits may not be sufficient to prevent disease. What is currently needed is a better understanding of the qualities of dusts that impact both measurement and the biological effects of crystalline silica – thus, it would benefit all efforts for more research energy to be directed to the characterization of mine dusts.

One prominent aspect in which monitoring efforts could be enhanced is by more extensive efforts towards characterization of the mineral composition and the particle size-related qualities (such as morphology and elemental composition) of aerosolized dusts from which respirable samples are collected. The size-distribution and mineral composition of dusts are characteristics which have important implications for the quantification of crystalline silica (43-57), yet very few attempts have been made to characterize occupational dusts containing crystalline silica, and still fewer attempts have been made to characterize mine dusts. The characteristics of dusts produced in mining environments vary according to the mineral composition of the dust, the particle size distribution of each component, and the particle size distribution of the overall dust (e.g. the sum of all of the components). These characteristics are influenced by the local geology – the materials present which are mechanically fractured in some way during the mining process – as well as the processes used in ore production, such as the types of machines that are used to break rock. As a result, dusts from different mines or different areas of the same mine are not necessarily similar in their physical and chemical properties (28, 30, 58, 59); many different samples need to be analyzed in order to enhance understanding of the qualities of mine dusts.

1.1 REGULATION AND MONITORING OF CRYSTALLINE SILICA EXPOSURE

The Mine Safety and Health Administration (MSHA), an agency of the U.S. Department of Labor, is responsible for enforcing the provisions of the Federal Mine Safety and Health Act of 1977 (Mine Act) (as amended by the 2006 MINER Act) (60). Its duties under the Act include establishing and enforcing regulations controlling the levels of respirable dust and crystalline silica to which workers may be exposed. The coal mining sector and the metal/non-metal mining sector each have distinct (though similar) standards for respirable dust and respirable crystalline silica (61-64). The dust standards for coal mines vary according to the percent of crystalline silica in the respirable dust of that particular mine, determined from previous respirable dust samples, while the dust standard for metal/non-metal mines varies sample by sample, according to the crystalline silica content of each individual sample. Equation 1 defines the dust standard currently in effect for surface and underground coal mines (63, 64), according to whether that particular mine has (a) crystalline silica content in the dust greater than 5% or (b) less than or equal to 5%.

$$\begin{aligned} \text{(a) Limit} &= \frac{10}{\% \text{ crystalline silica}} \text{ mg m}^{-3} \\ \text{(b) Limit} &= 2 \text{ mg m}^{-3} \end{aligned}$$

Equation 1 Dust standard for coal mines

Equation 2 defines the current standard for surface and underground metal/non-metal mines (61, 62) where crystalline silica content is greater than 1%.

$$\text{Limit} = \frac{10}{\% \text{ crystalline silica} + 2} \text{ mg m}^{-3}$$

Equation 2 Dust standard for metal/non-metal mines

These standards effectively set an exposure limit of $100 \mu\text{g m}^{-3}$ for crystalline silica. However, multiple studies have documented the wide variation in crystalline silica content of dusts, even within the same operation (29, 30, 65). Such variation has important implications for preventing exposure to crystalline silica, in that high variability makes it difficult for industrial hygienists and workers to anticipate dust concentrations (and therefore, exposure levels) in certain areas of the mine, particularly in areas where no previous exposure data exists to provide guidance. The well-documented variation in crystalline silica content of respirable dust suggests that there may be variation in other characteristics of respirable dust as well, and these characteristics may also impact efforts to monitor and prevent crystalline silica exposure.

Currently, monitoring for respirable dust and crystalline silica is completed in several stages. First, a dust sample is collected using a size-selective sampling device, so that only the respirable fraction of particles is collected on the sample filter. After sample collection is complete (typically at the end of a full-shift of work, or upon completion of a specific task), it is sent to an accredited laboratory. There, the filter is analyzed gravimetrically to determine the total mass of material collected. Along with sampling time and flow rate, the net mass of collected particles is then used to calculate the average concentration of respirable dust to which the worker was exposed over the course of the sampling period. This concentration is referred to as the time-weighted average (TWA) concentration: at any given time during sampling, the actual dust

concentration experienced by the worker may have been higher or lower, but the integrated sample provides an average concentration for the entire sampling period. Then, the laboratory quantifies crystalline silica in the sample. From the mass of crystalline silica determined, the average concentration of crystalline silica exposure is calculated; using the net mass of dust determined gravimetrically, the overall percentage of crystalline silica in the dust sample can also be determined.

For coal mine samples, crystalline silica is quantified using a transmission infrared (IR) method. The IR analysis of minerals was first described in 1950 by Hunt et al. (66). In the United States, the MSHA P7 method (67) and the National Institute for Occupational Safety and Health (NIOSH) method 7603 (57), are the most commonly used IR methods. In general, IR spectroscopy detects distinct polymorphs (different crystalline phases) of silica via the energy absorbed by the Si – O bond when light in the IR region of the spectrum passes through a sample. The intensity of the absorption signal is proportional to the quantity of crystalline silica present in the sample; this proportional response can be exploited to create a calibration curve by measuring known quantities of crystalline silica and observing the intensity of the resulting IR absorption. Once a calibration curve has been constructed, the equation of the curve can be used to determine the mass of crystalline silica present in a sample, based on the intensity of the IR response. The IR spectrum for the quartz polymorph of crystalline silica is shown in Figure 2. The doublet peak between 800 cm^{-1} and 780 cm^{-1} is the accepted analytical peak for crystalline silica quantification. The IR spectrum of crystalline silica also contains a peak at 1085 cm^{-1} that cannot be used for a reliable measurement due to its broadness, which makes reliable integration of the peak difficult. Other, higher frequency, peaks are not used due to their commonality with numerous silicate minerals (50), which would preclude accurate quantification in all but pure samples of crystalline silica.

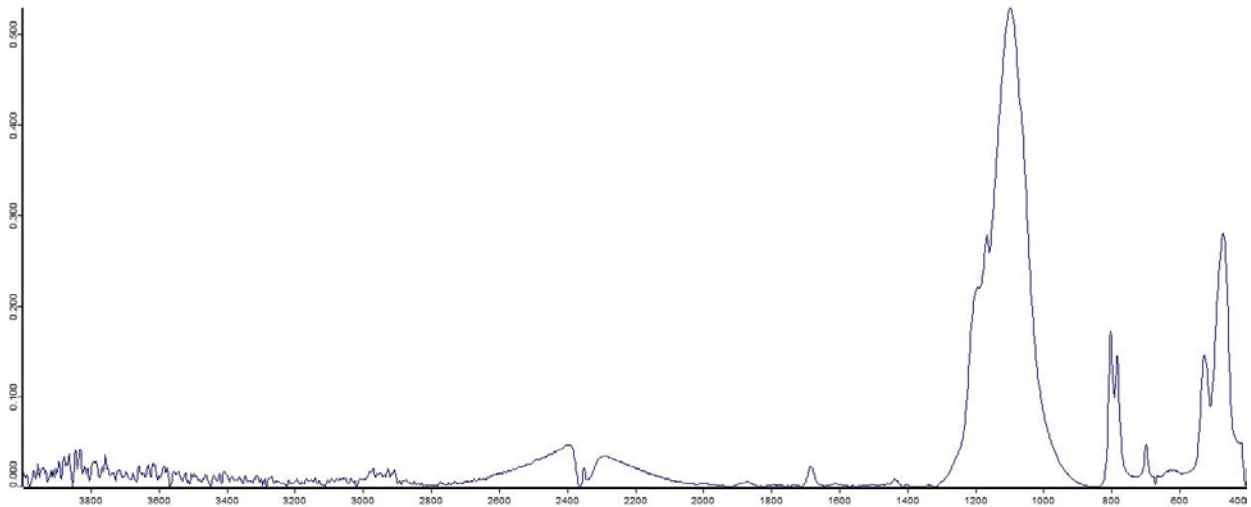


Figure 2 IR spectrum of crystalline silica on PVC filter media

Sample preparation for IR methods used for coal mine samples begins with ashing – a thermal procedure used to remove carbonaceous material from the sample. This procedure also destroys the polyvinyl chloride (PVC) filter media conventionally used for sample collection, while leaving the relevant mineral content of the sample undisturbed. The ashed sample is then redeposited on a low-absorption filter medium (which does not absorb IR radiation in the region used to quantify crystalline silica, thus reducing interference effects from the filter itself) before being analyzed in the IR beam.

Certain advantages and disadvantages of the IR method have been discussed. Lorberau and Abell (68) noted that the costliness of IR methods is intermediate (due to the wide range of instrumentation available) and that sensitivity to crystalline silica is superior compared to other methods, but that interfering absorption bands from other silicate materials are a significant concern. Ferg et al. (69) demonstrated that the IR method demonstrates improved sensitivity over the X-ray diffraction method and is less subject to influence by sample preparation. Importantly, Toffolo and Lockington (54) have made the distinction that while the IR method is capable of identifying all three of the common crystalline silica polymorphs (e.g. quartz,

cristobalite, tridymite) in the presence of any of the others, it cannot accurately quantify any of the three polymorphs in the presence of others. The authors note that this is due to the lack of universally accepted standards for any of the three polymorphs, and while there are currently several materials commonly used as quartz standards (including materials certified and distributed by the National Institute of Standards and Technology), there remains no widely used standard for either of the other common crystalline forms.

For metal/non-metal samples in the U.S., crystalline silica is measured via X-ray diffraction (XRD), using NIOSH method 7500 (56) or MSHA method P2 (70). This method was first described for crystalline silica analysis by Clark and Reynolds in 1936 (71) and identifies crystalline silica based on the crystal lattice of the silica molecule. Because the various crystalline polymorphs of silica have distinct crystalline structures, XRD is capable of distinguishing one polymorph from another. When an X-ray of known incident angle is directed onto the sample (see Figure 3), the beam is diffracted (scattered) by the silicon atom at the center of the lattice. The angle of the diffracted beam is characteristic of the molecules that compose the crystalline silica lattice, as described in by Bragg's Law (Equation 3).

$$2d\sin(\theta)=\lambda_0$$

where d is the interplanar spacing of the crystal lattice, θ is the angle of incidence, and λ_0 is the wavelength of the characteristics X-rays

Equation 3 Bragg's Law

The intensity of the signal from the diffracted beam is proportional to the mass of crystalline silica present, allowing quantification of unknown masses of crystalline silica in samples. In addition to the primary diffraction angle, there are also secondary and tertiary diffraction angles for crystalline silica which can be used for quantification in the event of primary angle interference

due to confounding minerals; however, these peaks are not as sensitive. The XRD diffractogram for the quartz polymorph of crystalline silica is shown in Figure 4.

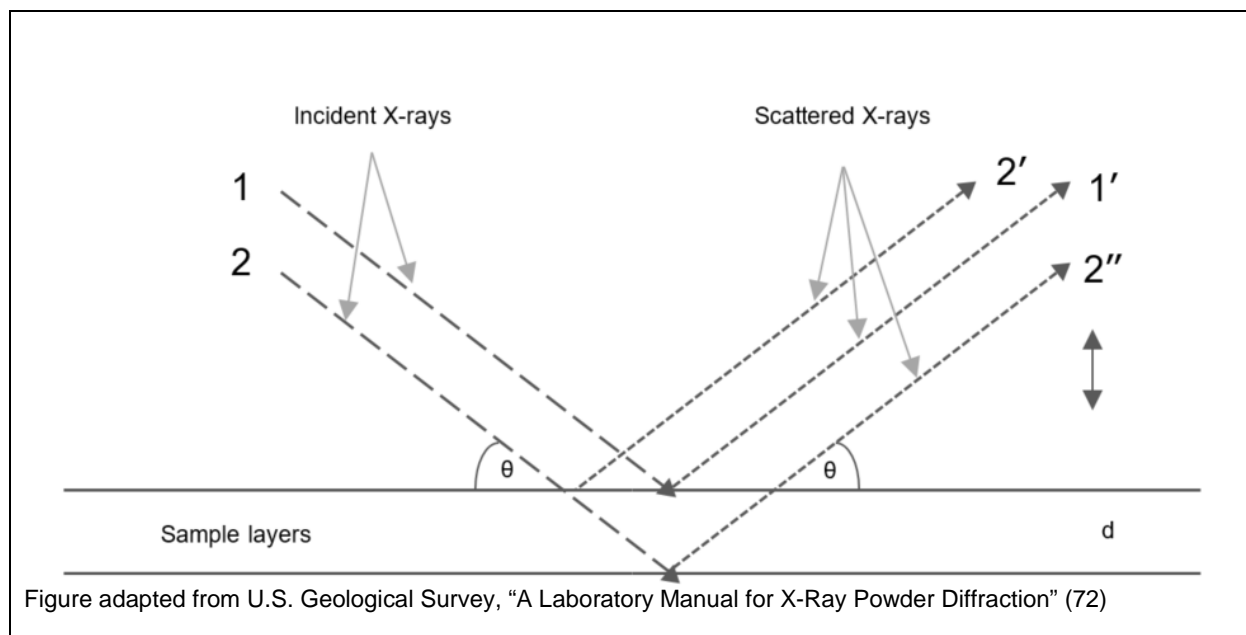


Figure 3 Scattering of X-rays

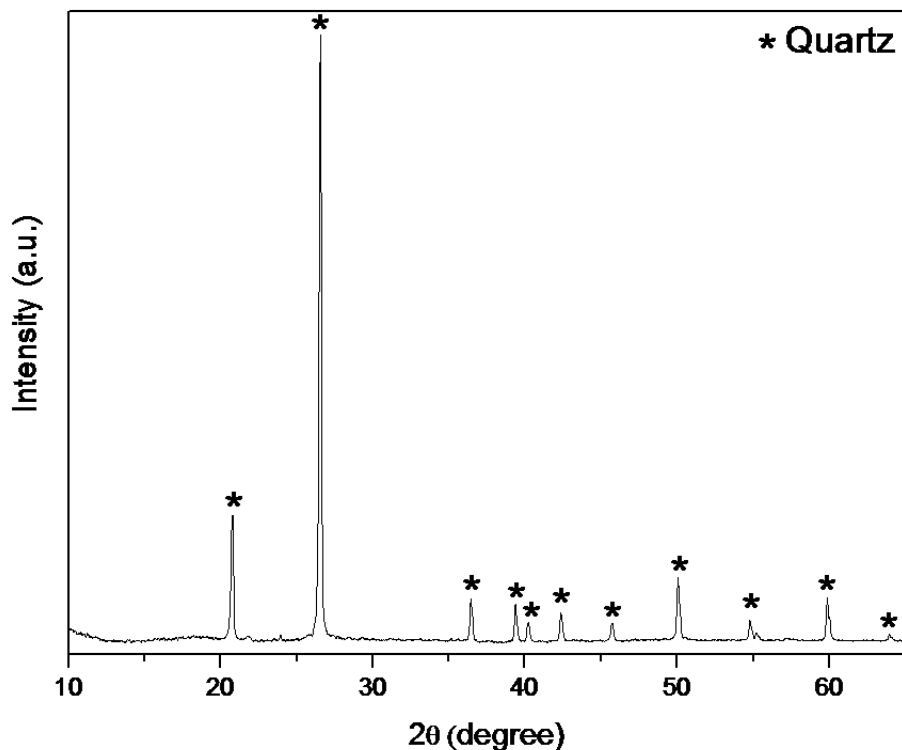


Figure 4 XRD diffractogram for crystalline silica

Sample preparation begins with filter removal by either a thermal method (e.g. ashing, as in IR methods) or by chemical dissolution (via a solvent such as tetrahydrofuran), and the sample is redeposited onto a silver membrane filter, which contributes little interference to the XRD diffractogram and thus allows more accurate quantification of crystalline silica. Once redeposition is complete, the sample is ready to undergo XRD analysis. Lorberau and Abell (68) noted that while XRD methods tend to be less prone to the effects of mineral interferences, the procedure is costlier due to complex instrumentation and the cost of silver membrane filters.

Both the IR and XRD methods are regarded as appropriate for crystalline silica analysis in exposure monitoring (56, 57, 67, 70). Dodgson and Whittaker (44) noted excellent correlation between the two methods, documenting less than 1% difference in quantity of crystalline silica determined. However, in this investigation both methods were carried out by the same

researchers and within the same laboratory, which may have contributed to the strong correlation. Inter-laboratory comparisons have historically been used to assess variability in crystalline silica analyses (73-75), both within and between methods. Recently, Cox et al. (32) documented concerns that inter-laboratory measurements of crystalline silica dust concentrations using XRD methods are neither precise nor accurate, particularly for samples with low crystalline silica loadings. This concern is particularly salient, as low sample loadings generally correspond to environmental concentrations that are near the action level – the threshold crystalline silica concentration (below the regulatory limit) for which a mine will take action to decrease dust and crystalline silica concentrations in order to prevent the limit from being exceeded in the future. Accurate quantification of crystalline silica at these levels is vital to protecting workers from crystalline silica exposures, before exposures can occur. While a discussion of the implications of the lack of confidence in the method is beyond the scope of this work, the observation of inconsistency points to an area ripe for improvement that could possibly be stimulated by detailed characterization of dusts.

While inter-laboratory variability certainly impacts the reliability of quantitative methods for crystalline silica, variability within the respirable dust samples can also impact the quality of crystalline silica monitoring efforts. Sirianni et al. (76) noted that particle size distributions vary both between workplaces and within workplaces, such as by specific work task, and that, likewise, the crystalline silica content of dusts has been demonstrated to vary widely according to the manner in which the dust is generated. Page (77) proposed that changes to the frequency of milling and grinding, as well as a shift towards more powerful machinery in mining, has resulted in a change in the size distribution of crystalline silica and other respirable mineral particles within coal mine dust. Furthermore, Cauda et al. (30) found that the crystalline silica content in respirable dusts from metal and sand and gravel mines is both higher and more variable than in dusts from other types of non-coal mining operations, and that control technologies may have selective efficiency for specific particle sizes.

Research characterizing mine dusts with regard to qualities such as mineral content (including crystalline silica content) and particle size distribution can provide a better understanding of factors that influence the observed variation (such as mine type or geographic region). Such research can also offer guidance on how to improve current monitoring strategies to offer more accurate assessments of crystalline silica exposure.

1.2 RELEVANCE OF PARTICLE SIZE TO DUST CONTROL AND EXPOSURE ASSESSMENT

The crystalline silica content of respirable dust samples used for exposure assessment is most often thought of as a “lump sum” (e.g. as the total mass of crystalline silica measured) – and indeed, even regulatory limits are based on the total quantified mass of crystalline silica in a sample. While this is a convenient and practical means to measure exposure, it fails to consider the individual particles that comprise the total mass of crystalline silica, and whether some of those particles may more efficiently initiate the development of silicosis. While all crystalline silica particles have the same chemical composition, the physical size of the particles in an aerosol often follows a lognormal distribution (78). Despite the fact that, currently, the particle size distribution of crystalline silica particles is not routinely measured, there are some considerations with respect to particle size that are worth noting.

There are several mechanisms that influence the deposition of particles from the air onto a surface, including gravitational settling, inertial impaction, and diffusion (78). These mechanisms are governed largely by the size of particles. For instance, larger particles have greater mass than smaller particles of the same composition and as a result settle (fall from the air) at a faster rate than the smaller particles. When large particles are entrained in an air stream, they are prone to impact, or collide, onto obstacles in their path, because the greater inertia of a

large particle prevents it from quickly changing direction when the direction of the air flow changes. Alternatively, the primary mechanism of movement for very small particles is diffusion (the random motion of particles due to their thermal energy), which does not influence large particles considerably. These mechanisms of particle movement are relevant to human exposure, as well as to the controls and protections that are used to prevent human exposure to particles.

Inertial impaction plays an important role for particles in the human respiratory tract, which is non-linear and requires directional change in both airflow and particle movement. This complexity causes particles of certain sizes to deposit in specific regions of the respiratory system. An international convention (79) has been defined for particles of inhalable, thoracic, and respirable particle sizes. The convention for each particle size is based on the cut-point diameter (d_{50}) at which point collection efficiency is 50% for that particular particle size, and the three size ranges defined by the convention correspond to the portion of the respiratory tract in which those particles are likely to deposit.

Particles smaller than 100 μm in diameter can enter the respiratory tract via the mouth or nasal passages; these particles are called *inhalable*. This fraction is defined below by Equation 4.

$$I(d)=0.5(1+e^{-0.06d})$$

where $I(d)$ is the collection efficiency of inhaled particles as a function of particle diameter d

Equation 4 Inhalable definition

Of the particles that are inhaled, those 10 µm and smaller can enter the airways (e.g. the trachea and bronchial region) and are referred to as *thoracic*, defined by Equation 5.

$$T(d)=I(d)[1-F(x)]$$

where $T(d)$ is the collection efficiency of thoracic particles as a function of particle diameter d , $x=\frac{\ln(\frac{d}{11.64})}{\ln(1.5)}$, and $F(x)$ is a lognormal function with median particle diameter 11.64 µm and GSD 1.5

Equation 5 Thoracic definition

Finally, particles 4 µm and smaller are called the *respirable* fraction (defined by Equation 6) and can penetrate deep into the lungs, including deposition in the alveolar region.

$$R(d)=I(d)[1-F(x)]$$

where $R(d)$ is the collection efficiency of respirable particles as a function of particle diameter d , $x=\frac{\ln(\frac{d}{4.25})}{\ln(1.5)}$, and $F(x)$ is a lognormal function with median particle diameter 4.25 µm and GSD 1.5

Equation 6 Respirable definition

As the foremost health outcomes of exposure to crystalline silica are respiratory diseases such as silicosis and lung cancer, it is important to consider how mechanisms of respiratory exposure and response might be affected by particle size. As discussed above, smaller particles are capable of penetrating more deeply into the lungs. However, there is also evidence that crystalline silica particles of different sizes induce varying degrees of inflammatory and fibrotic response in lung tissue, which affects the threshold dose of crystalline silica required for the development of an outcome like silicosis or lung cancer. Thus far, no consensus has been reached regarding the particle size characteristics which initiate the most potent inflammatory

response; however, it is clear that size and surface area are significant variables that should be considered and measured in exposure assessments.

The published data on health impact of specific size particles of crystalline silica is incomplete; the work that has been done is somewhat contradictory, with some studies indicating that toxicity may be dependent on dose by surface area (34) and others indicating that toxicity is dependent on particle size (39), mass concentration (33), or surface activity (80); likewise, some studies indicate that smaller particles induce more damage (34, 38) and others indicate that larger particles do (33, 39, 81). Therefore, the idea of differential toxicity on the basis of particle size is somewhat controversial. While there is no strong indication of a specific trend regarding particle size and inflammatory response, in general there is a demonstration that particle size does play a meaningful role in physiological response to crystalline silica.

Goldstein and Webster (33) exposed rats to surface-area equivalent doses of crystalline silica particles segregated into three size ranges (2-5 μm , 1-3 μm , and less than 1 μm). Sacrifice was performed at four months post-exposure, and lung tissue was histologically analyzed for degree of fibrosis. Chemical analysis was undertaken to determine crystalline silica content present in the lung tissue. The authors found that the two larger particle size ranges (2-5 μm and 1-3 μm) produced more fibrosis than the smallest size class (<1 μm), and that the degree of fibrosis was related to the mass of crystalline silica exposure rather than the surface area. Alternatively, Wiessner et al. (34) prepared crystalline silica particle solutions with average particle diameters of 11.2 μm , 7.8 μm , 5 μm , and 1 μm , and found that with exposures of equivalent surface area, the 1 μm particles induced more hemolysis than the larger fractions. However, the larger crystal preparations induced more inflammation and fibrosis 6 weeks post exposure. All three of the larger fractions elicited equivalent responses for both hemolysis and inflammation/fibrosis.

More recently, Mischler's 2013 (38) findings on the effects of submicron crystalline silica particles are an example of how knowledge of crystalline silica size distribution would be

beneficial. He evaluated particles of four mean diameters (4.1 μm , 2.1 μm , 0.7 μm , and 0.3 μm) and found that particles with a geometric mean of 0.3 μm generated mitochondrial reactive oxygen species (ROS) and resulted in cytokine expression that was significantly increased compared to ROS generation and cytokine expression from larger crystalline silica particles. This study is especially notable in that it considered nanoparticles separately, whereas most previous studies only considered particles down to 1-2 μm but did not separately evaluate smaller particles.

Ohyama et al. (39) compared the induction of lucigenin-chemiluminescence (CL) of four crystalline silica particle preparations with distinct median diameter (3.79 μm , 2.89 μm , 0.99 μm , 0.68 μm). They found that the larger crystalline silica particles were more active in inducing CL than were small particles. Similarly, Kajiwara et al. (81) compared the effects of two particle sizes instilled intratracheally, and found that 6 months post-exposure, inflammatory markers in pulmonary tissues and bronchoalveolar lavage fluid were more pronounced for rats exposed to 1.8 μm particles than for rats exposed to 0.74 μm particles.

The relevance of particle size to the health effect of crystalline silica is not limited to biological impacts alone, but also extends to engineering controls and personal protective equipment, which are used to limit exposure to crystalline silica. Engineering controls are employed by mines in areas where dust concentrations are elevated to unsafe levels, and include both prevention strategies (stopping dust from being generated) and suppression strategies (removing dust that has been generated). As complete prevention is often difficult to achieve, dust suppression is widely utilized and is crucial to protecting workers from exposure. Examples of dust suppression techniques include water sprays, ventilation, and air filtration systems; how each technique is used varies with the type of operation and the type of ore being mined. The effectiveness of these techniques is dependent on a number of factors, among which is particle size. For instance, water sprays tend to be more effective when the water droplet size is comparable to the size of the dust particles (82). For this reason, it is helpful to have knowledge of the size distribution of the dust that is generated by a particular task and within a particular

operation, so that the droplet size in the water spray can be adjusted to achieve maximum effect of dust reduction. In order to evaluate the efficacy of engineering controls in reducing dust and crystalline silica, additional respirable dust samples are collected and analyzed for dust and crystalline silica. Even the cyclone samplers used to collect such samples can have variable performance with regard to particle size (83) (though this effect would be expected to be minor for the respirable size range), making discrepancy in dust and crystalline silica size distribution even more important to consider.

Personal protective equipment such as half-mask respirators are commonly worn by workers in mines in areas where engineering controls have not successfully reduced dust concentration to safe levels. For protection against respirable crystalline silica, NIOSH recommends half-face particulate respirators with N95 filters or higher (84); previous recommendations (now superseded) also included dust and mist filter masks, which are known to have decreased filtering efficiency for particles smaller than 2 μm . Respirators of the appropriate type that are well-maintained and worn properly are quite effective in reducing dust exposure in areas of moderate dust concentration, yet even they are not uniformly effective for particles of all sizes (85). For example, Vo et al. (86) evaluated the performance of eight different respirator types, and for certain types found superior protection against 10-100 nm particles versus 100-400 nm particles. Again, knowledge of the dust size distribution in a mining environment is beneficial to workers by allowing them to select appropriate protective equipment when a more protective choice exists, and also permits workers and supervisors to make more informed judgements concerning the practical limitations of controls and protective equipment, in order to better protect workers against crystalline silica exposure.

1.3 PARTICLE SIZE EFFECTS IN ANALYTICAL METHODS FOR THE QUANTIFICATION OF CRYSTALLINE SILICA

The accuracy of spectroscopic analysis of particulate samples – including the analysis of crystalline silica in respirable dust – can be affected by the physical characteristics of individual particles that comprise respirable dust samples. Characteristics such as porosity (53), surface topography (87), refractive index (87), and particle morphology (45) have been discussed in the literature. The *amorphous layer* phenomenon (discussed in more detail below) has also been raised as a relevant factor. While these are all distinct concerns, many of these factors ultimately relate to the size of a specific particle (53, 87).

The so-called *particle size effect* is of concern for samples of mine dusts, as well as for the standard crystalline silica materials that are used to calibrate these methods in order to quantify crystalline silica. Both IR and XRD methods are susceptible to particle size effects and the resulting analytical bias, although the nature and causal mechanisms of this bias is distinct for each method. Gordon and Harris (46) outlined two distinct trends observed in XRD methods:

- 1) Decreasing XRD intensity for larger particles results from extinction, wherein none of the incident light (of any wavelength) is transmitted through the particle, whereas
- 2) Decreasing XRD intensity for smaller particles results from a greater proportional contribution of the amorphous surface layer of crystalline silica, which is present on crystalline silica particles and does not diffract X-rays in the same manner as crystalline silica.

The amorphous silica layer was first postulated by Nagelschmidt, Gordon and Griffin in 1952 (88), though it had been previously described less precisely by others (89). It has since been verified by numerous groups using a variety of techniques, and it is now well-accepted that a crystalline silica particle consists of an insoluble (crystalline) core surrounded by a layer of (amorphous) silica with a higher solubility. Nagelschmidt, Gordon, and Griffin concluded that this

layer has a maximum thickness of 0.3 μm . The phenomenon only becomes significant for small particles due to their large surface area to volume ratio; effects are negligible for larger particles. In partial support of this idea, Gordon and Harris (46) also found that when crystalline silica particles are leached with hydrofluoric acid to remove the amorphous layer, with the lower-solubility crystalline core left intact, the diffraction maximum occurs for particles 3 μm in diameter. Particles 1 μm in diameter achieved only 70% of the maximum intensity, while particles 0.5 and 0.4 μm achieved just 50% and 40% of the maximum intensity, respectively. Based on these findings, the authors asserted that the amorphous layer is not a true layer, per se, with clearly defined margins, but rather that a gradual and consistent increase in crystalline character occurs as the center of the particle is approached. For small particles, full crystallinity never occurs, even at the particle's core. As the crystalline structure of the silica molecule defines the characteristic signal for crystalline silica in both the IR and XRD methods, loss of crystalline character affects intensity of the analytical signal, and impacts the apparent mass of crystalline silica present.

Although both IR and XRD are affected by the amorphous layer, the effect in IR analysis is greater for larger particles (55), and the effect in XRD is greater for smaller particles (43). For a sample of very small particles (for instance, particles smaller than 500 nm), IR would provide a more accurate measure of crystalline silica mass, while for a sample of large particles (for example, particles between 6 and 10 μm), XRD would be more accurate. In occupational samples, a narrow range of particle size is rarely encountered, and even particles in the respirable size fraction range from nanometers to microns – a thousand-fold difference in magnitude. The effect of particle size on IR and XRD analysis is discussed in greater detail in the following sections.

1.3.1 Effect of Particle Size in IR Spectroscopy

The effects of particle size on IR analytical techniques have been well-documented (44, 49, 51-55). Generally, transmission IR techniques are subject to increasing signal attenuation with increasing particles size. The cause of this phenomenon has been widely studied, particularly with regard to analysis of crystalline silica.

Tuddenham and Lyon (55) found that increased absorbance and resolution in the region of the crystalline silica doublet (approximately 800 cm^{-1}) corresponded to decreasing particle size when they considered four size ranges of particle (less than $2\text{ }\mu\text{m}$, $5\text{-}6\text{ }\mu\text{m}$, $6\text{-}8\text{ }\mu\text{m}$, and $14\text{-}16\text{ }\mu\text{m}$), but they did not reach any conclusions for particles smaller than $1\text{ }\mu\text{m}$ in diameter. Lorberau (49) remarked upon particle size-related error of up to 30% in the quantification of crystalline silica, and also observed that the ratio of the two doublet peak heights varies with particle size. Reut et al. (52) estimated that the IR response is lowered 50-60% for particles between 2.2 and $7.2\text{ }\mu\text{m}$.

Lorberau also noted that while ratio of the doublet the peak heights is variable, it is less so than the integrated peak area of the doublet and thus could be a useful tool for correcting effects of particle size. Toffolo and Lockington (54) noted that an alternative absorption band for crystalline silica at 694 cm^{-1} demonstrates almost no size dependency for particles less than $10\text{ }\mu\text{m}$. While this would be ideal for analysis of respirable dust, this particular band is less intense than the preferred analytical peaks for crystalline silica, and thus its use would result in a decrease in method sensitivity for crystalline silica. The authors also remarked that laboratory determination of the percentage of crystalline silica in non-respirable and bulk dusts should not be undertaken without knowledge of the particle size distribution and the application of appropriate correction factors (discussed further below).

Otvos et al. (51) noted that anomalous effects of particle size are expected to be most significant when wavelength and particle size are similar, which is the case for respirable particles

that are evaluated at the analytical peak (doublet) for crystalline silica (occurring at 800 cm^{-1} , or $12.5\text{ }\mu\text{m}$). Likewise, Dodgson and Whittaker (44) found an inverse relationship between particle size and absorption of IR energy, with the precise relationship dependent on the wavelength of incident energy. The same investigation also found that methods accounting for particle size using absorbance ratios are affected by interfering IR absorbance from the presence of other minerals in the dust; this complicates the use of simple correction factors to adjust for particle size effects. The researchers ultimately concluded that it would not be worthwhile to apply particle size corrections to respirable dust samples as “these aerodynamically selected dusts are generally similar in size to the quartz standard.”

Alternatively, Salisbury and Eastes (53) presented the argument that it is not truly particle size that affects IR measurements of crystalline silica, but rather the porosity of the particles. Increased porosity of the surface of fine particles results in increased absorption by allowing photons to pass between grains. This results in deeper light penetration in to the layer, maximizing the chance of absorption and increasing the intensity of the analytical response.

1.3.2 Effect of Particle Size in X-ray Diffraction Spectroscopy

Effects of particle size on XRD analysis have likewise been well-studied (43, 45-47). Gordon and Harris (46) found that the intensity of the analytical diffraction line from crystalline silica was at a maximum intensity for particles $2\text{ }\mu\text{m}$ in diameter, and decreased for both larger and smaller particles, though the decrease was more substantial for decreasing particle size. Brindley and Udagawa (43) found that extinction in XRD analysis of crystalline silica is only of concern for particles larger than $40\text{ }\mu\text{m}$; thus, while this phenomenon is not relevant to the study of respirable dusts, it could be relevant when considering bulk mine dusts and the crystalline silica content therein. Hurst, Schroede, and Styron (47) observed an optimal size range for coherent diffraction domains of 200 nm to $5\text{ }\mu\text{m}$, but this does not include any portion of the particle that may not have

fully crystalline character, such as the amorphous layer. These authors also outline an extensive list of factors that should be considered in the process of interpreting XRD data in order to ensure accurate quantitative determination, including the size distribution of the coherent diffraction domain.

Edmonds, Henslee, and Guerra (45) attributed increased XRD sensitivity to crystalline silica in the larger particle size ranges to the greater relative volume of these particles, rather than the diameter of the particles. This echoes the theory of an amorphous surface layer that contributes disproportionately in the analysis of smaller particles, which have a larger ratio of surface area to volume. The authors also noted that analytical sensitivity is enhanced when smooth surface substrates, such as silver membrane filters, are used during analysis, in contrast to rougher surface of PVC filters. This is due to orientation effects (related to effects of particle size and morphology), wherein a substrate with rough surface features might “hide” or obscure particles from incident X-ray beams. While it is very common for samples to be collected on PVC filters (which are both inexpensive and easy to handle), the NIOSH 7500 XRD method does specify the use of silver membrane filters for sample redeposition. The analytical advantages of smooth substrate material are important to consider in the event that different filter materials are ever explored.

1.3.3 Significance of the Size Distribution of Calibration Material

For two dust samples having equivalent crystalline silica content but distinct size distributions, an IR method will quantify a greater mass of crystalline silica for the sample with the smaller size distribution, and an XRD method will quantify a greater mass for the sample with the larger size distribution, due to the effects of particle size on either method. This assumes that both methods are calibrated using material with equivalent size distributions. Typically, a crystalline silica reference material such as NIST SRM 1878a (respirable alpha quartz) would be used to complete

method calibration, by correlating known masses of the reference material (assumed to have 100% purity) to analytical signal intensity, and by subsequently constructing a calibration curve from which the mass of crystalline silica in a sample can be determined, based on the measured signal intensity from that sample. Because of the particle size effects discussed above and the resulting variability in signal intensity, the sample and the reference material should ideally have equivalent (or, at the very least, comparable) particle size distributions in order for the calibration to be valid. Unfortunately but perhaps understandably, evaluation of the particle size distribution of samples, much less comparison to the size distribution of the reference material, is not routine practice. To best knowledge, no such comparisons have been published for dusts from metal/non-metal mining operations, and only a few published works reference such comparisons for dusts from coal mines (77, 90). Importantly, Page (77) has published size information for several crystalline silica materials, which could be used for comparison to the size distribution of sample dusts. He found a median aerodynamic diameter of 2.23 μm for SRM 1878a, as well as for Min-U-Sil 5, the material from which SRM 1878a is derived and which is more readily available.

A lack of equivalency between size distribution of sample and reference material can result in inaccurate quantification of the mass of crystalline silica in a sample, and thus to exposure misclassifications. The importance of verifying agreement between the particle size distribution of a sample and that of the crystalline silica reference material is noted by numerous authors (45, 91, 92). Huggins et al. reported that the U.S. Bureau of Mines and MSHA estimated that discrepancies in measured crystalline silica values may be as high as 30% when the particle size distribution of the crystalline silica standard material differs significantly from the size distribution of the mine dust. It is worth noting that most investigations, to date, did not consider the size distribution of crystalline silica particles separately from the size distribution of dust particles, but rather assumed that the size distribution of respirable dust is equivalent to the size distribution of the crystalline silica component. This assumption has not been thoroughly evaluated and could have analytical implications, if the two size distributions are not in fact equivalent. Reut et al. (52)

determined that for a reference material with an approximate mass median diameter (MMD) of 2 μm and a sample with approximate MMD of 1.6 μm , crystalline silica is overestimated by 6%, but for the same reference material and a sample with MMD of approximately 8 μm , crystalline silica will be underestimated in the sample by 50%. Edmonds, Henslee, and Guerra observed that when the size distribution of a dust diverges from that of the crystalline silica standard, errors of up to 300% of the quantity of crystalline silica may occur. The authors also remarked that selecting a crystalline silica standard material based on its purity rather than its size distribution would lead to misrepresentative results that are nonetheless internally consistent, which may prevent the bias from being detected. Thus, determination of sample particle distribution, and selection of an appropriate standard is essential to ensure validity. Bhaskar et al. (93) remarked that in the case of dust samples that have been ashed, particle size distribution should be assessed *after* the ashing procedure, as the particle size distribution can change markedly as a result of the loss of carbonaceous particles in the sample.

1.4 MINERAL INTERFERENCE IN ANALYTICAL METHODS FOR THE QUANTIFICATION OF CRYSTALLINE SILICA

Dust samples rarely contain only a single species, and the presence of multiple species or a matrix can result in interference in analytical methods (56, 57). Spectroscopic interference occurs when other mineral species present in a sample contribute a signal in the analytical region for crystalline silica; such interference can be either positive (resulting in an overestimation of the quantity of crystalline silica) or negative (resulting in an underestimation of the quantity of crystalline silica). The potential effects of interfering signals from other minerals present in samples are well documented (48, 50, 56, 57)

In IR spectroscopy, there are two general type of interferences: broadband interferences (such as from particles of coal) absorb in a wide range of the spectrum and can distort the baseline of the spectrum such that accurate integration of the crystalline silica doublet becomes complicated; alternatively, structural interferents for crystalline silica (such as from particles of kaolinite and other silicates/aluminosilicates) contain similar bond structures, and therefore absorb IR wavelengths in a similar fashion despite being structurally distinct molecules. The presence of coal dust in samples is recognized as a source of interference, and can be addressed by removal of coal during sample preparation (94). Structural interferents must be corrected for mathematically, by identifying their presence in the sample spectrum and using other characteristic bands for that particular compound to adjust the signal intensity observed at 800 cm^{-1} (50). However, while kaolinite, an aluminosilicate clay, is considered to be the only mineral confounder of appreciable concern in respirable dust samples from coal mines (95), similar determinations have not been made for dust samples from other types of mining operations, which would be expected to contain a more diverse set of confounding minerals. Furthermore, it is unknown if generalizations of a similar degree can be made for dusts of other mine types, or if more specific determinations would need to be made for each set of samples.

Fortunately, while there is only a cursory knowledge of the most relevant confounders within each of the various types of mine dust, there is a much clearer understanding of the specific groups of minerals likely to be significant confounders for each method of analysis (56, 57). NIOSH Method 7500 (56) for XRD analysis of crystalline silica cites “barite, micas (muscovite, biotite), potash, feldspars (microcline, plagioclase), montmorillonite, sillimanite, zircon, graphite, iron carbide, clinoferrrosillite, wollastonite, sanidine, leucite, orthoclase, and lead sulfide” as the most relevant interferences for crystalline silica, and suggests use of the secondary or tertiary angles (which are less sensitive for crystalline silica, thus increasing the limit of detection) if interference from other minerals is found for the primary angle.

NIOSH Method 7603 (57) (nearly identical to MSHA P7, which does not offer guidance on mineral interference) for IR analysis of crystalline silica cites kaolinite and calcite as the most relevant minerals to consider in dust samples from coal mines. The method also notes that while cristobalite and tridymite both produce interfering peaks in the region of the 800 cm^{-1} crystalline silica doublet, neither has been found to occur in coal mine dust (although they may occur in the dusts from other types of mines). Ojima (50) referenced IR spectral interference from clays and micas which have absorption peaks in the region of the analytical peak for crystalline silica (800 cm^{-1}) and contribute to an apparent increase in crystalline silica concentration. Among the most often cited minerals creating interferences of this type are kaolinite, mullite, muscovite, pyrophyllite, montmorillonite and amorphous silica. Additionally, clinoenstatite, nontronite, antlerite, and chloritoid can also contribute to interference in the 800 cm^{-1} absorption band. Ojima also noted that other substances can contribute broadband interference in the quantification of crystalline silica by significantly affecting the baseline of the sample spectrum. Such minerals include graphite, silicon carbide, and iron oxide, among other highly absorbing mineral phases.

Dodgson and Whittaker (44) discussed common composition of coal mine dusts, which include the presence of interfering minerals such as calcite, mica, carbonates, montmorillonite, chlorite, feldspar, pyrite, iron oxides, anhydrite, gypsum, and kaolinite; they note that of these, only kaolinite is present in significant quantities in coal mine dusts. Toffolo and Lockington (54) echoed the finding that only kaolin clays and samples with significant amounts of muscovite are subject to significant interference in the 800 cm^{-1} region. Dodgson and Whittaker also cited previous work by Dixon and Fretwell (96) which determined that only minor errors were introduced by the presence of mineral interference – however, this study provides an upper limit of 30 μg for error in the quantification of crystalline silica. In 1968 when this study was published, dust and crystalline silica standards were significantly higher than they are today, and while 30 μg would have indeed been just a small contribution at that time, it represents a significant proportion of the current maximum allowable exposure. Furthermore, this paper cites the diluting effect of coal

dust as reducing the apparent error; the current P7 method developed by MSHA for analysis of crystalline silica in coal dust eliminates the contribution of carbonaceous materials via ashing of the sample prior to analysis.

There are two strategies used to correct for the interference resulting from confounding minerals. First, the spectrum of a pure sample of each interfering mineral can be subtracted from the IR spectrum of the sample. In theory, after spectrum subtraction is performed, the integrated peak area in the 800 cm^{-1} band is attributable entirely to the crystalline silica present in the sample and can be used to accurately quantify the mass of crystalline silica in the sample. Alternatively, the absorbance ratio method can be used to correct for mineral interference by using proportional peak heights in the spectrum of the interfering mineral. The integrated area of a distinct peak for the interfering mineral can be measured in the sample spectrum, and from the known ratio of the distinct peak to the interfering peak, the interference contributed by that mineral in the 800 cm^{-1} can be corrected. Lorberau (48) maintained that both the spectral subtraction method and the estimation of interferent concentration via calibration curves overcorrect for the interference and result in an overall underestimation of crystalline silica. On the contrary, Ojima (50) found that spectral subtraction (difference spectrum method) resulted in nearly complete correction of bias due to interference, while the absorbance ratio method resulted negative bias. What is most important to consider is that any strategy to address or correct mineral interference first requires a thorough understanding of the mineral components of which a dust is comprised.

1.5 PREVIOUS CHARACTERIZATION OF OCCUPATIONAL DUSTS CONTAINING CRYSTALLINE SILICA

To date, very few studies have undertaken detailed size and compositional characterization of any sort of occupational aerosol containing crystalline silica. Furthermore, the majority of the

research that does exist has focused on dust samples from coal mines, while little focus has been given to the mineral characteristics of dust from metal/non-metal mines, where variability could be expected due to the wide range of mined commodities represented by this group.

Though coal mine dust has been better characterized compared to other types of mine dusts, there is still relatively little published data concerning the size-related crystalline silica content of coal mine dusts. Huggins et al. (91) used scanning electron microscopy to size particles from underground and surface coal mines, and did the same for particles from four pure crystalline silica materials; no appreciable difference in size distribution between the mine dust particles and the pure crystalline silica materials was found. More recently, Page (77) completed a similar evaluation, making reference to changing mining technologies, machine power, and control technologies as contributing to a potential shift in the size distribution of coal mine dust. His work evaluated and compared the size distribution of dusts from 13 coal mines and four standard crystalline silica materials used in the IR and XRD methods. With regard to single particle analysis, DeNee (97) described a method for the characterization of mine dust using the scanning electron microscope; the analysis characterized morphological characteristics and particle agglomeration as well as elemental composition of particles. More recently, Sellaro et al. (98, 99) have described a standardized methodology for the analysis of respirable dust from coal mines using scanning electron microscopy with energy dispersive X-ray.

Apart from the study of coal mine dusts, only a few studies have endeavored to characterize the size distribution of occupational dusts specifically with regard to crystalline silica. Sirianni et al. (76) have characterized dust from a granite quarry with regard to the size distribution of the dust and the particle size-related crystalline silica content. They found that crystalline silica content varied with particle size and generally increased as particle size increased, but that this trend was somewhat variable. Qi et al. (100) have evaluated dust from the cutting of fiber cement siding with regard to particle size-related crystalline silica content and observed trends similar to the findings of Sirianni et al. Notably, the authors also remarked upon the complex nature of dust

characterization: namely, that reliable methods for characterization have not been developed (presumably, that there is no standardized approach for dust characterization), and that a diverse range of processes can generate respirable crystalline silica particles. This calls further attention for the need to characterize occupational dusts with regard to their crystalline silica (and mineral) content.

1.6 TOWARDS A MORE ACCURATE QUANTIFICATION OF CRYSTALLINE SILICA

When the mineral composition of a sample dust is known, quantitative results for crystalline silica determined from the IR or XRD methods can be corrected based on the known interferences contributed by other mineral components of the dust; likewise, adjustments may be made for particle size-related bias if the size distribution of that particular dust has been characterized. Such corrections can account for both positive (when interfering factors result in an overestimation of the quantity of crystalline silica in a sample) and negative (resulting in an underestimation of the quantity of crystalline silica) bias. While limiting the effects of negative bias are clearly important in protecting worker health against unsafe exposures to crystalline silica, avoiding positive bias is also important in order to prevent burdensome regulations that unfairly impact the mining operator while not offering additional protection to workers. To mitigate both types of bias and achieve a result that is as accurate as possible, it is important to have a thorough understanding of the characteristics of a particular dust that may impact the quantification of crystalline silica.

To minimize bias due to the effects of particle size in either the IR or the XRD method, the crystalline silica material used for calibration of the method should be matched to the sample material with regard to size distribution. Where this is not possible, adjustments should be made based on differences in the size distributions of the two materials. Both of these strategies require

a thorough understanding of the size characteristics of both the dust and the crystalline silica component; even for dusts which have previously been characterized, it may be necessary to re-evaluate size distribution when the mining process undergoes changes, such as equipment upgrades, exploration of new ore formations, or revisions in the control technologies that are used.

Most dusts will contain other minerals in addition to crystalline silica, and therefore corrections will be necessary in order to address signal interference from these minerals. When only one or two other minerals are present in a sample, this is a straightforward process, but it can become more complicated as the complexity of the mineral matrix of the dust increases. Madsen et al. (75) recommend that a multivariate approach to crystalline silica analysis be undertaken, which would require the component matrix of specific dust types to be well-defined. The authors note that it is unknown how rigorous this approach may be in the face of unknown matrices – thus, it is important to characterize a broad range of dusts, which contain a variety of other mineral species in assorted combinations.

Dodgson and Whittaker (44) note that mineral interferences tend to have a more substantial impact on quantification than do effects of particle size, and that mineral corrections should be carried out *before* adjustment for particle size effects. Furthermore, collection of respirable dust samples (including those for crystalline silica analysis) utilize size-selective sampling devices to separate respirable particles from larger particles, thus decreasing discrepancies between the particle size distributions of sample and calibration material; in some cases, this may make a size correction factor unnecessary. Nevertheless, Page (77) estimated that particle size effects in XRD quantification of crystalline silica are likely to result in a bias of 5-10%, up to as much as 18%, and Huggins (91) estimates a bias of up to 30% for IR. Lorberau and Abell (68) noted discrepancies that arose during proficiency analytical testing for the quantification of crystalline silica via XRD and IR methods, and speculated that discrepancies observed between two methods arose from the size distribution of the dust analyzed. Together,

these findings demonstrate that the possibility of effects due to particle size should not be assumed to be minimal, and should not be ignored.

Unfortunately, characteristics of mine dusts are not consistent from mine to mine, or even from task to task in the same mine: it is impossible to apply a uniform correction for all dusts. In order to develop correction factors for dusts of different types (and indeed, to determine what factors may constitute a “type of dust”), these dusts must first be characterized. Knowledge of qualities such as the size distribution of the dust particles generated, the crystalline silica content of the dust and the size distribution of crystalline silica particles, and the other mineral species present in the dust are of great value, as these factors have implications for the analytical methods discussed above. These qualities may vary according to: the type of mine commodity, the geology in the region of the mine, the locations within the mine (i.e. underground vs. surface vs. mill locations), and the types of equipment and processes employed in a specific air and for a particular task. While geology is expected to impact primarily the mineral composition of dust, it can also affect dust size distribution according to the hardness or brittleness of rock material and the mining equipment used to cut through the rock. In particular, as mining technologies evolve and equipment innovations result in new capabilities and higher production efficiency, changes to mining processes may result in changes to the size distribution of dusts generated. This phenomenon has been raised as a potential concern to crystalline silica monitoring efforts (30, 77), as the characteristics of dust could become even more dynamic in the future. A dedicated effort will be required to first achieve a comprehensive understanding of dust characteristics, and to then maintain that body of knowledge to ensure that accurate and appropriate correction methods are applied to analyses for crystalline silica.

In conjunction with these analytical considerations, detailed characterization of mine dusts would be beneficial for application toward exposure assessments, specifically with regard to quantitative metrics for crystalline silica based on properties other than mass. As more is learned about the role of particle size in crystalline silica-initiated inflammatory processes, it becomes

clear that respirable crystalline silica particles may not all be equivalent in terms of their impact on human health. This possibility increases the importance of understanding the size distribution of crystalline silica as a component of a dust, rather than understanding the size distribution of the whole dust alone.

Mass-based methods for the quantification of respirable crystalline silica consider all respirable crystalline silica particles together as an integrated sample. While mass-based measurements are convenient and have long been the standard, these methods are vulnerable to the lack of knowledge of particle size-related composition of mine dusts, for several reasons. First, lack of knowledge of the size distribution of crystalline silica particles relative to the size distribution of dust particles in general essentially necessitates the assumption that crystalline silica particles are distributed equally throughout all particle sizes, e.g. that each size fraction of dust has a comparable percentage of crystalline silica. While this may certainly be the case for some mine dusts, it may also be untrue for other mine dusts. As discussed above, uncharacterized particle size effects create the potential for analytical bias, as well as for exposure misclassification. Additionally, even within respirable dusts, some sizes of particles are more respirable than others – that is, their aerodynamic diameter allows them to penetrate deep into the lung before embedding in tissues. Furthermore, smaller particles may be more efficient in inducing fibrogenic response, either due to deeper lung penetration or increased surface area relative to larger particles. Dose response may be proportional to number concentration or surface area concentration rather than mass concentration, and this also has implications as far as the potential health effects of crystalline silica.

Clark and Reynolds (71) remarked that “exact quantitative knowledge concerning the chemical composition of the materials entering the lungs of workers” is necessary to the epidemiological study of respiratory disease such as silicosis. To achieve exact quantitative knowledge, the characterization of both the composition and the particle size characteristics of a mine dust must be undertaken.

1.7 SCOPE OF DISSERTATION AND STATEMENT OF HYPOTHESIS

While a few studies have investigated properties of aerosols of occupational dust with regard to crystalline silica, more research is necessary in order to understand properties of crystalline silica particles within a diverse range of dusts, relative to properties of the dust particles in general.

A considerable obstacle to improving exposure assessment for crystalline silica and therefore to limiting worker exposure is the lack of comprehensive efforts to characterize properties of mine dusts, specifically with regard to particle size and crystalline silica content. Few dusts from mining environments have been characterized, and no standardized method exists by which to characterize mine dusts with regard to their composition as well as with regard to particle size. Numerous works have focused on one or the other but none have combined the two aspects. Further, while recent works have begun to investigate factors such as particle size that may contribute to increased toxicity, and past works have addressed, in general, particle size-related factors that may contribute to measurement bias, little work to date has been done to characterize the qualities of mine dusts that might contribute significantly to measurement uncertainty in the quantification of crystalline silica.

The lack of investigation of particle size-related crystalline silica and mineral content of metal/non-metal mine dusts represents a serious gap in knowledge that must be addressed. Without a better understanding of particle size-related characteristics of dusts, it is not possible to assess the accuracy of current monitoring methods, which leaves workers vulnerable to excessive exposures to crystalline silica that may, inadvertently, go undetected. The lack of knowledge regarding size distribution of crystalline silica, specifically, also precludes monitoring and toxicological assessment based on dosing metrics other than mass – such as particle number or surface area. This study describes a method by which to achieve detailed characterization of mine dusts, and illustrates why future and continued efforts towards such characterization are required. This method is used to characterize three different dusts, all from gold mining

operations, and will illustrate that the qualities of mine dusts are varied, even within dusts from similar types of mines. Based on the premise that the particle size-related crystalline silica and mineral composition of mine dusts is variable, impacting the accuracy of monitoring methods for crystalline silica, this work seeks to explore three hypotheses, outlined below.

First, the size distributions of three gold mine dusts are measured and the crystalline silica content of each particle size fraction is quantified, in order to test the hypothesis that the size distribution of a particular dust is not equivalent to the size distribution of the crystalline silica component of that dust, and that crystalline silica is not uniformly distributed through all particle size ranges of dust.

Secondly, two distinct analytical methods for the quantification of crystalline silica are used to characterize specific size fractions of dust for their crystalline silica content. Comparisons are made between the crystalline silica determined by each method, in order to test the hypothesis that the particle size distribution of crystalline silica affects accuracy of analytical methods for the quantification of crystalline silica, and that this effect is not constant from dust to dust.

Finally, single-particle analysis is undertaken via electron microscopy to identify silica and non-silica particle classes. The relative abundance of these particle classes are determined for specific size ranges of the three dusts, in order to test the hypothesis that, like crystalline silica, other particle classes vary in abundance by particle size, and that such variation is not constant from dust to dust.

2.0 DETERMINATION OF THE SIZE DISTRIBUTION OF CRYSTALLINE SILICA IN GOLD MINE DUST

Exposure to crystalline silica and the development of silicosis are important health concerns in the mining industry. Exposure monitoring is used to address and prevent overexposures to respirable crystalline silica in the workplace. Current monitoring methods use gravimetric analysis to assess total respirable dust concentrations, and infrared (IR) or X-ray diffraction (XRD) methods to quantify crystalline silica within the dust. From these two analyses, the proportional crystalline silica content of the dust is calculated. An implicit assumption of this method is that size distributions of respirable dust (particles smaller than 4 μm) dust and of the crystalline silica component of respirable dust are equivalent, but to best knowledge this assumption has never been evaluated.

Understanding the particle size distribution of crystalline silica, in addition to the size distribution of the overall dust, is important for several reasons. First, accurate knowledge of the size distribution of crystalline silica is important to the quantification of crystalline silica. Analytical methods for the quantification of crystalline silica must be correctly calibrated in order to accurately quantify the mass of crystalline silica present in a sample; calibrations are established using known standard materials. However, both analytical methods are affected by particle size, requiring a close match between the size distributions of sample material and the calibration material. Lack of comparability between the two materials will result in a method calibration that either over- or under-estimates the crystalline silica present in samples. Without knowledge of the size distribution of the crystalline silica component, a good match cannot be guaranteed, and accurate results cannot be assured.

Secondly, both personal protective equipment (such as commonly employed half-face filtering respirators) and control technologies (such as water sprays and ventilation systems) have

variable efficiency with respect to particle size. More appropriate controls and protections can be chosen with knowledge of the size distribution of crystalline silica particles present in the environment; alternatively, with the knowledge that the controls in place may not be adequate for the particle sizes present, administrative controls such as shift rotation may be implemented to keep worker exposures to a minimum.

Finally, biological activity of crystalline silica particles does not appear to be consistent across all particle sizes. While this aspect of the mechanism of crystalline silica toxicity is not well understood, it is clear that there is some effect of either particle size or particle surface area that contributes to both inflammatory and fibrotic processes involving crystalline silica particles. In order to further explore the dose response relationship of crystalline silica exposure (as for development of new permissible exposure levels), it is important to understand the particle size distribution of crystalline silica within various mine dusts; it is not sufficient to understand solely the size distribution of the overall dust, which may be largely comprised of inert, so-called *nuisance dust* particles, which may be substantially different in size from crystalline silica particles. Crystalline silica particle size is also significant in that specific health outcomes and relevant toxicological dose may ultimately be demonstrated to be related to particle size or surface area rather than simply particle mass. Furthermore, since current exposure metrics rely on mass-based assessments, which are inherently biased towards larger, more massive particles, exposure assessments are likely underestimating exposure to smaller particles that contribute less significantly to mass-based measurements, but which could have greater impact on human health (38).

When the particle size distributions of samples have been evaluated in the literature, it has typically been for the whole dust, rather than for the crystalline silica component of the dust. Presumably, this is because it is relatively straightforward to evaluate the size distribution of a dust, as it can be performed gravimetrically. However, to evaluate the size distribution of crystalline silica particles, additional steps must be taken to quantify crystalline silica mass

spectroscopically. These steps do require some extra effort, but they are not unduly time-consuming, labor intensive, or cost-prohibitive. While it is not practical to evaluate the crystalline silica size distribution for each and every dust sample collected, it does seem more feasible to put forth such effort for a number of mine dusts with similarities and differences in relevant qualities, so that potential patterns may be unveiled.

2.1 METHODS

Three gold mine dusts were selected from samples previously collected at a mine in Alaska, a mine in Nevada, and a mine in South Africa. In general, these samples of bulk dust have been collected at mine sites by NIOSH researchers (or by other researchers or health and safety personnel at a mine on behalf of NIOSH researchers) from settled dust that has accumulated on surfaces near the production areas of the mine. Such samples often represent a composite of dust from various areas and processes around the mining operation; thus, they are not necessarily representative of any particular source of exposure, but are rather an approximate “average” of potential exposures throughout the mine. Once brought to the lab, bulk dusts are stored in glass vials and kept in a cool, dry environment. Prior to being aerosolized in a laboratory aerosol chamber, samples are sieved to remove particles larger than 32 μm (leaving smaller particles undisturbed), which are difficult to re-aerosolize in a consistent manner and are of little interest for worker exposure.

Independently of one another, each dust was re-aerosolized in a calm-air Marple aerosol chamber (101), using a TSI 3400A fluidized bed aerosol generator (TSI, Shoreview, MN) and neutralized through a TSI 3012A NRC Aerosol Neutralizer (TSI, Shoreview, MN). The aerosol chamber is 2.44 m in height with hexagonal cross section (inside diameter 1.19 m). The aerosolized dust is introduced from the top of the chamber and there is mixed by an air jet that

enters the chamber from the side. The thoroughly mixed aerosol flows downward through a 10-cm thick honeycomb structure where turbulence is reduced, providing a low-velocity downward flow through the portion of the chamber where sampling occurs. This chamber has been used extensively in recent years for evaluation of dust monitors (102, 103), and conditions inside the chamber can be controlled such that spatial variability is less than 5% (101). Respirable dust concentration within the chamber was monitored by Tapered Element Oscillating Microbalance (TEOM 1400, Thermo Scientific, Waltham, MA).

2.1.1 Characterization of Size Distribution: APS + SMPS

As the respirable portion of mine dust is expected to include particles as large as 10 μm and as small as several nanometers, the aerosol of each dust was characterized by two different spectrometers in order to characterize this complete size range. A TSI 3321 aerodynamic particle sizer (APS; TSI, Shoreview, MN) measured particles from 0.5 μm to 20 μm , while a TSI scanning mobility particle sizer (SMPS; EAD 3080; CPC 3010; TSI, Shoreview, MN) measured particles from 14 nm to 673 nm. The SMPS was operated with sheath air of 3 liters per minute (lpm) and aerosol flow rate of 0.3 lpm. The two instruments simultaneously extracted aerosol from the mid-section of the Marple chamber via conductive tubing (OD 6 mm). Aerosols were evaluated under a variety of chamber conditions (relative humidity; air flow; dust concentration) to ensure that size distributions remained consistent, independent of chamber conditions. Resulting APS aerodynamic and SMPS electromobility size distributions were merged using the Data Merge Module (TSI, Shoreview, MN), applying a lognormal fit for the composite distribution. To optimize the merged data, specific settings and corrections were applied: the density of each dust was estimated and assumed constant, and a shape factor of 1.2 was selected (104, 105). For the SMPS data, the multiple charge correction was selected, and for the APS data, the efficiency counting correction was selected. The merged distribution was exported as a function of the

aerodynamic size of the particles, as this metric is more germane to the objectives of this study than the electromobility size.

2.1.2 Characterization of Size Distribution: Gravimetric Inversion

Size distributions can also be determined by inversion of gravimetric data, wherein discrete bins of a range of particle size are measured by the mass of material collected; this data is then converted into a continuous distribution by considering the stage efficiency and particle loss functions for each particle size and for each collection stage. Stage efficiency functions and mathematical representations can be developed empirically, or, for well-documented instrumentation, can be estimated from functions reported in the literature (106), with the assumption that both the calibration instrument and the experimental instrument were operated under the same conditions during sampling, and that the calibration aerosols and sample aerosol had sufficiently similar properties.

A cascade impactor is used to collect particles in specific ranges of aerodynamic diameter. An aerosol enters the inlet of the impactor and flows over a plate or stage; particles must move around the plate in order to continue in the airflow, but larger particles cannot move quickly enough and are deposited on the stage via impaction. Smaller particles continue to the next stage where the process is repeated, and so on until the air reaches an after-filter, where all particles still entrained in the airstream are collected. A greased substrate is often used to increase the collection efficiency of a stage by preventing particles from bouncing off the stage and becoming re-entrained. The sharpness of a stage indicates how precisely the stage separates particles, and the d_{50} or cut-point of the stage indicates the particle size that is collected by the stage with 50% efficiency. The Micro-orifice Uniform Deposit Impactor (MOUDI) (107) is one type of cascade impactor; it employs stage rotation and precisely oriented stage nozzles (where airflow enters the stage) to achieve a more uniform sample deposit than other types of impactors. In addition, the

sharp cuts of each stage of the MOUDI achieves better particle separation than other types of impactors. Stage cut-points and approximate sharpness are shown in Table 1.

Table 1 MOUDI stage cut-points

| Stage | d₅₀ (μm) | Approximate Sharpness |
|--------------|----------------------------|------------------------------|
| Inlet | 18 | 1.35 |
| Stage 1 | 9.9 | 1.18 |
| Stage 2 | 6.2 | 1.10 |
| Stage 3 | 3.1 | 1.05 |
| Stage 4 | 1.8 | 1.11 |
| Stage 5 | 1.00 | 1.07 |
| Stage 6 | 0.56 | 1.08 |
| Stage 7 | 0.32 | 1.16 |
| Stage 8 | 0.18 | 1.13 |
| Stage 9 | 0.097 | 1.20 |
| Stage 10 | 0.057 | 1.33 |
| Final Filter | - | - |

A MOUDI (model 110-R, MSP Corporation Minneapolis, MN), positioned outside of the sampling chamber, extracted dust from the chamber via conductive tubing (OD 30 mm) and was used to fractionate and collect dust on pre-weighed, greased 47-mm foil substrates (MSP Corporation, Shoreview, MN). Sample substrates and after-filter were post-weighed to determine the net mass of dust collected on each stage. An inversion of gravimetric data (108) was performed using estimates of stage efficiency functions and particle losses for the MOUDI, and a size distribution of the dust was constructed, including MMD and GSD for each dust.

2.1.3 Characterization of Particle Size-related Crystalline Silica Content

While greased substrates are useful for reducing particle bounce, the grease interferes with chemical analyses and is difficult to remove from dust particles post-collection. To characterize crystalline silica content, samples were collected with the MOUDI on 47 mm PVC filters. As PVC

filters are subject to increased particle bounce compared to greased substrates, a mechanism was devised to limit the effects of bounce while still maintaining chemical integrity of the samples. Sampling was completed in two phases: in the first, greased foil substrates (as described in the previous section) were placed on the inlet and even numbered stages of the MOUDI, and PVC filters were placed on odd numbered stages; in the second, the arrangement was reversed so that PVC filters were on even numbered stages (shown in Figure 5). By alternating greased foils with PVC filters, the effects of large particles bouncing onto a sample (positive bias) are greatly decreased, as the majority of large particles will adhere to the greased stage above the sample. Negative bias due to particles bouncing off of the filter is still possible; however, crystalline silica and non-crystalline silica particles will bounce off the filter with approximately the same frequency, and the proportionate crystalline silica content measured in the sample will be unaffected.

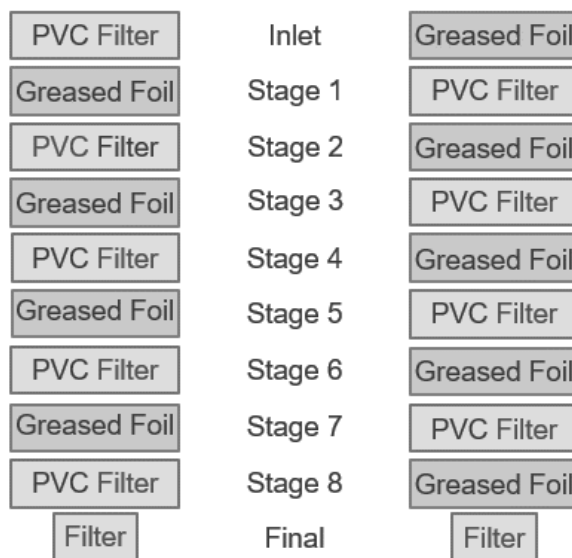


Figure 5 Arrangement of PVC filters and foil substrates on MOUDI stages

PVC filters and greased substrates were pre-weighed prior to sample collection. Dusts were aerosolized in the manner described above. Though the MOUDI 110-R is capable of

segregating aerosols into 10 defined size fractions, plus the inlet stage and after-filter, dusts were segregated into either 6 or 8 (plus inlet and after-filter) fractions for this phase of the study. The lowest stages (representing the smallest particles) were eliminated due to the size distributions of the dusts, where negligible particle concentrations in the smallest size ranges would have required prohibitive sampling times in order to collect at least 5 µg of crystalline silica. Particles that would have been collected on these stages were instead collected on the after-filter. Chamber concentrations of respirable dust and sampling times by stage are listed for each of the three dusts in Appendix A. Where allowed by time constraint and sufficient material, two samples per stage were collected. Sampling times varied by stage, according to the proportion of particle mass in the particular size range and the estimated percent of crystalline silica in the dust, such that crystalline silica mass in collected samples was expected to fall within the analytical range for the method (e.g. 5 µg – 500 µg). Typical sampling times ranged from 30 minutes to 12 hours.

Following sample collection, PVC filters and greased substrates were post-weighed to determine net mass collected on each sample. PVC filters were designated for analysis by an IR method (P7) or an XRD method (NIOSH 7500). Where two samples had been collected for a stage, one sample was analyzed by each method; where only one sample could be collected, that sample was analyzed by the optimum method for that range of particle size. P7 and NIOSH 7500 analysis was completed by RJ Lee Group, Inc., Monroeville, PA. Due to limited commercial availability of the filter medium required for P7 analysis (109), P7 samples for two of the dusts (Nevada, Alaska) were analyzed by Mine Safety and Health Administration (MSHA) analytical laboratories in Pittsburgh, Pennsylvania. Since both laboratories are accredited and follow the published P7 method, no significant bias is expected as a result of this change. From the net mass of the sample (determined gravimetrically) and the mass of crystalline silica in the sample (determined by IR or XRD), the proportion of crystalline silica was determined for each sample.

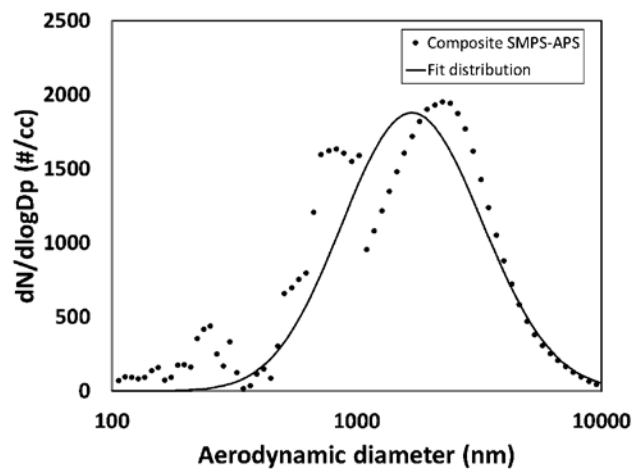
2.1.4 Construction of a Crystalline Silica Size Distribution

Particle size-related crystalline silica content was calculated for each MOUDI stage, as well as the inlet and after filter. For the inlet, Stage 1, and Stage 2, XRD data was used to determine percent crystalline silica (by mass); for Stages 3-8 and the after filter, IR data was used to determine percent crystalline silica. Percent crystalline silica for each stage was applied to raw gravimetric data that was used to determine size distributions of whole dust; the same inversion procedures was applied to the resultant quantities in order to obtain a size distribution of crystalline silica particles within the dust. To validate the unimodal or near-unimodal nature of the crystalline silica size distribution, data bins were also plotted as column charts.

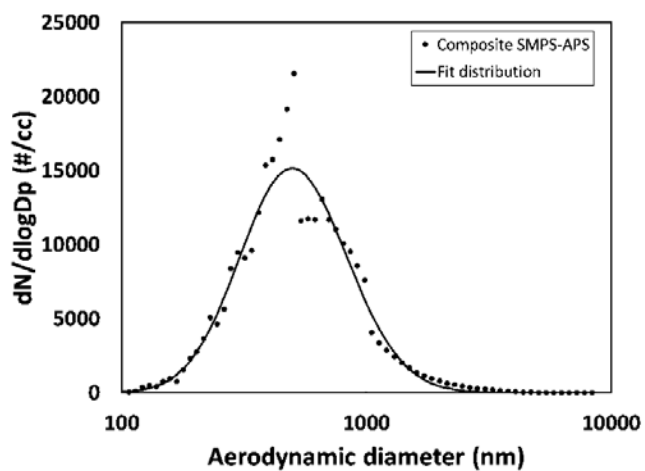
2.2 RESULTS

2.2.1 Size Distributions: APS + SMPS

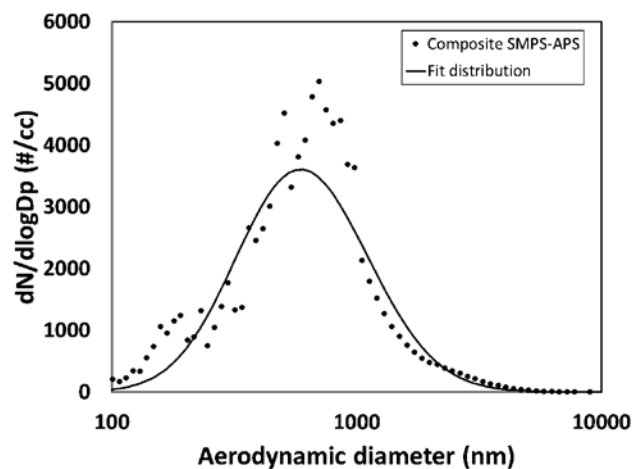
The particle number size distribution of each dust, as a function of particle aerodynamic diameter, are shown in Figure 6. Each plot displays the composite particle size distribution from the merged SMPS and APS data, as well as the proposed fit distribution. For all three dusts, a unimodal distribution was selected as the best fit to the composite data. The count median diameter (CMD) and geometric standard deviation (GSD) of each dust were determined from the fit distributions. The CMDs were determined to be 1680 nm (GSD=1.96), 498 nm (GSD=1.72), and 590 nm (GSD=1.94), for the dust from Alaska, Nevada and South Africa, respectively.



Alaska



Nevada



South Africa

Figure 6 Particle number size distributions from merged SMPS-APS data

2.2.2 Size Distributions (Total Dust, Crystalline Silica): Gravimetric Inversion

The particle size distribution of each dust and the crystalline silica component thereof was constructed, based on mass, from inversion of gravimetric data collected with the MOUDI. The gravimetric inversion method is based upon the methods described by O'Shaughnessy and Raabe (108) and Roberts et al. (106). Figure 7 (top) shows the particle mass size distributions of the three total dusts generated by inversion of gravimetric data from the MOUDI; as the particle mass size distribution of the Nevada and South Africa dusts are quite similar, these two plots overlap one another. Figure 7 (bottom) shows the particle mass size distribution of the crystalline silica component of the three dusts, generated by applying the size-related proportional crystalline silica content to gravimetric data from the MOUDI and subsequent inversion of these values. The size distribution of each dust is normalized to the largest fraction, and thus reaches unity. Figure 8 shows the respirable particle mass size distribution of total dust and crystalline silica, generated by applying the respirable particle convention (79) to Figure 7 (top) and (bottom), respectively. By applying the respirable convention, large particles that are not relevant to worker exposure are no longer considered; as these plots represent only a specific fraction of the size distributions shown in Figure 7, they do not reach unity. MMD and GSD for each size distribution are summarized in Table 2.

For all three dusts, the MMD was determined to be larger for crystalline silica than for the total dust. This difference was fairly small for the dusts from Alaska and South Africa, but was quite pronounced for the dust from Nevada, where the MMD of crystalline silica particles was 2.76 μm larger than for dust particles overall. Additionally, the GSD of the three crystalline silica size distributions was smaller than the overall distributions, indicating a more narrow range of particle sizes for crystalline silica than for the overall dust.

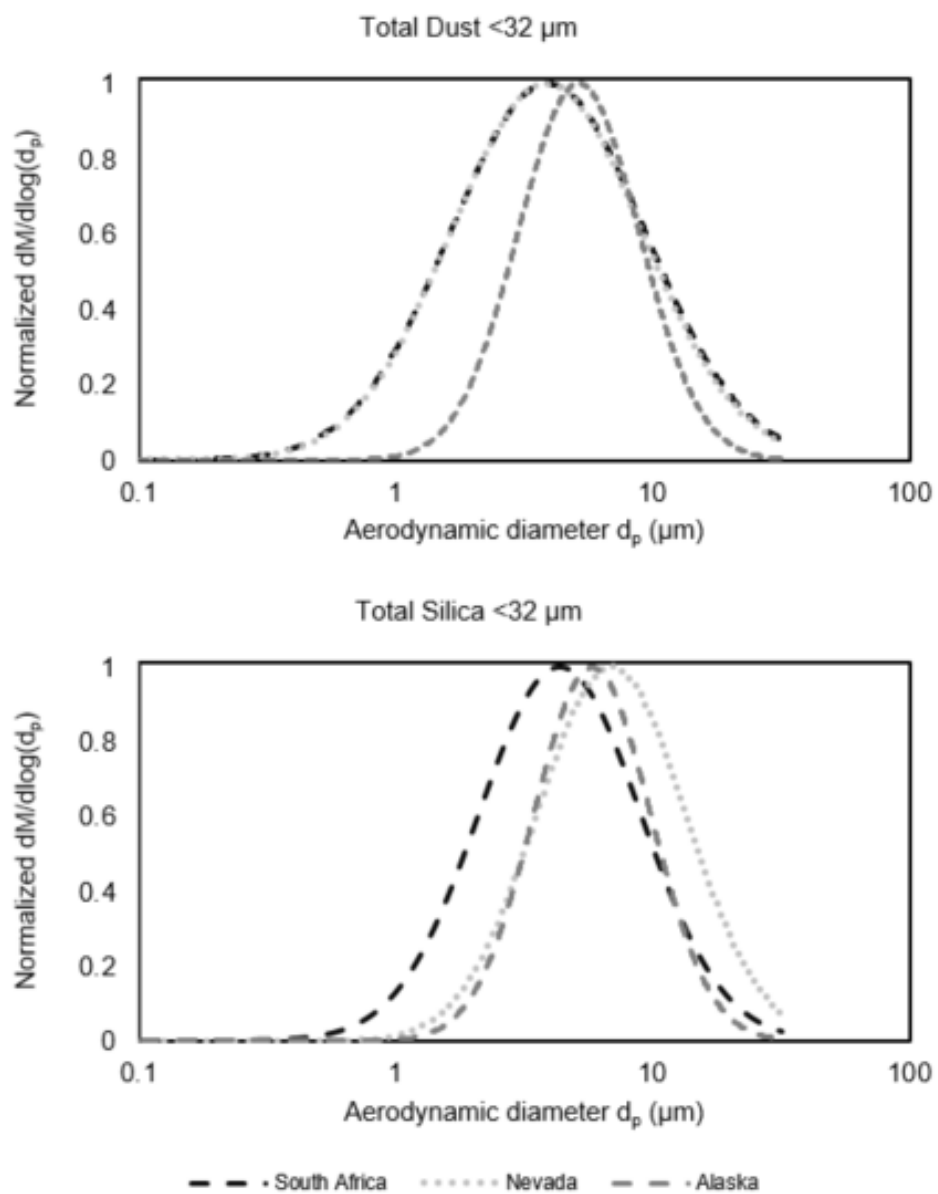
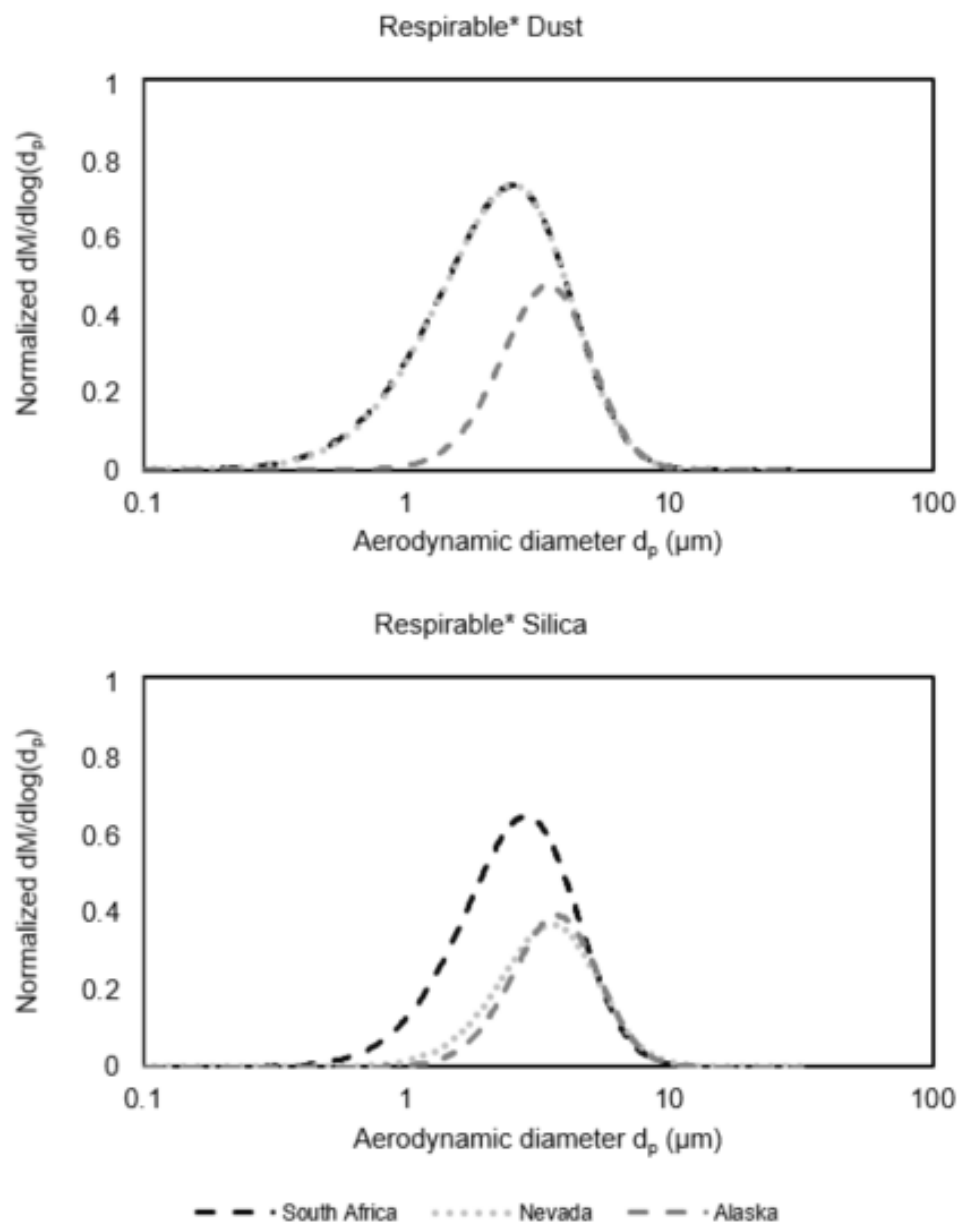


Figure 7 Particle mass size distributions: particles <32 μm



*respirable fraction calculated using the respirable convention described in Chapter 1 (79)

Figure 8 Particle mass size distributions: respirable fraction

Table 2 MMD and GSD of the size distributions of total dust and total crystalline silica

| Dust | | Stages | MMD | GSD |
|---------------|--------------|--------|--------|------|
| Alaska: | total dust | 6 | 5.1656 | 1.72 |
| | total silica | 6 | 5.8324 | 1.69 |
| Nevada: | total dust | 6 | 3.8845 | 2.36 |
| | total silica | 6 | 6.6486 | 2.09 |
| South Africa: | total dust | 8 | 3.9206 | 2.39 |
| | total silica | 8 | 4.3609 | 2.07 |

2.2.3 Characterization of Particle Size-related Crystalline Silica Content

Although it is useful to compare the size distributions of crystalline silica and the overall dust, such comparisons do not directly provide information about the relative amount of crystalline silica associated with a particular particle size in a specific dust.

Using the kernel functions for each stage of the MOUDI – which incorporate the collection efficiency function of a stage as well as a function approximating particle losses to the interior wall surfaces of the impactor – and the proportional crystalline silica content determined for each stage of the MOUDI (shown in Table 3), a continuous curve was determined for the proportional crystalline silica content of each particle size of the dust, shown along with the size distribution of each total dust in

Figure 9. It is necessary to consider that this curve depicts proportional crystalline silica content *by mass* within each particle size range: determination of proportional crystalline silica content *by particle count* within particle size ranges is beyond the capabilities of the current methods. Such determinations are possible with more sophisticated methods and is discussed further in Chapter 4.

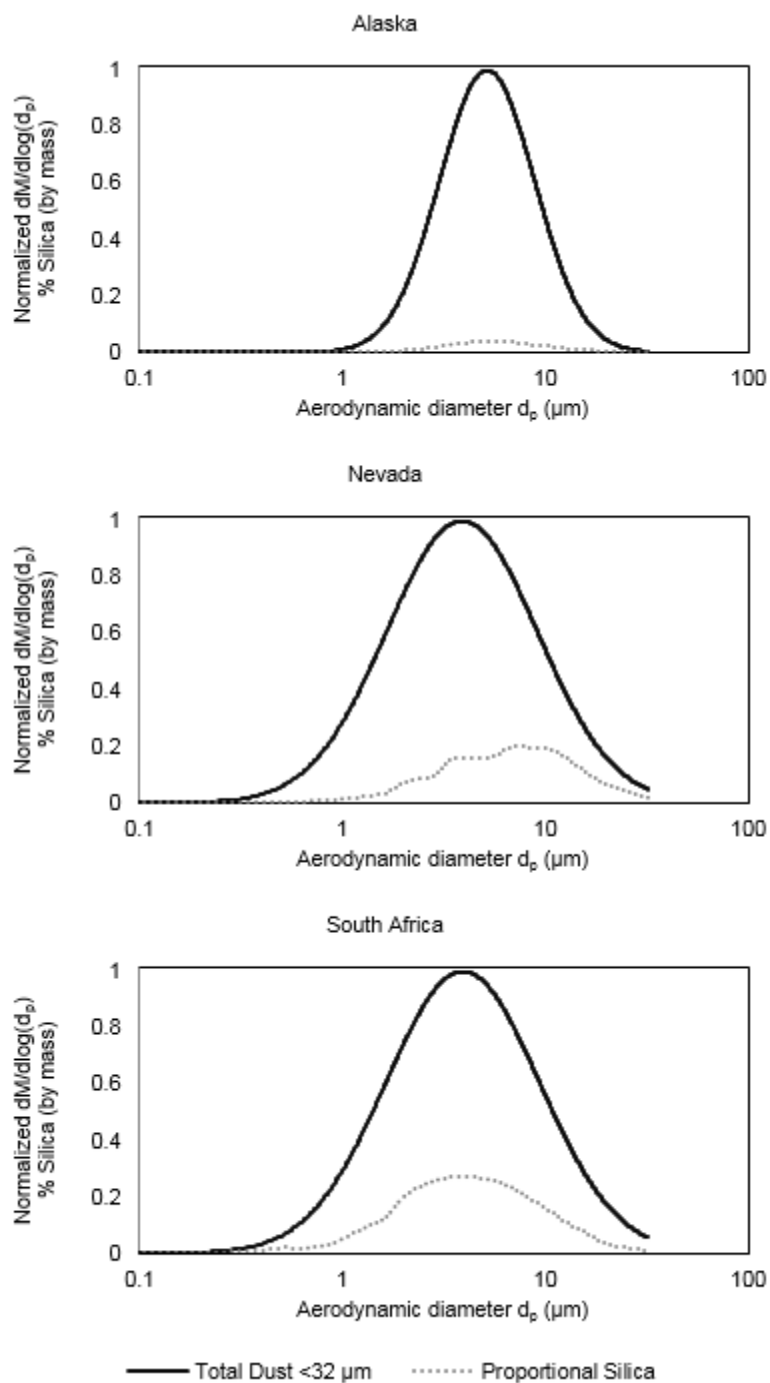


Figure 9 Proportional crystalline silica content, by particle size

The IR and XRD data used to construct the plots in Figures 7-9 is shown below in Table

3. The crystalline silica masses shown represent the composite of quantification by XRD (for Inlet, Stage 1, and Stage 2 samples) and IR (for Stages 3-8 and final samples).

Table 3 Proportional crystalline silica content (%) from IR and XRD data

| MOUDI Stage | d ₅₀ | Alaska | Nevada | South Africa |
|-------------|-----------------|--------|--------|--------------|
| Inlet | 18 µm | 8.17 | 41.25 | 17.80 |
| Stage 1 | 10 µm | 5.31 | 42.86 | 27.66 |
| Stage 2 | 5.6 µm | 3.99 | 26.58 | 28.70 |
| Stage 3 | 3.2 µm | 3.63 | 15.71 | 27.37 |
| Stage 4 | 1.8 µm | 2.91 | 9.88 | 27.54 |
| Stage 5 | 1.0 µm | 1.37 | 5.00 | 20.20 |
| Stage 6 | 560 nm | 0.72 | 4.26 | 13.87 |
| Stage 7 | 320 nm | - | - | 30.83 |
| Stage 8 | 180 nm | - | - | 46.84 |
| Final | - | 0.98 | 4.07 | 11.30 |

2.3 DISCUSSION

With respect to both count and mass distribution, the dusts from Nevada and South Africa are similar to one another and have compositions that include appreciable amounts of small particles, while the dust from Alaska is composed of somewhat larger particles. The GSDs of both the particle count and particle mass size distributions of dust from Nevada and South Africa are also quite similar; they indicate that a broader range of particle sizes comprises these two dusts than the dust from Alaska. One explanation for this is that the crystalline silica component of the dust represents particles produced by one type of source: the fracturing of rock. Alternatively, the total dust contains particles produced by a variety of sources, including emissions from vehicles and mining equipment, re-suspended soil particles, and particles from long-range atmospheric transport. The size distributions of particles from these sources are likely to be somewhat smaller

(in the case of vehicle emissions) or somewhat larger (as for re-suspended particles) than from the fracture of rock, thus the broader size distribution of total dust relative to crystalline silica.

NIOSH has previously documented high variability in the overall crystalline silica content of dust samples collected from mining operations (30), and these findings are in agreement with such variability. Within distinct size fractions of a particular dust, the proportional crystalline silica content was also quite variable. Fractions of each dust with the least and greatest proportion of crystalline silica differed by a factor of approximately four for the dust from Nevada, and by a factor of greater than ten for the dusts from Alaska and from South Africa. The mass distribution of crystalline silica for all three of the dusts was similar to the mass distribution of the corresponding total dust, and the MMD for crystalline silica was slightly larger than the MMD for the corresponding dust. While it is not possible to assess the statistical significance of this difference using the current data set, it is telling that the same trend is apparent in all three of the dusts. Additionally, the same trend is observed for a dust of fairly low crystalline silica content (5%) as well as for a dust of moderately high crystalline silica content (20%), which suggests that the trend is not dependent on the relative abundance of crystalline silica within the dust.

That the size distribution of crystalline silica generally trends towards larger particles and is narrow than the distribution of the overall dust is encouraging for exposure controls used within these three mines. The effectiveness of a control technology is typically evaluated based on reductions in total respirable dust concentration, as respirable dust can be assessed in a straightforward manner via gravimetric analysis. These findings indicate that a control technology that is effective in reducing respirable dust concentrations should, in theory, be as effective in reducing concentrations of crystalline silica particles. However, all three dusts and their crystalline silica components contain substantial quantities of submicron particles, which have longer settling times and are capable of deeper penetration into the lungs, relative to particles larger than one micron. Any control technology used to reduced overall respirable dust concentrations should be evaluated for its effectiveness in reducing concentrations of submicron particles as well.

From a monitoring perspective, it is also encouraging that, for two of the three dusts characterized, the size distribution of crystalline silica was extremely comparable to the size distribution of the total dusts. It has been previously documented that appreciable differences between the size distribution of a sample dust and the size distribution of the crystalline silica reference material used for calibration of the analytical method can result in a significant bias in the quantification of crystalline silica in samples (91). While it is not common practice to assess the size distribution of either a dust sample or the crystalline silica component thereof, it is more likely that the size distribution of the whole dust would be known or could be estimated, and substantially less likely that the size distribution of crystalline silica would be. It seems that the size distribution of the total dust may, in some instances, be an appropriate proxy for the size distribution of crystalline silica. However, it is necessary to characterize the size distribution of many other types of dust, and the crystalline silica component of each, before such a generalization could be made with confidence; it should also be determined for which types of dusts such an assumption would *not* be appropriate. In this study, the dust from Nevada showed a size distribution of the crystalline silica component that differed more appreciably from the size distribution of the dust. It is possible that this is common within that geographic region, or perhaps with the technologies and equipment used in that particular mine. Further studies can shed additional light and data upon such speculations.

In summary, this study has demonstrated that crystalline silica is not present in uniform proportion throughout the entire size range of a mine dust, and while the size distribution of crystalline silica is sometimes very similar to the size distribution of the dust, at other times it differs more appreciably. This is a strong demonstration that further study is needed, both to characterize the size distributions of dust produced in mines, as well as to characterize the crystalline silica content of those dusts. This work presents a replicable method by which to do so.

3.0 COMPARISON OF PARTICLE SIZE-RELATED ANALYSIS OF CRYSTALLINE SILICA BY IR AND XRD METHODS

Infrared (IR) and X-ray diffraction (XRD) methods are both widely utilized for quantifying crystalline silica in respirable dust samples. Outside of the United States, XRD is the predominant method used for analysis of crystalline silica in dust samples from all types of mines (75), while in the United States, each of the two methods is utilized in specific mining sectors. For largely historical reasons, the IR method is used in the coal mining industry in the form of the Mine Safety and Health Administration (MSHA) P7 method (67) (analogous to NIOSH method 7603 (57)), while XRD (MSHA P2 (70), analogous to NIOSH method 7500 (56)) is used in the metal/non-metal mining industry. Both methods have comparable limits of detection (5-10 µg per sample) (56, 57), and are considered to be approximately equivalent to one another for quantification of crystalline silica in respirable dust (68, 92, 94). However, these validations have only assessed integrated respirable samples of crystalline silica standard materials; as the accuracy of each method can be affected by the size of the particles present in the sample, it is prudent to verify the inter-method reliability for specific particle sizes of real-world occupational dust samples.

Given variability in the size distributions of mine dusts, as well as in the size distribution of the crystalline silica component of those dusts, it is essential to evaluate how particle size can contribute to discrepancies between the IR and XRD methods, and how such discrepancies are likely to affect exposure assessments for respirable crystalline silica. Understanding such variability and the discrepancies that can result is essential to efforts towards improvement of occupational monitoring for crystalline silica exposure.

3.1 METHODS

The selection of dusts and collection of samples was completed as described in Chapter 2. Briefly, three previously selected and prepared gold mine dusts from Alaska, Nevada, and South Africa were each aerosolized in a calm-air chamber at 25°C and 40%RH, using a fluidized bed dust generator.

3.1.1 Collection of Size-fractionated Samples

Size-segregation of particles was completed using the Microorifice Uniform Deposit Impactor (MOUDI). Samples for crystalline silica analysis were collected on pre-weighed 47 mm PVC filters, which were alternated with pre-weighed 47 mm greased foil substrates to limit particle bounce, as described in Chapter 2. Duplicate samples were collected for each dust and size fraction and analyzed by both IR and XRD methods, so that the results of the two methods could be compared for all particle size ranges. Following sample collection, samples were post-weighed to determine the net mass of dust collected, and were sent to analytical laboratories for crystalline silica quantification via P7 and NIOSH 7500. While the ideal method of conducting such a comparison is to collect simultaneous samples of exactly the same mass, this was not possible to accomplish using the MOUDI; sequential samples were collected, keeping chamber and sampler conditions constant so that overall sample mass would be comparable. Sampling times were varied according to dust and size fraction, as described in Chapter 2 and summarized in Appendix A.

Additionally, samples of respirable dust were collected for each type of dust using the size-selective Dorr-Oliver cyclone, which is used to collect samples for respirable dust monitoring in both coal and metal/non-metal mines. The cyclones were operated at a flow rate of 1.7 liters per minute (lpm), and samples were collected on pre-weighed 37 mm PVC filters.

3.1.2 Comparison of IR and XRD Methods

Using data from the gravimetric analysis of filters and crystalline silica quantification from the IR and XRD methods, percent crystalline silica by mass was determined for each sample. Data was then organized according to origin of dust (Alaska, Nevada, South Africa), particle size range (Inlet through Stage 8, see Table 1), and analytical method (IR, XRD) for the quantification of crystalline silica. To facilitate comparison between IR and XRD methods, the proportional crystalline silica content of each sample was determined from gravimetric data and crystalline silica quantification. This was necessary because MOUDI sample pairs were collected sequentially rather than simultaneously, and the total mass collected was similar but not identical for the two samples. Cyclone sample pairs were collected simultaneously but were treated the same as MOUDI samples, for consistency.

For each pair of particle size-fractionated samples, the ratio of the IR-determined proportional crystalline silica content and the XRD-determined proportional crystalline silica content was calculated. The same calculations were performed for respirable dust samples collected via cyclone.

3.2 RESULTS

To facilitate comparison between methods, results are presented in Table 4 as mass percent crystalline silica determined by either method, for each size fraction of the three dusts. Two samples (both analyzed by XRD) yielded crystalline silica results below the limit of detection (5 μg); a value of one half the limit of detection was used to determine the approximate mass percent crystalline silica content in those samples.

Figure 10 shows the ratio of crystalline silica results from the two methods. To enable comparison between all three dusts, the ratios shown for the <0.56 μm fraction of the South Africa dust represents the sum of crystalline silica quantified in the three smallest particle fractions (0.32, 0.18, <0.18 μm) by the two methods, divided by the sum of the total dust collected for the same three samples. This was necessary because the 0.32 μm and 0.18 μm fractions were not collected separately for the Alaska and Nevada dusts, but instead were collected as part of the <0.18 μm fraction.

Table 4 Crystalline silica composition (mass %) by IR and XRD

| | Alaska | | Nevada | | South Africa | |
|----------------------------|--------|------|--------|-------|--------------|--------------------|
| d_{50} (μm) | IR | XRD | IR | XRD | IR | XRD |
| 18 | 1.05 | 8.17 | 6.67 | 41.25 | 11.16 | 17.80 |
| 9.9 | 2.31 | 5.31 | 14.54 | 42.86 | 18.18 | 27.66 |
| 6.2 | 3.44 | 3.99 | 19.16 | 26.58 | 20.29 | 28.70 |
| 3.1 | 3.63 | 5.43 | 15.71 | 22.13 | 27.37 | 20.48 |
| 1.8 | 2.91 | 4.75 | 9.88 | 13.72 | 27.54 | 25.96 |
| 1.00 | 1.37 | 3.71 | 5.00 | 6.77 | 20.20 | 15.84 |
| 0.56 | 0.72 | 2.54 | 4.26 | 4.60 | 13.87 | 9.57 |
| 0.32 | - | - | - | - | 30.83 | 9.68 |
| 0.18 | - | - | - | - | 46.84 | 6.10% [‡] |
| <0.56*, <0.18 [§] | 0.98 | 1.79 | 4.07 | 3.50 | 11.30 | 8.93% [‡] |
| <i>respirable</i> | 2.99 | 4.49 | 12.00 | 15.55 | 16.45 | 20.48 |

* For the Nevada, Alaska dusts

[§] For the South Africa dust

[‡] Results below XRD method LOD (5 μg); crystalline silica percentage calculated using 0.5*LOD

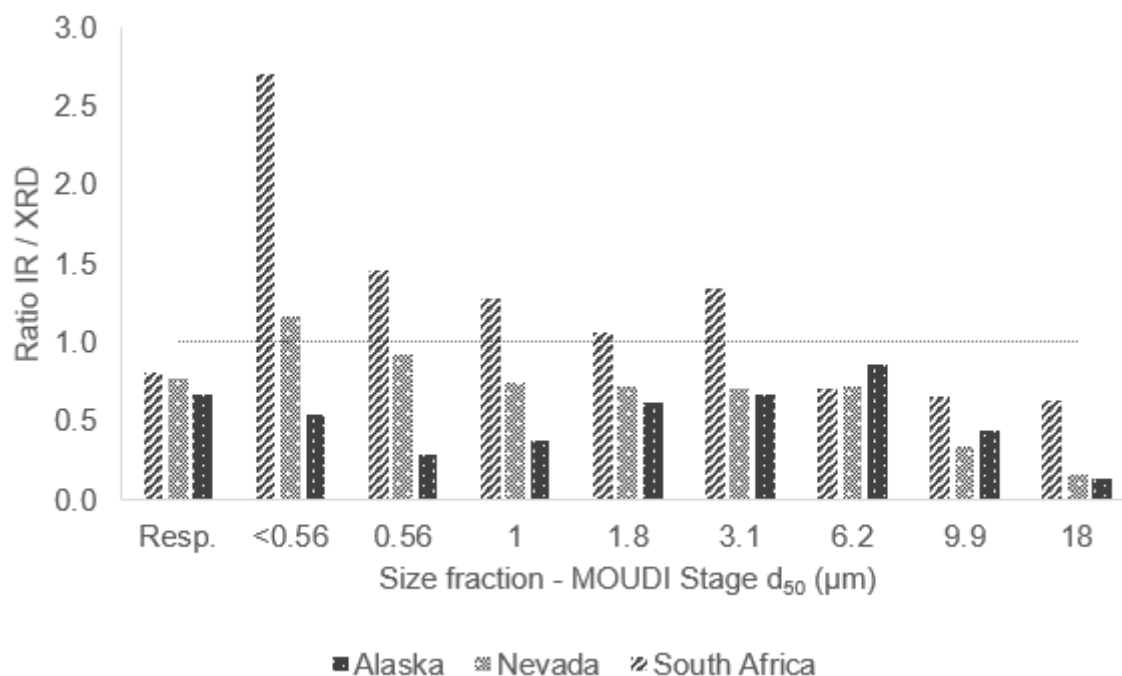


Figure 10 Ratio of IR to XRD quantification of crystalline silica, by particle size

For all three dusts, considerable differences were observed between the proportion of crystalline silica determined by the IR and XRD methods of analysis. Generally, these differences were the most pronounced for the largest particle size fractions (9.9 μm , 18 μm and larger) and for the smallest particle size fractions (<0.5 μm , 0.56 μm). Differences between the two methods were also observed in the mid-particle size ranges, as well as for samples of respirable dust, but these differences were more moderate. For most samples, the XRD analysis determined a greater proportion of crystalline silica than the IR method, though the IR method quantified a greater proportion of crystalline silica in 7 (of 11) fractions of the South Africa dust.

3.3 DISCUSSION

Differences between the IR and XRD methods were most pronounced in the smallest and largest particle size fractions. This observation was as expected due to the inverse relationship between the impacts of particle size effects in IR analysis versus those in XRD analysis. This is also supported by good agreement between the two methods (for all three dusts) for crystalline silica in respirable dust samples, which contain particles ranging from the smallest fraction to the largest fraction but are composed largely of particles in the mid-range size fractions (approximately 3-6 μm).

It is interesting that the XRD method determined a greater quantity of crystalline silica in nearly all samples of the Alaska and Nevada dusts (with the exception of the $<0.56 \mu\text{m}$ fraction of the Nevada dust). If particle size effects alone are considered, the XRD method would be expected to determine a greater quantity of crystalline silica (than the IR method) in the 6.2 μm , 9.9 μm , and 18 μm fractions, but would be expected to determine a lesser quantity in the $<0.56 \mu\text{m}$ and 1.0 μm samples. The discrepancy observed between the expected trend and the results for these samples indicates that other factors, in addition to particle size effects, impact the quantity of crystalline silica measured in these samples. The most likely explanation is that other minerals present in the samples contribute to the intensity of the absorption peak at 800 cm^{-1} that is used to quantify crystalline silica in the IR method. These contributions may be positive (increasing the apparent amount of crystalline silica in the sample) or negative (decreasing the apparent amount of crystalline silica in the sample), depending on the particular mineral. The XRD method is susceptible to positive and negative interference from mineral confounders as well, although the two methods may be affected differently by the same mineral.

More detailed study of the dust compositions, would be necessary to completely disentangle the effects of interfering minerals coupled with effects of particle size. Such an examination would likely include a thorough characterization of the minerals that compose each

dust. For each mineral identified, the effect of particle size on the quantification of that mineral by itself (for both the IR and XRD methods) should then be evaluated. Evaluation of the particle-size related effects when crystalline silica and only one other mineral are combined would also be useful. It would be helpful to reach an understanding of how such effects change when the distribution of crystalline silica is 1) larger than, 2) smaller than, or 3) approximately equivalent to the distribution of the interfering mineral. This degree of characterization would involve an enormous effort and would be quite time consuming, making it impractical to attempt to parse these effects for specific individual dusts. However, it would be more feasible to determine common dust compositions (for example, crystalline silica, calcite, and dolomite; or crystalline silica, feldspar, and muscovite) and to then undertake detailed characterization of these dust types. Mathematical modeling, such as the partial least squares method (110-112), has been previously used to understand and correct for the effects of confounding minerals on the IR spectrum on crystalline silica; such a method would also be useful here to understand the effects of mineralogy and particle size on both the IR and XRD methods of analysis.

Due to the time and materials necessary to collect a single sample of a specific particle size range, multiple samples were not collected, which would have enabled a statistical analysis of the significance of differences between the two methods. Again, the continued evaluation of IR and XRD analysis for crystalline silica specific to particle size would eventually yield enough aggregate data for such a statistical analysis to be completed.

Formal evaluation of the magnitude of analytical discrepancy (between the IR and XRD methods) that may be observed in real-world samples is beyond the scope of the study, but it should be noted that, assuming the discrepancy is uniform across all size fractions, differences in quantity of crystalline silica determined in the mid-size ranges (between approximately 1 and 6 μm) of particles are likely to have the most impact, because these particles comprise the majority of the size distribution (by mass). Conversely, even large differences in quantification of crystalline silica in the smallest particle size fractions are unlikely to have an appreciable impact

when measurements are made on the basis of mass, because these particles typically (though not necessarily) have a negligible impact on the total mass of a respirable dust sample, despite possibly contributing significantly in terms of particle number. However, the mid-range particle sizes are generally where the two methods show the most agreement. Presumably, this is due to the opposing effects of particle size with the two methods: accuracy of the IR method is poor for large particles and improves as particle size decreases, and accuracy of the XRD method is poor for small particles and improves as particle size increases (within the respirable size range), and so results for both methods are fairly consistent in this region of overlap.

It should be noted that the magnitude of discrepancy between the two methods for a given size fraction is not constant among the three dusts. A likely explanation for this is that each dust has a distinct mineral composition (see Table 5 in Chapter 4), and the other minerals present may also affect the mass of crystalline silica that is quantified in each sample. As discussed previously, the IR and XRD methods are both susceptible to mineral interference, and the magnitude of such effects may vary according to the method, to the particular mineral, and to the size of particles in the sample (both crystalline silica and non-silica particles). While this matter complicates the determination of crystalline silica, it illustrates the point that the size distribution of a particular dust, with regard to the crystalline silica component of that dust as well as with regard to the total dust (which includes the other mineral components of the dust), contributes to the accuracy of crystalline silica quantification. Thus, an understanding of the size distribution is important to the understanding of the accuracy and limitations of the exposure assessment. Even if current methods and corrections cannot fully account for the discrepancy in order to provide a completely accurate quantification of crystalline silica, it is important to understand whether the qualities of a particular dust may lead to an overestimation of crystalline silica or to an underestimation of crystalline silica; only then can appropriately conservative precautions be taken. When there is doubt, the higher estimation of crystalline silica content in a sample should always be used for

exposure monitoring purposes, in order to protect workers from unacceptably high crystalline silica exposures.

4.0 CHARACTERIZATION OF PARTICLE SIZE-RELATED COMPOSITION OF GOLD MINE DUST

In dusts generated in mines, pure crystalline silica is rarely present on its own. Rather, crystalline silica exists within a matrix of other materials such as vehicle exhaust, smoke, and dusts from other mineral components of solid rock. This mineral material is particularly relevant to exposure assessments for crystalline silica, as numerous minerals – including other silicates and aluminosilicates which occur commonly with crystalline silica – can contribute to analytical interference that impacts the accuracy of monitoring methods. Typically, if the presence of such interfering materials are known, and if the nature of the interference is sufficiently well-characterized (i.e. the magnitude of the bias and whether it is positive or negative), it is possible to apply correction factors in order to reach a more accurate determination of crystalline silica. However, given the known effects of particle size on the signal intensity of both IR and XRD methods, it would also be useful to have an approximate knowledge of the particle size distributions of the non-silica minerals that occur in a particular mine dust, to compare to the size distribution of crystalline silica within that same dust.

Additionally, toxicological evidence suggests that contamination on the surface of crystalline silica particles by metallic species such as iron may impact the inflammatory effect of crystalline silica particles by promoting release of free radicals (36, 40, 41, 113). To that effect, it would be beneficial to have a more thorough understanding of how crystalline silica particles exist within a mine dust: are crystalline silica particles generally standalone, not associated with other chemical species; do they exist as components of multi-mineral aggregates; or, are they associated with metallic species?

One method frequently employed (114-117) to characterize single particles is scanning electron microscopy with energy dispersive spectroscopy (SEM-EDS). While the electron

microscopy portion of the analysis constructs an “image” of the particle that can be used to qualitatively and quantitatively assess morphological characteristics of the particles, the energy dispersive component uses X-ray fluorescence to characterize the elemental composition of the particle. These methods have traditionally relied on time-consuming manual analysis by an experienced spectroscopist, thus limiting the number of particles that could be analyzed in a practical time frame. More recently, automated computer-controlled methods have been developed (118-120), capable of analyzing in a few minutes what would have previously taken several hours of human analysis. By facilitating analysis of a greater number of particles, automated analysis produces a large data set that offers a more comprehensive representation of the sample.

4.1 METHODS

The selection of dusts and the collection of samples was completed as described in Chapter 2. The three previously selected and prepared gold mine dusts were again aerosolized in a calm-air chamber at 25°C and 40% RH, using a fluidized bed dust generator. Size-segregation of particles was completed using the MOUDI.

Respirable samples of each dust were also collected using Dorr-Oliver cyclones operated at 1.7 lpm. Respirable dust samples were analyzed by X-ray diffraction (XRD) using the Rietveld refinement (121) to ascertain the specific mineral composition of the respirable fraction of each dust.

4.1.1 Collection of Size-fractionated Samples for Single Particle Analysis

Size-fractionated samples were collected one stage at a time; greased foil substrates were used on all non-sample stages to minimize the possibility of positive bias via particle bounce. Samples were collected from all eleven MOUDI size-fractions, unlike in the analysis of Chapters 2 and 3, as SEM-EDS is not mass dependent and rather focuses on individual particles, such that sufficient sample loadings could be achieved in a reasonable period of time, even for those dusts which contained very little material in the ultrafine size range. Respirable dust concentration in the aerosol chamber was kept low ($0.5 \text{ mg}\cdot\text{m}^{-3}$) in order to maintain better control of particle loading on collected samples; sampling time was varied by stage depending on the relative particle concentration of each size fraction. For the six size fractions with the largest particles (collected on the Inlet stage through Stage 5), samples were collected on 47 mm polycarbonate filters ($0.2 \text{ }\mu\text{m}$ pore, Whatman, Pittsburgh, PA). For the five size fractions with the smallest particles (collected on Stages 6 through 100, samples were collected on Formvar film 200 mesh copper TEM grids (Electron Microscopy Sciences, Hatfield, PA) to facilitate analysis of particles smaller than $1 \text{ }\mu\text{m}$ (122). Due to the small size (approximately 3 mm diameter) of the TEM grids and the difficulty in predicting particle deposition, 5 grids were arranged on the stage as shown in Figure 11, in order to maximize the probability of collecting a sample with optimal particle density for microscopy analysis. Grids were lightly affixed to the stage using a spray adhesive diluted in isopropanol; this achieved a slightly tacky surface on the sampling stage, to which the grid could adhere (to prevent loss in the air flow during sampling) without becoming permanently attached to the stage. Sampling times for SEM-EDS sample collection are shown in Appendix A.

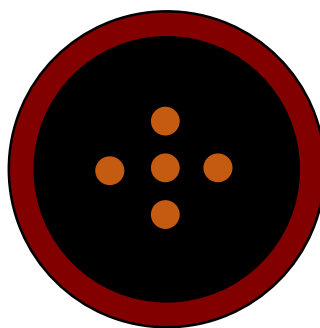


Figure 11 Arrangement of TEM grids on MOUDI stage

4.1.2 Size-fractionated Single Particle Analysis via SEM-EDS

Using a computer-controlled SEM-EDS method, up to 1,500 particles per size fraction were analyzed in order to yield approximately 200 silicon-containing particles per sample. A prescribed set of rules was used to classify particles according to their elemental composition, as determined by EDS X-ray counts. Briefly, the X-ray spectrum for each particle was compared to each rule sequentially to determine if the conditions of the rule were met (“TRUE” versus “FALSE”). If the conditions of a rule were met (“TRUE”) by a particle, the particle was assigned to the particle class defined by that rule; if the conditions were not met (“FALSE”), the conditions of the next rule were evaluated, and so on until the particle was successfully assigned to a class. This procedure was completed for all particles. Examples of particle classification rules are included in Appendix C.

To evaluate single-particle data, each MOUDI stage was considered separately for each dust. The composition as number percent and mass percent of total particles was determined for each particle class. Based on number percent and mass percent data over all size fractions, the four most abundant particle classes were identified for each dust.

4.2 RESULTS

XRD results of mineral composition of each respirable dust are shown in Table 5. In addition to crystalline silica (in the form of quartz), the respirable fractions of the three dusts each contain five to seven mineral species, including silicate and aluminosilicate minerals (chlorite, feldspar, muscovite, and pyrophyllite). Importantly, none of the dusts were found to contain amorphous material, thus all silica present can be assumed to be crystalline.

Table 5 Mass percent mineral composition of respirable dust

| | | South Africa | Nevada | Alaska |
|--|--|--------------|-------------|------------|
| | SiO₂ Quartz | 36.9 | 19.3 | 8.9 |
| | KAl ₃ (SO ₄) ₂ (OH) ₆ Alunite | - | 55.2 | - |
| | CaCO ₃ Calcite | - | - | 17.9 |
| | (Mg,Fe) ₃ (Si,Al) ₄ O ₁₀ (OH) ₂ ·(Mg,Fe) ₃ (OH) ₆ Chlorite | 8.2 | 8.4 | - |
| | CaMg(CO ₃) ₂ Dolomite | - | - | 51 |
| | KAlSi ₃ O ₃ K-Feldspar | 4.2 | - | - |
| | CaSO ₄ ·2H ₂ O Gypsum | 0.9 | 3.5 | 2.5 |
| | KFe ₃ (OH) ₆ (SO ₄) ₂ Jarosite | - | 7.8 | - |
| | KAl ₃ Si ₃ O ₁₀ (OH) ₂ Muscovite | 23.6 | 5.7 | 5.7 |
| | FeS ₂ Pyrite | - | - | 6.6 |
| | Al ₂ Si ₄ O ₁₀ (OH) ₂ Pyrophyllite | 26.3 | - | - |
| | (Zn,Fe)S Sphalerite | - | - | 2.4 |
| | (Zn,Fe)S Wurtzite | - | - | 0.8 |

For the nine samples collected and analyzed via electron microscopy for each dust, a total of approximately 10,000 particles per dust was analyzed. The total number of particles evaluated for each dust and size fraction are shown below in Table 6. Grid samples of the Alaska and South Africa dust contained appreciable numbers of salt particles, mostly composed of sodium chloride. The origin of these particles is not known definitively but they may have been generated in the sampling process; as they are not salient to the original objectives of this analysis, they were rejected from the particle analysis and are not included in the total particle counts of Table 6.

Additionally, although samples were collected for the Stages 9 and 10 size ranges, analysis was complicated by extremely light particle loadings; these size ranges are excluded from the following results.

Table 6 Total particles analyzed by CCSEM

| d_{50} (μm) | Alaska | Nevada | South Africa |
|----------------------------|--------|--------|--------------|
| 0.18 | 988 | 704 | 684 |
| 0.32 | 1751 | 800 | 1182 |
| 0.56 | 744 | 664 | 566 |
| 1.0 | 1423 | 1441 | 1958 |
| 1.8 | 1371 | 1486 | 1826 |
| 3.1 | 1243 | 1682 | 1186 |
| 6.2 | 841 | 1360 | 558 |
| 9.9 | 565 | 1362 | 675 |
| 18 | 799 | 1438 | 1398 |
| Total | 9725 | 10937 | 10033 |

Tables 7-9 show the relative abundance, by count and by weight, of all particle classes determined for the three dusts (n= 24 particle classes), over nine particle size ranges; not all particle classes are observed in all three dusts. The Si-rich particle class was observed in each size range of the three dusts. Of all the minerals detected by XRD in the three dusts, crystalline silica is the only mineral containing silicon alone (oxygen is not included in the EDS analysis); therefore, the Si-rich class represents standalone crystalline silica particles. Particle classes containing silicon and/or aluminum (e.g. Si-Al-K, Si-Al-Ca, Si-Al-Mg, Si-Al-Fe, Si-Al-Na, Si-Al-S, Si-Al, and Si-Al (mixed)) are abundant across the size fractions of each of the three dusts. The Si-Al (mixed) class includes particles that do not fall strictly into one of the Si-Al-___ particle classes, but are nonetheless similar to these particles types (i.e. such a particle may contain silicon, aluminum, iron, and magnesium). Particles in the Miscellaneous and C-rich classes tend to be abundant in most size fractions of the three dusts; however, since these classes are less likely to describe specific mineral types than other particle classes – i.e. the Miscellaneous class contains all particles which were not rejected but do not adhere to any of the prescribed rule; the

C-rich class may contain carbonaceous minerals but may also contain carbonaceous non-mineral material, or the strong contribution of carbon may be an artifact from the substrate materials, which contain carbon (this effect is stronger in smaller particles due to increased penetration of X-rays) – they are excluded from the remainder of the analysis.

Table 7 Particle class relative abundance (% count and weight): Alaska

| Stage d ₅₀ (μm) | 0.18 | | 0.32 | | 0.56 | | 1.0 | | 1.8 | | 3.1 | | 6.2 | | 9.9 | | 18 | |
|----------------------------|------------|------------|------------|------------|------------|------------|------------|------------|------------|------------|------------|------------|------------|------------|-------------|------------|-------------|------------|
| Particle Class | C | W | C | W | C | W | C | W | C | W | C | W | C | W | C | W | C | W |
| Si-rich | 1.1 | 0.6 | 1.4 | 0.7 | 1.6 | 0.1 | 2.6 | 1.1 | 4.2 | 2.4 | 3.7 | 2.9 | 3.6 | 1.8 | 16.6 | 7.1 | 16.4 | 5.9 |
| Si-Al-K | 1.4 | 6.1 | 5.3 | 14.8 | 12.6 | 24.4 | 7.4 | 18.7 | 7.7 | 26.5 | 8.3 | 27.4 | 7.1 | 20.4 | 13.8 | 29.8 | 19.9 | 26.3 |
| Si-Al-Ca | 0.4 | 1.3 | 1.1 | 2.2 | 0.4 | 0.3 | 0.1 | 0.6 | 0.0 | 0.0 | 0.1 | 0.1 | 0.0 | 0.0 | 0.4 | 0.8 | 0.3 | 0.3 |
| Si-Al-Mg | 0.6 | 4.8 | 2.3 | 5.4 | 1.5 | 2.2 | 0.4 | 0.5 | 0.1 | 0.1 | 0.1 | 0.6 | 0.0 | 0.0 | 0.7 | 2.0 | 1.0 | 1.0 |
| Si-Al-Fe | 0.3 | 1.1 | 0.3 | 1.3 | 0.0 | 0.0 | 0.0 | 0.0 | 0.0 | 0.0 | 0.0 | 0.0 | 0.0 | 0.0 | 1.2 | 0.0 | 0.4 | 0.4 |
| Si-Al-Na | 0.0 | 0.0 | 0.0 | 0.0 | 0.0 | 0.0 | 0.2 | 0.4 | 0.1 | 0.2 | 0.0 | 0.0 | 0.0 | 0.0 | 0.2 | 0.0 | 0.4 | 0.1 |
| Si-Al-S | 1.9 | 5.6 | 1.9 | 2.7 | 1.2 | 1.3 | 0.3 | 1.7 | 0.1 | 0.3 | 0.0 | 0.0 | 0.5 | 1.6 | 0.2 | 0.0 | 0.1 | 0.0 |
| Si-Al | 5.5 | 21.1 | 1.0 | 2.7 | 0.4 | 1.5 | 2.2 | 2.5 | 0.7 | 0.6 | 0.6 | 0.1 | 0.5 | 0.4 | 47.3 | 47.5 | 44.2 | 43.7 |
| Si-Al (mixed) | 4.4 | 15.0 | 19.4 | 49.8 | 27.4 | 59.5 | 9.3 | 24.8 | 8.8 | 24.5 | 6.4 | 15.4 | 5.5 | 9.5 | 7.8 | 9.7 | 10.3 | 18.9 |
| Ca-Si | 0.3 | 0.1 | 0.9 | 0.7 | 0.4 | 0.1 | 0.1 | 0.0 | 0.4 | 0.2 | 0.5 | 1.9 | 0.4 | 0.4 | 0.2 | 0.0 | 0.5 | 0.0 |
| Ca-Mg | 28.5 | 9.3 | 36.4 | 7.4 | 27.6 | 4.3 | 44.1 | 22.9 | 35.9 | 21.0 | 36.5 | 27.6 | 39.4 | 34.8 | 0.4 | 0.1 | 0.0 | 0.0 |
| Ca-S | 5.9 | 1.5 | 4.2 | 0.9 | 3.9 | 0.4 | 1.1 | 2.4 | 0.9 | 1.1 | 1.0 | 0.5 | 0.5 | 0.3 | 1.4 | 2.0 | 1.3 | 2.1 |
| Al-S | 0.1 | 0.0 | 0.4 | 0.3 | 0.8 | 0.0 | 0.1 | 0.1 | 0.0 | 0.0 | 0.0 | 0.0 | 0.1 | 0.3 | 0.0 | 0.0 | 0.0 | 0.0 |
| Fe-S | 2.3 | 0.4 | 3.3 | 1.2 | 3.4 | 0.4 | 7.2 | 4.9 | 11.5 | 3.2 | 11.2 | 5.9 | 10.8 | 7.1 | 1.4 | 0.0 | 0.5 | 0.0 |
| Si-S | 0.3 | 0.1 | 0.2 | 0.0 | 0.0 | 0.0 | 0.0 | 0.0 | 0.0 | 0.0 | 0.1 | 0.0 | 0.0 | 0.0 | 0.0 | 0.0 | 0.0 | 0.0 |
| Fe-rich | 0.4 | 0.1 | 0.1 | 0.0 | 1.9 | 0.1 | 0.6 | 0.5 | 0.7 | 1.0 | 2.4 | 2.8 | 3.7 | 2.2 | 1.8 | 0.0 | 1.5 | 0.2 |
| S-rich | 0.9 | 0.1 | 4.7 | 0.4 | 1.6 | 0.1 | 0.1 | 0.0 | 1.0 | 0.6 | 1.5 | 1.8 | 3.4 | 3.3 | 0.0 | 0.0 | 0.0 | 0.0 |
| Ca-rich | 4.5 | 1.0 | 3.7 | 1.1 | 5.0 | 1.8 | 8.9 | 5.4 | 9.2 | 6.3 | 7.5 | 6.3 | 10.7 | 12.5 | 1.2 | 0.0 | 0.4 | 0.0 |
| Zn-rich | 0.2 | 0.3 | 0.1 | 0.0 | 0.1 | 0.0 | 0.0 | 0.0 | 0.0 | 0.0 | 0.0 | 0.0 | 0.0 | 0.0 | 0.0 | 0.0 | 0.0 | 0.0 |
| Ti-rich | 1.2 | 0.3 | 0.7 | 0.1 | 1.9 | 0.1 | 1.7 | 1.1 | 0.8 | 0.3 | 0.6 | 0.1 | 0.5 | 0.1 | 0.7 | 0.4 | 0.3 | 0.0 |
| Pb-rich | 3.3 | 3.9 | 3.8 | 0.8 | 1.3 | 0.1 | 1.6 | 2.5 | 1.3 | 0.9 | 2.2 | 2.0 | 3.8 | 2.9 | 0.0 | 0.0 | 0.0 | 0.0 |
| C-rich | 18.3 | 22.5 | 0.7 | 1.3 | 1.2 | 0.5 | 5.3 | 6.3 | 11.9 | 3.8 | 13.0 | 3.3 | 5.5 | 1.1 | 4.1 | 0.3 | 2.4 | 0.2 |
| Misc. | 18.1 | 4.8 | 8.2 | 6.3 | 5.8 | 2.6 | 6.8 | 3.4 | 4.8 | 7.0 | 4.4 | 1.3 | 4.2 | 1.4 | 0.7 | 0.2 | 0.4 | 1.0 |

Table 8 Particle class relative abundance (% count and weight): Nevada

| Stage d ₅₀ (μm) | 0.18 | | 0.32 | | 0.56 | | 1.0 | | 1.8 | | 3.1 | | 6.2 | | 9.9 | | 18 | |
|----------------------------|------------|------------|------------|------------|------------|------------|------------|------------|------------|------------|-------------|------------|-------------|-------------|-------------|-------------|-------------|-------------|
| Particle Class | C | W | C | W | C | W | C | W | C | W | C | W | C | W | C | W | C | W |
| Si-rich | 4.8 | 2.5 | 3.3 | 2.3 | 5.3 | 3.4 | 9.9 | 4.8 | 8.2 | 3.5 | 11.1 | 7.2 | 19.9 | 14.2 | 16.9 | 19.7 | 13.6 | 14.6 |
| Si-Al-K | 0.3 | 1.0 | 1.9 | 8.3 | 3.9 | 18.1 | 6.6 | 16.4 | 7.8 | 20.8 | 7.4 | 20.0 | 3.5 | 15.0 | 4.6 | 14.8 | 4.4 | 19.5 |
| Si-Al-Ca | 0.0 | 0.0 | 0.0 | 0.0 | 0.2 | 0.0 | 0.3 | 1.2 | 0.4 | 0.5 | 0.2 | 0.1 | 0.1 | 0.0 | 0.0 | 0.0 | 0.1 | 0.2 |
| Si-Al-Mg | 0.1 | 0.2 | 0.1 | 0.6 | 0.0 | 0.0 | 0.6 | 0.3 | 0.1 | 0.0 | 0.2 | 0.1 | 0.1 | 0.5 | 0.1 | 0.0 | 0.1 | 0.1 |
| Si-Al-Fe | 0.4 | 0.2 | 0.3 | 0.4 | 0.0 | 0.0 | 0.1 | 0.1 | 0.2 | 0.1 | 0.2 | 0.1 | 0.1 | 0.1 | 0.1 | 0.3 | 0.1 | 0.1 |
| Si-Al-Na | 0.3 | 1.5 | 0.3 | 0.2 | 0.5 | 0.2 | 0.3 | 0.4 | 0.7 | 3.3 | 0.1 | 0.0 | 0.3 | 0.1 | 0.3 | 0.2 | 0.1 | 0.0 |
| Al-Si-S | 7.8 | 5.6 | 14.9 | 12.6 | 11.6 | 5.0 | 2.2 | 1.7 | 1.5 | 2.4 | 1.7 | 1.6 | 0.4 | 0.8 | 0.4 | 2.1 | 0.4 | 1.6 |
| Si-Al-S | 3.8 | 2.1 | 5.9 | 5.0 | 10.5 | 9.1 | 4.9 | 3.0 | 2.4 | 2.0 | 1.1 | 0.7 | 0.7 | 1.7 | 0.9 | 1.5 | 0.6 | 1.3 |
| Si-Al | 13.8 | 19.2 | 17.6 | 22.0 | 13.4 | 8.5 | 20.7 | 20.4 | 16.3 | 14.3 | 14.3 | 11.5 | 9.9 | 9.1 | 11.5 | 12.2 | 9.5 | 16.5 |
| Si-Al (mixed) | 15.6 | 12.0 | 21.5 | 20.8 | 22.0 | 34.9 | 3.3 | 4.1 | 5.5 | 10.3 | 5.1 | 7.5 | 5.3 | 6.0 | 6.8 | 14.0 | 5.4 | 11.4 |
| Ca-Si | 0.0 | 0.0 | 0.3 | 0.3 | 0.6 | 0.2 | 0.2 | 0.4 | 0.5 | 0.9 | 0.1 | 0.2 | 0.1 | 0.2 | 0.1 | 0.0 | 0.3 | 2.3 |
| Ca-Mg | 0.0 | 0.0 | 0.0 | 0.0 | 0.0 | 0.0 | 0.0 | 0.0 | 0.1 | 0.0 | 0.0 | 0.0 | 0.0 | 0.0 | 0.0 | 0.0 | 0.7 | 2.5 |
| Ca-S | 0.0 | 0.0 | 0.1 | 0.0 | 0.3 | 1.2 | 0.6 | 0.5 | 0.3 | 0.0 | 0.3 | 0.1 | 0.4 | 0.2 | 0.3 | 0.4 | 0.2 | 0.0 |
| Al-S | 23.2 | 14.8 | 19.4 | 17.4 | 21.8 | 13.2 | 39.8 | 24.5 | 38.9 | 28.8 | 42.6 | 32.0 | 29.4 | 29.3 | 28.2 | 23.2 | 19.1 | 18.9 |
| Fe-S | 8.7 | 7.5 | 7.4 | 6.0 | 0.0 | 0.0 | 5.8 | 4.2 | 6.5 | 3.6 | 8.6 | 9.4 | 10.4 | 11.7 | 7.0 | 8.3 | 4.5 | 5.4 |
| Ca-rich | 0.3 | 0.3 | 0.1 | 0.3 | 0.0 | 0.0 | 0.3 | 0.1 | 0.6 | 0.5 | 0.5 | 0.2 | 0.5 | 0.0 | 0.2 | 0.3 | 0.8 | 1.6 |
| Ti-rich | 1.7 | 1.3 | 1.8 | 0.5 | 3.5 | 0.4 | 0.2 | 0.0 | 0.4 | 0.0 | 0.3 | 0.1 | 0.1 | 0.0 | 0.2 | 0.1 | 0.1 | 0.2 |
| Pb-rich | 0.0 | 0.0 | 0.0 | 0.0 | 0.0 | 0.0 | 0.0 | 0.0 | 0.3 | 1.2 | 0.1 | 7.3 | 0.0 | 0.0 | 0.0 | 0.0 | 0.1 | 0.2 |
| rich | 1.0 | 19.7 | 0.0 | 0.0 | 0.6 | 4.2 | 2.3 | 13.7 | 7.2 | 7.1 | 4.5 | 1.3 | 12.0 | 6.3 | 18.0 | 0.3 | 38.3 | 2.9 |
| Misc. | 18.2 | 12.4 | 5.4 | 3.4 | 5.9 | 1.7 | 1.9 | 4.3 | 2.2 | 0.7 | 1.7 | 1.0 | 6.8 | 4.7 | 4.3 | 2.6 | 1.6 | 0.7 |

Table 9 Particle class relative abundance (% count and weight): South Africa

| Stage d ₅₀ (µm) | 0.18 | | 0.32 | | 0.56 | | 1.0 | | 1.8 | | 3.1 | | 6.2 | | 9.9 | | 18 | |
|----------------------------|------------|------------|------------|------------|------------|------------|------------|------------|------------|------------|-------------|------------|-------------|------------|-------------|------------|------------|------------|
| Particle Class | C | W | C | W | C | W | C | W | C | W | C | W | C | W | C | W | C | W |
| Si-rich | 7.7 | 1.2 | 4.6 | 1.2 | 6.4 | 2.1 | 5.0 | 1.5 | 3.6 | 1.3 | 10.9 | 3.0 | 12.2 | 6.4 | 11.9 | 6.7 | 5.6 | 6.0 |
| Si-Al-K | 2.5 | 8.1 | 5.3 | 9.9 | 5.3 | 12.0 | 8.6 | 28.5 | 12.0 | 31.9 | 11.4 | 38.1 | 7.9 | 21.6 | 10.1 | 31.8 | 8.7 | 28.8 |
| Si-Al-Ca | 0.3 | 0.1 | 0.7 | 0.5 | 1.9 | 0.2 | 1.2 | 1.0 | 1.3 | 3.0 | 0.1 | 0.0 | 0.0 | 0.0 | 0.3 | 0.2 | 0.2 | 0.7 |
| Si-Al-Mg | 0.1 | 0.1 | 1.4 | 2.0 | 0.9 | 0.3 | 2.1 | 3.0 | 1.9 | 0.9 | 0.3 | 0.7 | 0.4 | 0.4 | 0.6 | 0.1 | 0.1 | 0.1 |
| Si-Al-Fe | 2.3 | 1.3 | 1.6 | 0.9 | 2.1 | 0.5 | 0.6 | 0.7 | 0.8 | 0.1 | 0.4 | 0.6 | 0.0 | 0.0 | 0.2 | 0.1 | 0.3 | 0.0 |
| Si-Al-Na | 0.9 | 1.0 | 0.6 | 0.4 | 0.2 | 0.0 | 1.6 | 2.0 | 1.3 | 0.3 | 0.2 | 0.3 | 0.0 | 0.0 | 0.2 | 0.0 | 0.0 | 0.0 |
| Si-Al-S | 0.7 | 0.5 | 0.7 | 0.8 | 0.9 | 0.2 | 1.4 | 1.7 | 1.6 | 0.7 | 0.0 | .00 | 0.0 | 0.0 | 0.2 | 0.0 | 0.0 | 0.0 |
| Si-Al | 20.2 | 34.9 | 29.6 | 37.4 | 27.2 | 40.8 | 30.5 | 24.5 | 26.5 | 17.9 | 40.8 | 38.3 | 34.4 | 51.4 | 35.1 | 43.2 | 20.2 | 36.4 |
| Si-Al (mixed) | 12.4 | 13.8 | 22.9 | 31.2 | 17.5 | 32.1 | 31.9 | 29.7 | 28.5 | 37.3 | 12.3 | 14.7 | 8.1 | 16.9 | 8.7 | 14.5 | 3.2 | 5.3 |
| Ca-Si | 0.6 | 1.5 | 0.8 | 0.2 | 0.2 | 0.0 | 0.2 | 0.0 | 0.5 | 0.1 | 0.1 | 0.1 | 0.2 | 0.0 | 0.2 | 0.3 | 0.2 | 1.0 |
| Ca-Mg | 0.0 | 0.0 | 0.3 | 0.2 | 0.0 | 0.0 | 0.1 | 0.0 | 0.1 | 0.0 | 0.1 | 0.0 | 0.0 | 0.0 | 0.0 | 0.0 | 0.2 | 0.5 |
| Ca-S | 0.1 | 0.2 | 0.2 | 0.2 | 0.0 | 0.0 | 0.3 | 0.1 | 0.4 | 0.1 | 0.5 | 1.1 | 1.1 | 1.4 | 0.4 | 0.3 | 0.5 | 3.6 |
| Al-S | 0.4 | 0.1 | 0.2 | 0.1 | 0.0 | 0.0 | 0.1 | 0.0 | 0.1 | 0.0 | 0.1 | 0.1 | 0.0 | 0.0 | 0.0 | 0.0 | 0.0 | 0.0 |
| Fe-S | 3.4 | 2.6 | 6.4 | 2.6 | 2.8 | 1.1 | 0.9 | 0.2 | 2.5 | 0.4 | 0.7 | 0.2 | 0.9 | 0.1 | 0.4 | 0.1 | 0.6 | 0.9 |
| Ca-rich | 0.7 | 7.0 | 0.7 | 0.1 | 0.2 | 0.1 | 0.3 | 0.1 | 0.5 | 0.1 | 0.7 | 0.2 | 0.7 | 0.1 | 0.7 | 0.1 | 0.7 | 0.1 |
| Fe-rich | 5.6 | 4.0 | 3.6 | 2.8 | 2.5 | 0.2 | 0.4 | 0.1 | 0.6 | 0.2 | 0.8 | 0.2 | 1.8 | 0.0 | 0.9 | 0.4 | 0.9 | 1.1 |
| S-rich | 6.9 | 1.4 | 1.0 | 0.2 | 0.2 | 0.1 | 0.0 | 0.0 | 0.1 | 0.0 | 0.0 | 0.0 | 0.0 | 0.0 | 0.0 | 0.0 | 0.0 | 0.0 |
| Zn-rich | 0.1 | 0.0 | 0.1 | 0.0 | 0.0 | 0.0 | 0.0 | 0.0 | 0.0 | 0.0 | 0.0 | 0.0 | 0.0 | 0.0 | 0.0 | 0.0 | 0.0 | 0.0 |
| Ti-rich | 12.9 | 3.7 | 14 | 4.4 | 3.7 | 0.4 | 0.8 | 0.1 | 1.0 | 0.2 | 1.0 | 0.3 | 0.4 | 0.0 | 0.3 | 0.1 | 0.4 | 0.0 |
| Pb-rich | 1.5 | 0.5 | 0.3 | 0.1 | 0.0 | 0.0 | 0.1 | 0.0 | 0.5 | 0.5 | 0.0 | 0.0 | 0.0 | 0.0 | 0.0 | 0.0 | 0.0 | 0.0 |
| C-rich | 6.0 | 11.8 | 1.4 | 4.2 | 23.7 | 9.4 | 10.1 | 5.6 | 12.2 | 5.0 | 18.0 | 2.0 | 31.7 | 1.8 | 29.0 | 1.7 | 57.2 | 14.9 |
| Misc. | 14.6 | 6.5 | 3.6 | 0.7 | 4.4 | 0.6 | 4.0 | 1.3 | 4.0 | 0.3 | 1.8 | 0.1 | 0.4 | 0.0 | 0.9 | 0.4 | 1.0 | 0.7 |

Figure 12 displays examples of SEM images of three particle classes, as well as the corresponding EDS spectra which were used to classify the particles.

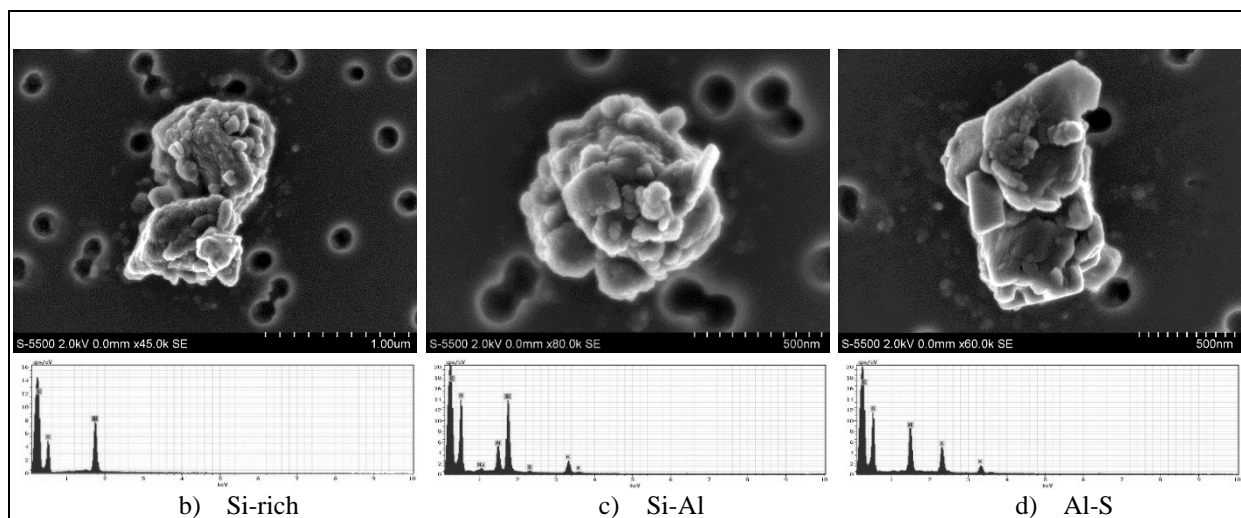


Figure 12 SEM particle images and corresponding EDS spectra

Figures 13-15 show plots of the four most abundant classes (of total particles counted) for each dust, by count and weight, across nine particle size ranges. The Si-rich particle class, representing standalone silica particles, is included in all plots, even if it was not among the four most abundant particle classes. Finally, the relative abundance of Si-rich/silica particles is shown by count (determined by EDS) in Figure 16, and by weight (as determined by EDS) and mass percent (as determined by IR and XRD; see Chapter 3) in Figure 17.

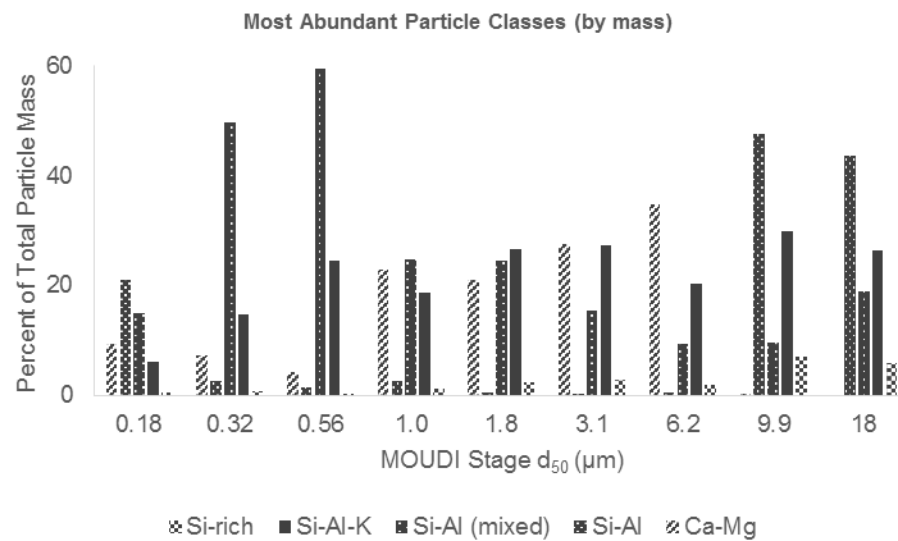
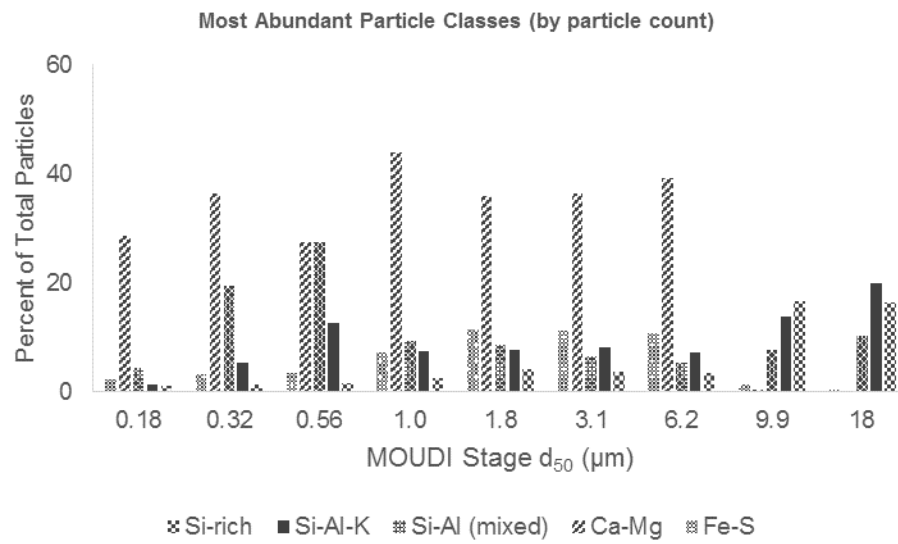


Figure 13 Particle size-related trends in most abundant particle classes: Alaska

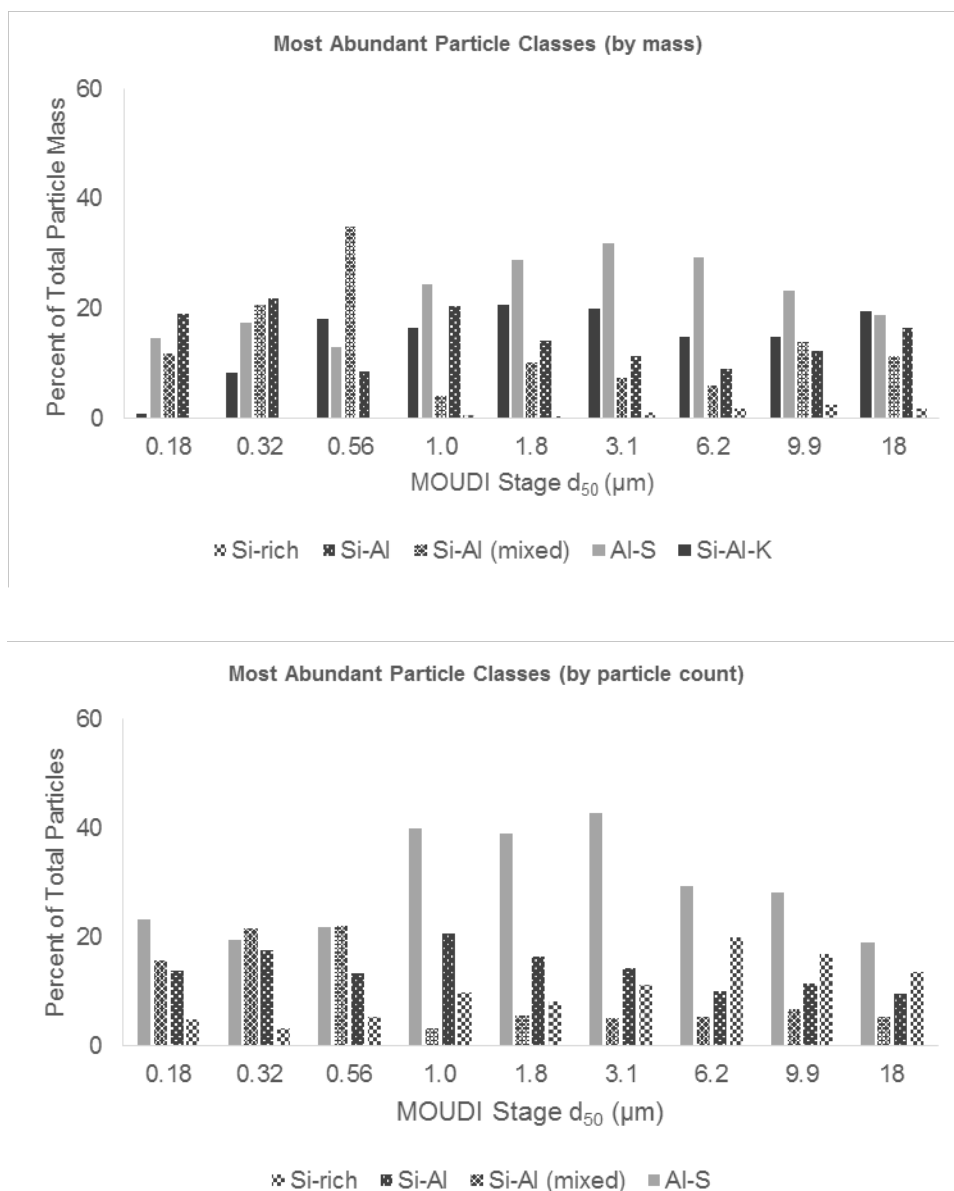


Figure 14 Particle size-related trends in most abundant particle classes: Nevada

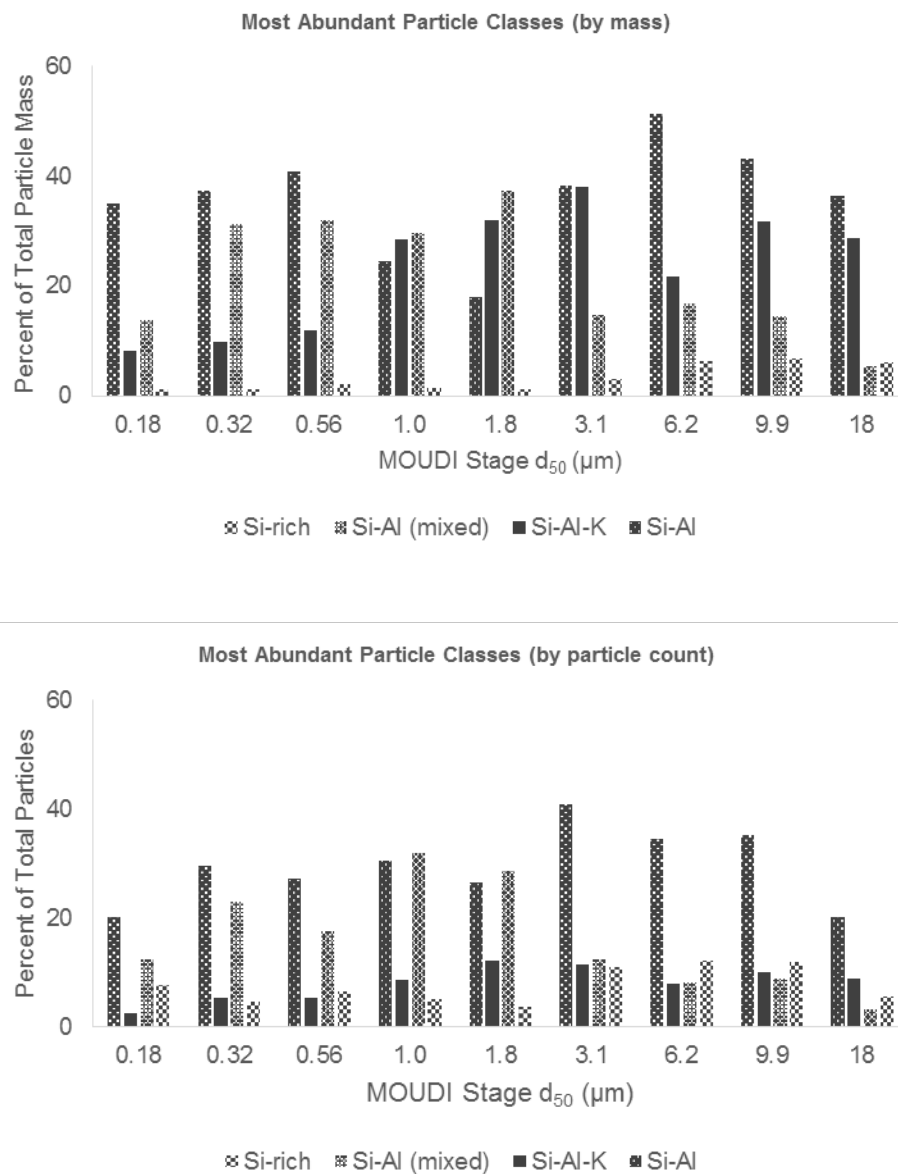


Figure 15 Particle size-related trends in most abundant particle classes: South Africa

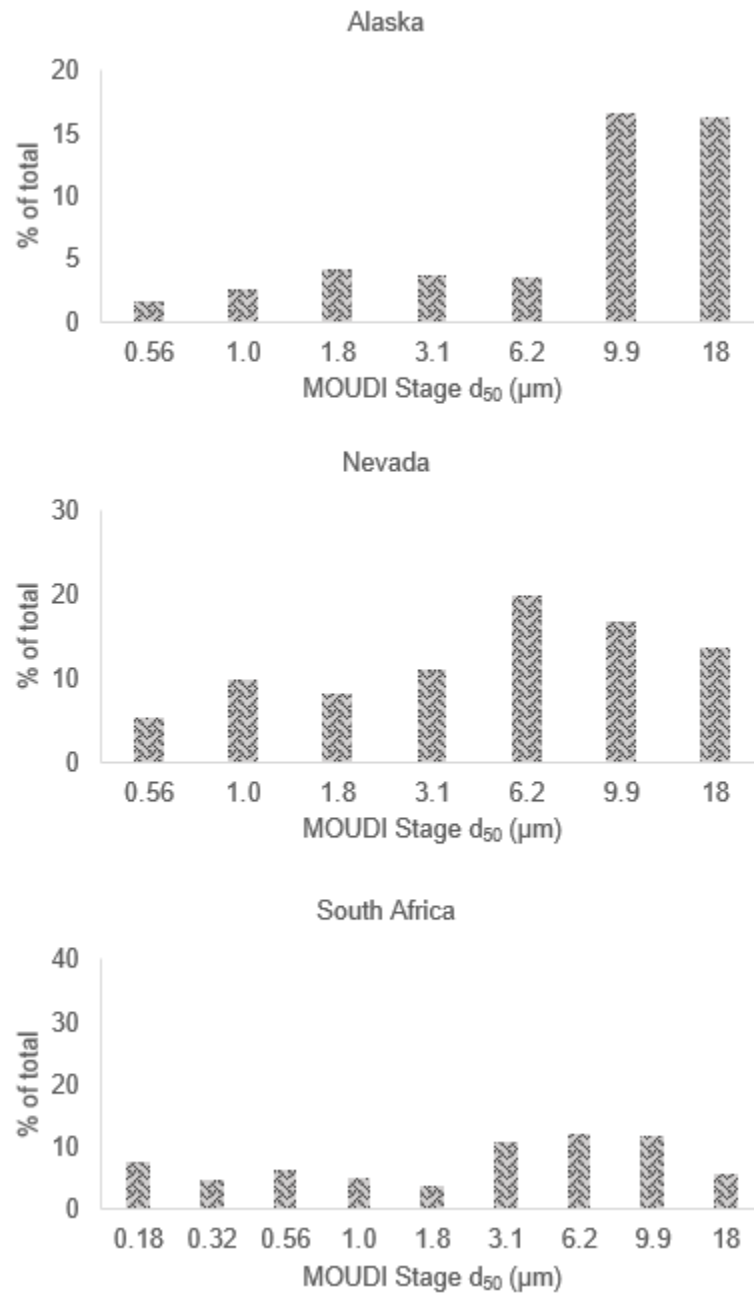


Figure 16 Particle size-related trends in silica, determined by EDS (count)

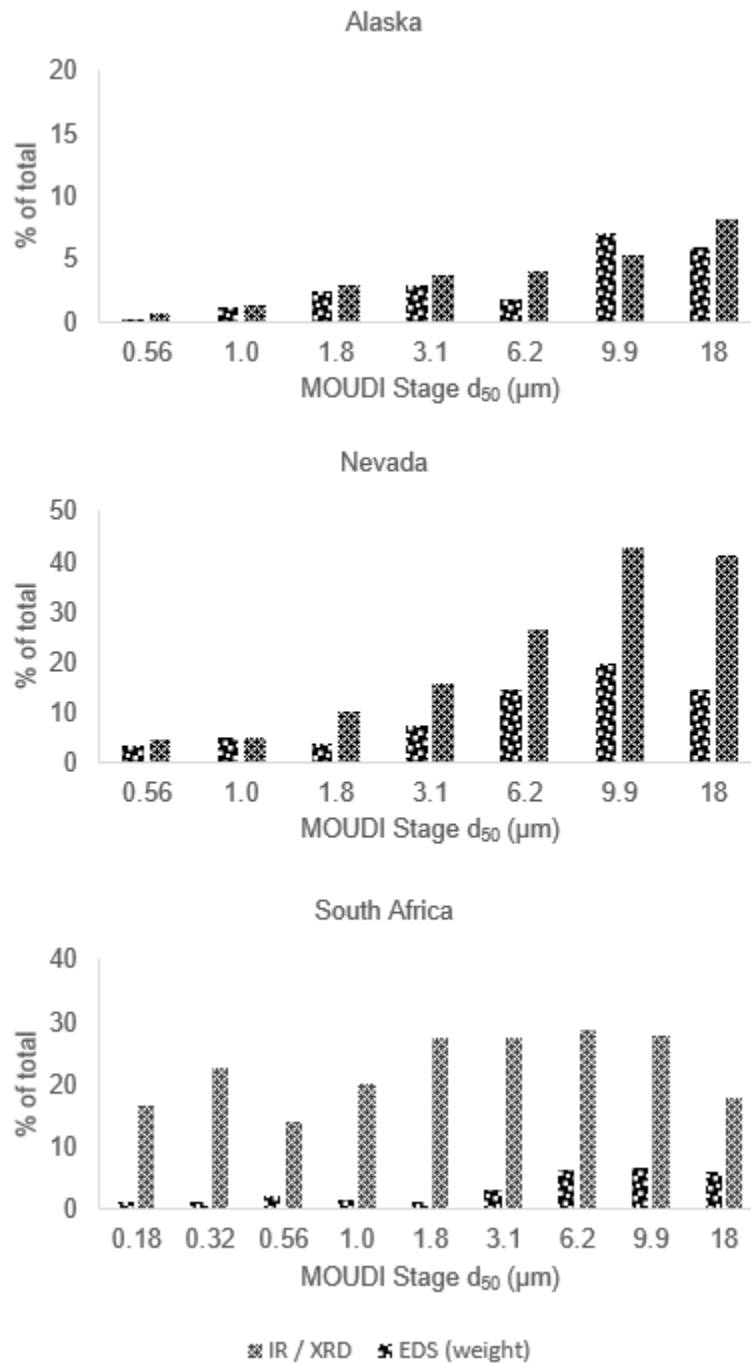


Figure 17 Particle size-related trends in silica, determined by EDS (weight) and IR/XRD

4.3 DISCUSSION

Figures 13-15 show the four most abundant particle types (excluding C-rich and Miscellaneous classes) for each of the three dusts, with respect to both particle number and particle weight. Particle classes that are abundant in terms of particle number are generally abundant in terms of particle weight as well, although this is not uniformly true. The discrepancy between the particle classes that are more abundant with respect to particle number and those that are more abundant with respect to particle weight is largely due to differences in particle density among different particle types. For example, Fe-rich particles may only contribute moderately to the total number of particles, but contribute more significantly to the total particle weight, due to the relatively high density of the iron atom and the resulting greater mass of these particles. Together the four most abundant classes encompassed an average of 61.6% of the total particle number, or 74.5% of total particle weight; each of the three dusts also contains approximately 15 additional particle classes, which each comprise only a minor proportion of the dust particle number (average 1.3%, excluding C-rich and miscellaneous particles) or total particle weight (average 1.2%, not excluding C-rich and miscellaneous particles).

For the Nevada and South Africa dust, Si-rich particles are among the four most abundant particle classes with regard to count; Si-rich particles are also among the four most abundant particle classes by weight for the South Africa dust. It is unsurprising that the Si-rich class is so prominent in these two dusts but not in the Alaska dust, as the South Africa dust contains the most silica of the three, followed by Nevada, while the dust from Alaska contains the least (when IR and XRD results for crystalline silica are considered). Particles containing both silicon and aluminum (Si-Al-K, Si-Al-Mg, Si-Al-Ca, Si-Al-Fe, Si-Al-Na, Si-Al-S Si-Al, and Si-Al (mixed)) are also quite abundant throughout all three dusts. This finding has particular significance as these particle classes likely correspond to silicate minerals which may have chemical or crystalline structures analogous to that of silica, such that they are more likely to contribute confounding

effects to the analysis of crystalline silica by methods such as IR or XRD. This finding is also not surprising, as silicate minerals (chlorite, feldspar, muscovite, and pyrophyllite) are observed in the Rietveld XRD refinement analysis of all three dusts. Figure 17 shows a comparison of size-related trends in silica abundance determined by IR / XRD and by EDS (particle weight) methods. It is readily apparent that the crystalline silica quantification results from XRD and IR methods are not equivalent in magnitude to the abundance of Si-rich particles determined EDS. There are several potential reasons for this, first and foremost among which is that crystalline silica may not always exist as a standalone particle, but rather may joined with one or more particles of other minerals to form an aggregate. In this case, the EDS analysis would not identify such an aggregate as a Si-rich particle but would instead classify it as another particle type.

Additionally, it should be considered that EDS is not measuring crystalline silica directly, but rather detects elemental silicon, which is used here as a proxy for silica. Relative abundance is shown for EDS data based on particle count (a direct measurement) as well as particle weight (an indirect measurement, calculated from particle count and corresponding estimates of particle volume and density). It is important to recognize that because these analytical techniques each use distinct metrics to determine the abundance of silica in each sample, they will not necessarily yield results of comparable magnitude; however, for each dust, the overall trends in abundance of silica with progression of particle size are similar across analytical methods.

The presence of co-toxicants, such as iron particulates and diesel particulate matter, have been suggested as a mechanism for the increased toxicity of certain dusts (40-42), and size-related trends in the abundance of either of these species would be salient to discussion of the health impacts. The above analysis did not indicate appreciable abundance of particles rich in both silicon and iron (which could indicate a silica particle with iron inclusion) however, these particles may be low in abundance to begin with, and this analysis was not optimized with this particular purpose in mind, which may contribute to the apparent absence (or near-absence). Likewise, this analysis was not intended to look at diesel particulates specifically; since diesel

particles are largely submicron (123) and have distinct morphology (124-126), a dedicated approach would be required to identify and accurately measure these particles. Such an analysis would have impeded the primary objectives of this study but would be interesting to pursue in a standalone investigation.

In each dust, there were several particle classes that were particularly high in abundance with respect to particle count or particle weight; the same particle classes were often fairly abundant with respect to both. For the Alaska dust, such particle classes included Si-Al-K, Si-Al (mixed), Si-Al, Fe-S, and Ca-Mg particle. Based on results from Rietveld XRD refinement, these classes most likely correspond to muscovite (for Si-Al-K, Si-Al-mixed, and Si-Al; the variability in apparent elemental composition may be related to variation in particle size as well as in particle orientation), pyrite or possibly sphalerite/wurtzite (for Fe-S), and dolomite (Ca-Mg). For the Nevada dust, abundant particle classes included Si-Al, Si-Al (mixed), Si-Al-K, Si-rich, and Al-S, which most likely correspond to chlorite (again, for Si-Al-K, Si-Al, and Si-Al (mixed)), silica (Si-rich), and alunite (Al-S). Finally, for the South Africa dust, abundant particle classes include Si-rich, Si-Al (mixed), Si-Al-K, and Si-Al, most likely corresponding to silica (Si-rich), chlorite (Si-Al (mixed)); also Si-Al-K and Si-Al) and pyrophyllite (Si-Al), also feldspar and muscovite (Si-Al-K).

Because the EDS technique does not measure specific crystalline structures but rather detects individual elements and determines the proportional intensity of the fluorescent signal for each element, the abundance of individual particle classes can be used to approximate abundance of specific minerals, but shouldn't be considered an absolute measurement of these minerals. As discussed in Chapter 3, mineral confounders specific to a particular type of dust may influence the accuracy of IR and XRD methods, especially when particle size is also considered as a factor. In order to reconcile these effects, detailed size-related characterization of multiple mineral species is required, and this is a time-consuming process. Single-particle data from EDS can be used to prioritize the minerals for which size-related characterization is required, based on which minerals are most abundant and therefore may have effects of the greatest

magnitude. While certain minerals may have a large relative effect on the accuracy of crystalline silica quantification, a particular mineral would not necessarily be a concern if it comprised only 1-2% of the total mineral composition of a dust.

5.0 DISCUSSION AND CONCLUSIONS

While other authors have emphasized the importance of well-characterized aerosols (76, 100, 127) to the accurate measurement and evaluation of exposure to crystalline silica, there remains a stark lack of data characterizing mine dusts, particularly from non-coal mines. This work takes a step towards addressing that need, by proposing a method by which such characterization can be accomplished, by characterizing the particle size-related crystalline silica content of three gold mine dusts, and by evaluating particle size-related elemental composition of mine dust particles. The variability in particle size-related qualities observed in these three dusts further demonstrates the need to characterize additional aerosols from a variety of types of mines.

5.1 IMPLICATIONS OF THE PARTICLE SIZE DISTRIBUTION OF CRYSTALLINE SILICA

This study determined that, for the three dusts evaluated, the particle size distributions of the total dust and of the crystalline silica component of dust are not identical, and demonstrated that the size distribution of crystalline silica particles was generally somewhat larger than the size distribution of the overall particles. When only the respirable fraction of particles was considered for each dust, the difference in size distribution was even more pronounced. Thus, it should not be assumed that the crystalline silica component of a dust will have the same size distribution as the whole dust. Personal protective equipment and control technologies utilized to suppress dust in mines should be chosen with the size distribution of crystalline silica in mind, rather than the respirable dust alone, so that respirable crystalline silica concentrations are always decreased equivalently or greater than respirable dust concentrations. In certain situations where the difference in size distribution is especially pronounced, or where total dust concentration or

crystalline silica percentage in the dust is especially high, to select and evaluate protections and controls based reduction of the respirable dust alone may result in a false sense of security, where workers are being overexposed to crystalline silica while exposure estimates suggest otherwise. Shepherd et al. (128) assessed reductions in crystalline silica and dust concentrations in construction environments using local exhaust ventilation. They used four-stage personal cascade impactors to measure crystalline silica exposure and found that while ventilation decreased exposure to all three health-relevant size fractions (inhalable, thoracic, respirable), there was a slightly smaller reduction in inhalable crystalline silica relative to thoracic crystalline silica. The authors also emphasized that the majority of crystalline silica exposure for these workers was due to inhalable crystalline silica particles rather respirable particles, underlining once again the value of understanding the size distribution of crystalline silica within the dust in question.

The discrepancy between the size distribution of the complete dust and the size distribution of crystalline silica also suggests that periodic evaluation of the size distribution of the crystalline silica component of dusts is necessary in order to ensure comparability to the crystalline silica standards used for calibrations of laboratory methods. Conducting these comparisons based on the size distribution of the total dust would be insufficient. As discrepancy between sample and crystalline silica standard size distribution has been shown to result in appreciable bias in the quantification of crystalline silica, this check of validity should not be neglected.

5.2 IMPLICATIONS OF PARTICLE SIZE-RELATED DISCREPANCY IN CRYSTALLINE SILICA ANALYSES

Results reported in Chapter 3 indicated that there is a particle size-related lack of agreement in crystalline silica quantified by the IR and XRD methods, but that mineral composition is also likely to contribute to the discrepancy. Clearly this inconsistency must be addressed, as both methods are used for industrial hygiene as well as for regulatory compliance purposes. Unfortunately, the solution is not immediately clear. What can be said with confidence is that knowledge of the size and compositional characteristics of a dust can be informative of the potential limitations of either method with regard to the quantification of crystalline silica. For instance, the crystalline silica content of a dust with MMD of 1.5 μm and a high percentage of feldspar minerals (a known XRD interference) is likely to be underestimated by the XRD method. It may or may not be possible to apply corrections – either general adjustments or corrections that apply if certain conditions are met – in order to arrive at a more accurate quantity of crystalline silica. Regardless, with knowledge of the methods limitations, appropriately conservative measures can be taken: for instance, assuming that the crystalline silica content has been underestimated by a certain factor, and taking subsequent corrective actions based on the higher concentration value.

5.3 IMPLICATIONS OF SINGLE-PARTICLE ANALYSIS OF SIZE-FRACTIONATED SAMPLES

This study determined that, like crystalline silica, other particle classes (used as a proxy for other mineral types) vary in abundance according to particle size and are not uniformly consistent throughout the dust. This variation does not appear to be constant between different dusts for the same particle class, but it should be considered that the three dusts do not have equivalent

mineral composition, and this is likely to impact the particle-size related trends observed for each dust with regard to particle class. Though this study did not undertake mathematical modeling to correlate the assigned particle classes with specific mineral species, such an effort would be an interesting and possibly useful addition to future studies of this kind. Such a method would likely require analysis of a greater number of particles than what was analyzed in this study.

As discussed in Chapter 3, particle size effects coupled with mineral interference may impact the comparability of crystalline silica measurements by the IR and XRD methods. Further investigation of this possibility is warranted based on the above observations that particles of different types vary in abundance by particle size. The findings of this investigation could be confirmed by collection of size-segregated samples of dust for spectroscopic analysis (as described in Chapter 2) of different minerals. Given the findings of Chapter 3, it would be advisable to use multiple methods (including but not necessarily limited to IR and XRD) to evaluate mineral composition, as there may also be discrepancy in measurements of minerals other than crystalline silica.

Finally, the conclusion that the relative abundance of crystalline silica particles determined by EDS is not equivalent to the mass percent of crystalline silica determined by IR / XRD suggests that crystalline silica may not always exist as a standalone particle, but rather may be physically associated with one or more particles of distinct mineral composition (for example, an agglomerated particle of crystalline silica, chlorite, and muscovite). As this study was not specifically designed to investigate such particle-particle associations in detail, more specific conclusions cannot be reached, but this topic would be an interesting and potentially important area for future studies.

5.4 EVALUATION OF STUDY LIMITATIONS AND STRENGTHS

This investigation of the particle size-related characteristics of gold mine dusts incorporated several different techniques to achieve a detailed characterization of each dust. The use of multiple techniques allowed for methods that were complementary to one another, in order to optimize the data collected, while also incorporating a level of redundancy, so that results of one method could be compared to and validated by another. Notable limitations and strengths of the study design are discussed below.

5.4.1 Limitations

One limitation of this study arises from the use of re-aerosolized bulk material, collected from settled dust. Allowing dust to settle naturally can skew the size distribution towards larger particles, which have greater mass and settle more quickly, and “cleans” the dust of submicron material which takes longer to settle. However, given sufficient time, most submicron particles will still settle from the air and can be collected with other settled particles, and two of the three dusts studied did indeed contain substantial numbers of submicron particles. Another consideration is raised by Hicks and Yager (129), who found, in a study of coal fly ash at a power plant, that bulk dust had diminished crystalline silica content relative to airborne dust; the authors noted that this is important for occupational hygiene assessments that use the crystalline silica content of settled material as a proxy for crystalline silica exposure. However, the study of coal fly ash considered the total crystalline silica content of bulk material against the total crystalline silica content of respirable airborne dust. Within any given size fraction of dust, crystalline silica particles are very likely to have density – and thus, mass – similar to particles of other mineral composition in that size class, and they will settle at a similar rate. This means that while the overall size distributions of dust and of crystalline silica may be impacted by the practice of using

settled material, the relationship between the two size distributions (e.g. the proportional crystalline silica content in each size fraction) should not be impacted. Likewise, it is important to note that the methods using in this study – particularly the sieving of dusts to remove large particles, and aerosolization via the fluidized bed aerosol generator – do not create new particles (i.e. by breaking larger particles) and thus do not affect the size distribution in the particle size range that is of interest to human health.

Another disadvantage of studies utilizing bulk dust is that such dust is not necessarily representative of the dust in a particular area of the mine or from a specific mining task. As Sirianni et al. (76) have observed, different tasks produce dust with variable size distributions both for total dust and for crystalline silica. While it may not always be practical to characterize multiple dusts from a single operation, such an endeavor would be worthy of consideration in certain situations, such as when a particular task or area is producing respirable dust with uncharacteristically high crystalline silica content, or if respirable dust and/or crystalline silica in a particular area proves difficult to control.

While the methods used in this study provide a straightforward and thorough method for laboratory characterization of mine dusts and dusts from other occupational settings, these methods require cumbersome equipment setups that may not always be practical for in-field use, though not entirely impossible depending on the mine environment. In-field use of the MOUDI would require a sampling pump capable of supporting the required 30 lpm flow rate; a mechanism by which to remove and replace sample filters and substrates without exposing them to contamination and without moving the MOUDI; and sufficiently high dust concentrations (or sufficiently long sampling times, possibly on the order of days) to ensure that enough material is collected. Such dust concentrations would likely require the use of respiratory protection for anyone attending to the sampling setup.

Small modifications to the basic premise of this method could make it more feasible for those who desire to characterize dusts in the field rather than in the laboratory. Smaller cascade

impactors are available, including models small enough to be worn by workers for exposure assessments (130-132). A smaller, less cumbersome impactor would also facilitate multiple days of sampling, which could allow for sampling in a lower dust concentration environment; however, multiple samples may need to be combined to have sufficient material for crystalline silica analysis.

The generalizations available from this summary are limited by the sample size of this study, as only three mine dusts from one commodity type (gold) were considered. The three dusts were all from different geographic regions, so no generalizations can be drawn regarding the characteristics of dust with respect to location, except to say that the observed differences *could* be related to geographical trends in the general characteristics of dust; this avenue warrants further exploration. Future analyses should compare the characteristics of dusts from the same general region (i.e. the American Southwest) as well as the same commodity type.

This study investigated physical and chemical attributes of mine dusts but did not explore differences in the biological effects of exposure to these dusts, thus there are a number of points regarding the toxicity of crystalline silica that are not addressed. In particular, freshly fractured crystalline silica has recently been implicated as a more efficient producer of reactive oxygen species than aged crystalline silica particles (37). Because this current study utilized settled material that had been stored in the laboratory prior to use, it can provide no information on the size distribution of freshly fractured crystalline silica relative to aged crystalline silica; this would be a useful area for further study and would be especially interesting in conjunction with toxicological work. Additionally, size and surface area have both been implicated as more potent indicators of dose than mass, but such metrics have a tendency to be overlooked because it is much more convenient to assess the mass of a sample of particles than it is to assess other physical characteristics. This study indicated that the count and mass distributions of whole dusts and of the crystalline silica component are unique, and that perhaps additional attention should be devoted to developing practical means of assessing exposures based on particle number or

surface area concentrations, rather than mass concentrations alone. In addition to providing incomplete information about exposures, mass-based exposure metrics have the added disadvantage of skewing dose assessment towards larger particles, which have greater mass but smaller ratios of surface area to volume, and may not be as biologically active as smaller particles in the fibrogenic mechanisms that lead to silicosis (38). Comparison of mass-, diameter-, and surface area-based dose assessments from real-world dusts are beyond the scope of this work, but would certainly be a valuable contribution to the field.

5.4.2 Strengths

The foremost advantage of this series of evaluations is that, while somewhat labor intensive, the methods are basic in principle and are easily replicated using commercially available instrumentation and techniques. This is vital towards encouraging more research in this field and towards facilitating the characterization of a broad range of aerosols. Furthermore, while the cost of SEM-EDS may be prohibitive and difficult to justify for an individual mine, size-segregated crystalline silica analysis using a cascade impactor is not far beyond the scope of routine sampling performed for industrial hygiene and exposure assessment purposes. Using standardized gravimetric and spectroscopy methods (services available from accredited occupational hygiene laboratories), industrial hygienists can assess the size distribution of dust and of crystalline silica in a specific mine, or in several tasks across a mine. Assuming similar and well-documented methodologies, such as the one described here, are used, results from both researchers and health and safety professionals would be readily comparable, allowing the collective evaluation of a wide range of mine dusts that will enhance understanding of these dusts in general.

Though the use of re-aerosolized bulk material does have certain drawbacks (discussed above), this practice facilitated high dust concentrations in a laboratory chamber, whereas such concentrations would have been unsafe (and hopefully never encountered) in the mining

workplace. High dust concentrations permitted the collection of multiple samples over the course of just a few days, whereas weeks of sampling may have been required to collect sufficient material at lower concentrations. Additionally, better control over sampling time, dust concentration, and other ambient conditions resulted in less censored data due to samples below the method limits of detection for crystalline silica. Elimination of variables such as wind, precipitation, ventilation, work practices and rate of dust generation avoids any bias due to dynamic field sampling conditions.

This study employs numerous techniques that validate each other through partial redundancy, while enhancing each other with complementary capabilities. Size distributions were determined using two explicit approaches: combined use of APS and SMPS capability enabled construction of count distributions for particles, while gravimetric data collected with the MOUDI enabled construction of mass distributions. With some degree of data manipulation, either method can provide both types of distribution, but this requires a precise understanding of the density of the dust, and any error in estimating dust parameters can significantly skew the results. Combined use of both methods provides accurate and straightforward determination of both types of size distribution. Though these two types of particle size distribution are distinct and cannot directly be compared to one another, similarities in general size trends are consistent within each dust. These same trends are observed in the pseudo-“count distributions” constructed using silica data from the single-particle analysis.

5.5 IMPLICATIONS OF THE OVERALL FINDINGS OF THIS STUDY

This work, using gold mine dusts, has demonstrated that the crystalline silica component of a dust cannot be assumed to have a size distribution equivalent to that of the complete dust, and that other mineral components of a dust are also likely to have unique size distributions. Additionally,

dusts from these three mines are not consistent with regard to the size distribution of the total dust, the overall crystalline silica content, the size distribution of the crystalline silica component, or the mineral composition, despite originating from mines of the same type.

Accurate quantification of the crystalline silica content of samples is a complex undertaking and is subject not only to the particle size distribution of the sample but also to its mineral composition and the analytical method that is used. Currently it is not certain how the discrepancies in this area can best be addressed or corrected. Nevertheless, it is crucial to recognize these impediments, to estimate if they are likely to result in an overestimation or underestimation of crystalline silica within a sample, and to take action accordingly to limit worker exposure to respirable crystalline silica. It is also necessary to expand this field of study so that a comprehensive understanding of the salient characteristics of mine dusts can be reached, and to eventually successfully address analytical discrepancies in the measurement of crystalline silica.

This work raises several additional questions, for which continued efforts will be necessary to arrive at answers:

- 1) **Is the composition of dust from other metal mine-commodity types (i.e. copper, iron) and from non-metal commodity types (i.e. stone, sand, gravel) also variable with respect to crystalline silica and minerals?** Evaluations of the particle size-related crystalline silica composition of granite quarry dust (76) indicated that crystalline silica composition varies according to the size range of particles sampled, which would seem to indicate that this trend is not isolated to gold mine dust and that researchers could reasonably expect other types of dust to exhibit similar trends. Further study is needed to confirm this.
- 1) **Dusts from mines of the same commodity type do not exhibit the same compositional characteristics; what other relationships might predict similarities between different dusts?** A logical place to start would be to compare dusts according

to region of origin, as close geographic areas may have similar geological features which would strongly impact the composition of dusts generated. Further study may indicate that the combination of commodity type and geographical region is a better indicator of dust characteristics, or it may indicate that factors other than commodity or location are more relevant.

Ultimately, further research is required to gain a more comprehensive study of variation in these characteristics among different mine dusts, as well as to understand how to more accurately assess exposures to crystalline silica.

Geochemist Paul Anderson remarked in a 1975 publication (133) that “[F]or accurate results there is no general or routine method [for the quantification of crystalline silica]. Each sample must be evaluated and handled specifically to minimize analytical errors. Each sample is a minor research effort.” This work demonstrates the feasibility of such a research effort for an individual dust and provides a method by which to accomplish it, while also underlining that this need still exists. More recently, Cauda, Miller, and Drake (127) have outlined a method for the in-field analysis of crystalline silica in mine dust samples, such that exposure monitoring can be conducted on-site at the end of a shift, rather than waiting the days or weeks required for laboratory analysis to be completed. Such a method would allow results of exposure monitoring to be communicated almost immediately to site management and the affected workers, so that interventions could be implemented quickly and further exposures prevented. Such a technique would have an enormous impact on efforts to reduce silicosis, but as the authors note, specific knowledge of the mineral matrices of a dust is necessary in order to develop a method that is accurate and reliable in quantifying crystalline silica, even in the presence of confounders.

Detailed characterization of mine dusts, such as has been accomplished by the methods presented in this study, will build a body of knowledge that can improve control of dust and crystalline silica in occupational environments, as well as improve the accuracy of exposure monitoring for crystalline silica. Both of these accomplishments will contribute to decreasing

occupational exposures to crystalline silica. Given the millions of people in the U.S. and globally who are exposed to crystalline silica – and who are thus susceptible to silicosis – the prevention of such exposures would have profound public health implications.

APPENDIX A: SUMMARY OF SAMPLING CONDITIONS AND TIMES

Table 10 Collection times of size-fractionated samples for crystalline silica analysis

| <i>Chamber concentration</i> | Alaska | Nevada | South Africa |
|------------------------------------|------------------------|------------------------|----------------------|
| | 8.5 mg·m ⁻³ | 2.5 mg·m ⁻³ | 3 mg·m ⁻³ |
| <i>Sampling Times (min)</i> | | | |
| <i>Inlet</i> | 360 | 180 | 60 |
| <i>Stage 1</i> | 180 | 90 | 60 |
| <i>Stage 2</i> | 60 | 90 | 30 |
| <i>Stage 3</i> | 60 | 60 | 30 |
| <i>Stage 4</i> | 60 | 60 | 30 |
| <i>Stage 5</i> | 360 | 60 | 30 |
| <i>Stage 6</i> | 660 | 180 | 60 |
| <i>Stage 7</i> | - | - | 60 |
| <i>Stage 8</i> | - | - | 120 |
| <i>Final</i> | 1020 | 240 | 240 |

Table 11 Collection times of size-fractionated samples for SEM-EDS analysis

| <i>Chamber concentration</i> | Alaska | Nevada | South Africa |
|------------------------------------|------------------------|------------------------|------------------------|
| | 0.5 mg·m ⁻³ | 0.5 mg·m ⁻³ | 0.5 mg·m ⁻³ |
| <i>Sampling Times (min)</i> | | | |
| <i>Inlet</i> | 30 | 30 | 30 |
| <i>Stage 1</i> | 30 | 30 | 30 |
| <i>Stage 2</i> | 3 | 5 | 5 |
| <i>Stage 3</i> | 2 | 2 | 2 |
| <i>Stage 4</i> | 2 | 2 | 2 |
| <i>Stage 5</i> | 10 | 2 | 2 |
| <i>Stage 6</i> | 10 | 3 | 5 |
| <i>Stage 7</i> | 10 | 3 | 5 |
| <i>Stage 8</i> | 15 | 3 | 5 |
| <i>Stage 9</i> | 30 | 25 | 5 |
| <i>Stage 10</i> | 30 | 30 | 5 |
| <i>Final</i> | N/A | N/A | N/A |

APPENDIX B: PARTICLE SIZE DISTRIBUTION OF A CRYSTALLINE SILICA REFERENCE
MATERIAL

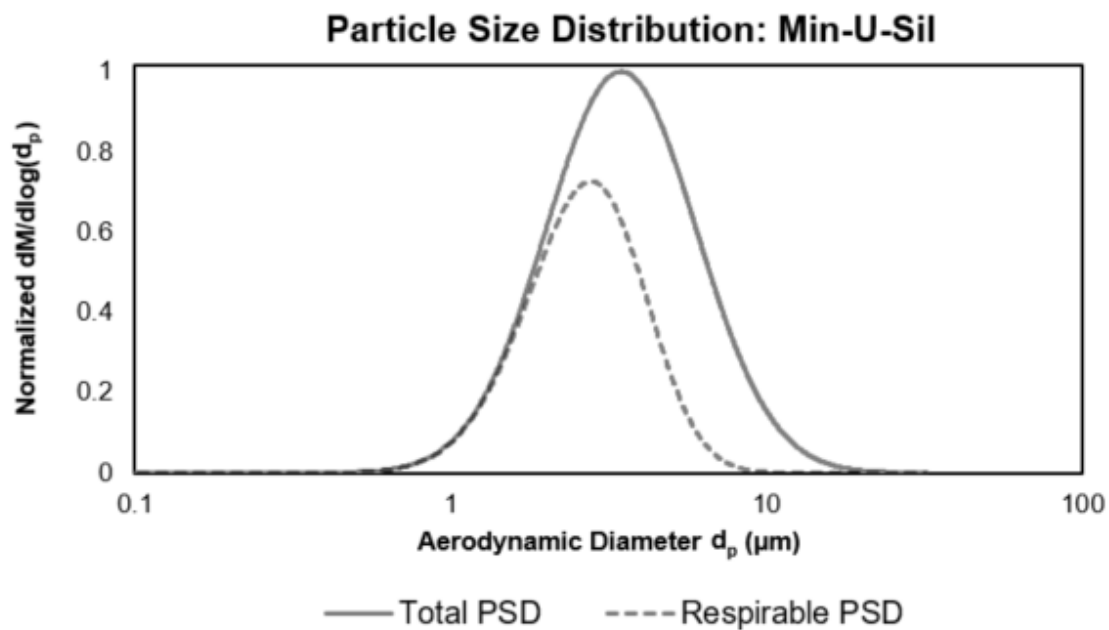


Figure 18 Particle mass size distribution of Min-U-Sil 5

APPENDIX C: EXAMPLES OF RULES FOR PARTICLE CLASSIFICATION BY EDS

Table 12 Particle classification rules for Nevada dust

| Particle Class | Rule |
|----------------|---|
| Si-Al-K | Si>20 and Al≥5 and K≥5 and K>2*Mg and K>2*Fe and K>2*Ca and K>2*Na and K>2*S |
| Si-Al-Ca | Si>20 and Al≥5 and Ca≥5 and Ca>2*Mg and Ca>2*Fe and Ca>2*K and Ca>2*Na and Si≥Ca and Ca>2*S |
| Si-Al-Mg | Si>20 and Al≥5 and Mg≥5 and Mg>2*Ca and Mg>2*Fe and Mg>2*K and Mg>2*Na and Mg>2*S |
| Si-Al-Fe | Si>20 and Al≥5 and Fe≥5 and Fe>2*Mg and Fe>2*K and Fe>2*Ca and Fe>2*Na and Si≥Fe and Fe>Ti and Fe>2*S |
| Si-Al-Na | Si>20 and Al≥5 and Na≥5 and Na>2*Mg and Na>2*Fe and Na>2*K and Na>2*Ca and Na>2*S |
| Al-Si-S | Al>20 and Si>10 and S>10 and Al>1.5*Si |
| Si-Al-S | Si>20 and Al≥5 and S≥5 and S>2*Mg and S>2*Fe and S>2*K and S>2*Ca and S>2*Na |
| Si-Al | Si>20 and Al≥3 and Si+Al+C>90 and K<3 and Ca<3 and Mg<3 and Fe<3 and Na<3 and S<3 |
| Si-Al (mixed) | (Si>20 and Al≥3 and Si>Ca and Si>Fe) or (Si>10 and Al≥3 and Si+Al+C>75) |
| Ca-Si | Ca≥15 and Si≥10 and Si>Mg and Si>S and Si>Al and Si>Mg |
| Ca-Mg | Ca≥10 and Mg≥10 and Mg≥S |
| Ca-S | Ca≥10 and S≥10 and Ca>Al and Ca>Fe |
| Al-S | Al>15 and S>10 and Al>Zn and Al>Fe |
| Fe-S | Fe>10 and S>10 |
| Si-rich | Si≥75 or [Si≥10 and C+Si>90 and Ca<3] |
| Ca-rich | Ca>40 or [Ca>20 and Ca+C>75] |
| Zn-rich | Zn>40 or [Zn>20 and C+Zn>75] |
| Ti-rich | Ti>40 or [Ti>20 and C+Ti>75] |
| Pb-rich | Pb>25 |
| C-rich | C>75 |
| Miscellaneous | true |

BIBLIOGRAPHY

1. Global, regional, and national age-sex specific all-cause and cause-specific mortality for 240 causes of death, 1990-2013: a systematic analysis for the Global Burden of Disease Study 2013. *The Lancet* 2015;385(9963):117-171.
2. Bang KM, Mazurek JM, Attfield MD. Silicosis mortality, prevention, and control - United States, 1968-2002. *Morbidity and Mortality Weekly Report* 2005;54(16):401-405.
3. Bang KM, Mazurek JM, Wood JM, White GE, Hendricks SA, Weston A. Silicosis mortality trends and new exposures to respirable crystalline silica - United States, 2001-2010. *Morbidity and Mortality Weekly Report* 2015;64(5):117-120.
4. Mazurek JM, Schleiff PL, Wood JM, Hendricks SA, Weston A. Notes from the field: Update: Silicosis mortality - United States, 1999-2013. *Morbidity and Mortality Weekly Report* 2015;64(23):653-654.
5. Attfield MD, Bang KM, Petsonk EL, Schleiff PL, Mazurek JM. Trends in pneumoconiosis mortality and morbidity for the United States, 1968–2005, and relationship with indicators of extent of exposure. *Journal of Physics: Conference Series* 2009;151(1):012051.
6. Esswein EJ, Breitenstein M, Snawder J, Kiefer M, Sieber WK. Occupational exposures to respirable crystalline silica during hydraulic fracturing. *Journal of Occupational and Environmental Hygiene* 2013;10(7):347-356.
7. Akgun M, Mirici A, Ucar EY, Kantarci M, Araz O, Gorguner M. Silicosis in Turkish denim sandblasters. *Occupational Medicine* 2006;56(8):554-558.
8. National Institute for Occupational Safety and Health (NIOSH). Work-related lung disease surveillance report. In: Services DoHaH, editor. Cincinnati, OH; 1991.
9. Leung CC, Yu ITS, Chen WH. Silicosis. *Lancet* 2012;379(9830):2008-2018.
10. Erren TC, Glende CB, Morfeld P, Piekarski C. Is exposure to silica associated with lung cancer in the absence of silicosis? A meta-analytical approach to an important public health question. *International Archives of Occupational and Environmental Health* 2008;82(8):997-1004.
11. Pelucchi C, Pira E, Piolatto G, Coggiola M, Carta P, La Vecchia C. Occupational silica exposure and lung cancer risk: a review of epidemiological studies 1996–2005. *Annals of Oncology* 2006;17(7):1039-1050.
12. Soutar CA, Robertson A, Miller BG, Searl A, Bignon J. Epidemiological evidence on the carcinogenicity of silica: factors in scientific judgement. *The Annals of Occupational Hygiene* 2000;44(1):3-14.
13. IARC. IARC monographs on the evaluation of carcinogenic risks to humans: silica, some silicates, coal dust and para-armid fibrils. Vol 68. Lyon, France: World Health Organization, International Agency for Research on Cancer.; 1997.

14. Barboza CEG, Winter DH, Seiscento M, Santos UdP, Filho MT. Tuberculosis and silicosis: epidemiology, diagnosis and chemoprophylaxis. *Jornal Brasileiro de Pneumologia* 2008;34(11):961-968.
15. Hanifa Y, Grant AD, Lewis J, Corbett EL, Fielding K, Churchyard G. Prevalence of latent tuberculosis infection among gold miners in South Africa. *The International Journal of Tuberculosis and Lung Disease* 2009;13(1):39-46.
16. Churchyard GJ, Kleinschmidt I, Corbett EL, Murray J, Smit J, De Cock KM. Factors associated with an increased case-fatality rate in HIV-infected and non-infected South African gold miners with pulmonary tuberculosis. *The International Journal of Tuberculosis and Lung Disease* 2000;4(8):705-712.
17. Park HH, Girdler-Brown BV, Churchyard GJ, White NW, Ehrlich RI. Incidence of tuberculosis and HIV and progression of silicosis and lung function impairment among former basotho gold miners. *American Journal of Industrial Medicine* 2009;52(12):901-908.
18. Rees D, Murray J, Nelson G, Sonnenberg P. Oscillating migration and the epidemics of silicosis, tuberculosis, and HIV infection in South African gold miners. *American Journal of Industrial Medicine* 2010;53(4):398-404.
19. Corbett EL, Churchyard G, Clayton TC, Williams BG, Mulder D, Hayes RJ, et al. HIV infection and silicosis: the impact of two potent risk factors on the incidence of mycobacterial disease in South Africa miners. *AIDS* 2000;14(17):2759-2768.
20. Steenland K. One agent, many diseases: Exposure-response data and comparative risks of different outcomes following silica exposure. *American Journal of Industrial Medicine* 2005;48:16-23.
21. Makol A, Reilly MJ, Rosenman KD. Prevalence of connective tissue disease in silicosis (1985–2006)—a report from the state of michigan surveillance system for silicosis. *American Journal of Industrial Medicine* 2011;54(4):255-262.
22. Gulumian M, Borm PJA, Vallyathan V, Castranova V, Donaldson K, Nelson G, et al. Mechanistically identified suitable biomarkers of exposure, effect, and susceptibility for silicosis and Coal-worker's Pneumoconiosis: A comprehensive review. *Journal of Toxicology and Environmental Health, Part B* 2006;9:357-395.
23. Dalal NS, Jafari B, Petersen M, Green FH, Vallyathan V. Presence of stable coal radicals in autopsied coal miners' lungs and its possible correlation to coal workers' pneumoconiosis. *Archives of environmental health* 1991;46(6):366-372.
24. Mikolajczyk U, Bujak-Pietrek S, Szadkowska-Stanczyk I. Exposure to silica dust in coal-mining: Analysis based on measurements made by industrial hygiene laboratories in Poland, 2001-2005. *Medycyna Pracy* 2010;61(3):287-297.
25. Naghizadeh A, Mahvi AH, Jabbari H, Derakhshani E, Amini H. Exposure assessment to dust and free silica for workers of Sangan iron ore mine in Khaf, Iran. *Bulletin of Environmental Contamination and Toxicology* 2011;87(5):531-538.

26. Verma DK, Rajhans GS, Malik OP, des Tombe K. Respirable dust and respirable silica exposure in Ontario gold mines. *Journal of Occupational and Environmental Hygiene* 2014;11(2):111-116.
27. Park RM, Chen W. Silicosis exposure–response in a cohort of tin miners comparing alternate exposure metrics. *American Journal of Industrial Medicine* 2013;56(3):267-275.
28. Joy GJ. Evaluation of the approach to respirable quartz exposure control in U.S. coal mines. *Journal of Occupational and Environmental Hygiene* 2012;9(2):65-68.
29. Watts WF, Huynh TB, Ramachandran G. Quartz concentration trends in metal and nonmetal mining. *Journal of Occupational and Environmental Hygiene* 2012;9(12):720-732.
30. Cauda E, Joy GJ, Miller AL, Mischler SE. Analysis of the silica percent in airborne respirable mine dust samples from U.S. operations. *Silica and Associated Respirable Mineral Particles* 2013;STP 1565:12-27.
31. Schatzel SJ. Identifying sources of respirable quartz and silica dust in underground coal mines in southern West Virginia, western Virginia, and eastern Kentucky. *International Journal of Coal Geology* 2009;78(2):110-118.
32. Cox J, L.A., Van Orden DR, Lee RJ, Arlauckas SM, Kautz RA, Warzel AL, et al. How reliable are crystalline silica dust concentration measurements? *Regulatory Toxicology and Pharmacology* 2015;73:126-136.
33. Goldstein B, Webster I. Intratracheal injection into rats of size-graded silica particles. *British Journal of Industrial Medicine* 1966;23(1):71-74.
34. Wiessner JH, Mandel NS, Sohnle PG, Mandel GS. Effect of particle size on quartz-induced hemolysis and on lung inflammation and fibrosis. *Experimental Lung Research* 1989;15(6):801-812.
35. Kozin F, Millstein B, Mandel G, Mandel N. Silica-induced membranolytic activity: A study of different structural forms of crystalline and amorphous silica and the effects of protein adsorption. *Journal of Colloid and Interface Science* 1982;88(2):326-337.
36. Vallyathan V, Shi X, Dalal NS, Irr W, Castranova V. Generation of free radicals from freshly fractured silica dust: potential role in acute silica-induced lung injury. *American Review of Respiratory Disease* 1988;138(5):1213-1219.
37. Porter DW, Barger M, Robinson VA, Leonard SS, Landsittel D, Castranova V. Comparison of low doses of aged and freshly fractured silica on pulmonary inflammation and damage in the rat. *Toxicology* 2002;175(1–3):63-71.
38. Mischler SE. A multistage cyclone array for the collection of size-segregated silica aerosols to test the hypothesis that ultrafine crystalline silica particles are more efficient in their activation of macrophages [Ph.D.]. Ann Arbor: University of Pittsburgh; 2013.
39. Ohyama M, Tachi H, Minejima C, Kameda T. Comparing the role of silica particle size with mineral fiber geometry in the release of superoxide from rat alveolar macrophages. *The Journal of Toxicological Sciences* 2014;39(4):551-559.

40. Fubini B. Surface chemistry and quartz hazard. *The Annals of Occupational Hygiene* 1998;42(8):521-530.
41. Castranova V, Vallyathan V, Ramsey DM, McLaurin JL, Pack D, Leonard S, et al. Augmentation of pulmonary reactions to quartz inhalation by trace amounts of iron-containing particles. *Environmental Health Perspectives* 1997;105(Suppl 5):1319-1324.
42. Benbrahim-Tallaa L, Baan RA, Grosse Y, Lauby-Secretan B, El Ghissassi F, Bouvard V, et al. Carcinogenicity of diesel-engine and gasoline-engine exhausts and some nitroarenes. *The Lancet Oncology*;13(7):663-664.
43. Brindley OW, Udagawa S. Sources of error in the X-ray determination of quartz. *Journal of the American Ceramic Society* 1959;42(12):643-644.
44. Dodgson J, Whittaker W. The determination of quartz in respirable dust samples by infrared spectrophotometry - I. The potassium bromide disc method. *Annals of Occupational Hygiene* 1973;16:373-387.
45. Edmonds JW, Henslee WW, Guerra RE. Particle size effects in the determination of respirable .alpha.-quartz by x-ray diffraction. *Analytical Chemistry* 1977;49(14):2196-2203.
46. Gordon RL, Harris GW. Effect of particle-size on the quantitative determination of quartz by X-ray diffraction. *Nature* 1955;175(4469):1135-1135.
47. Hurst V, Schroede P, Styron R. Accurate quantification of quartz and other phases by powder X-ray diffraction. *Analytica Chimica Acta* 1997;337:233-252.
48. Lorberau C. Investigation of the determination of respirable quartz on filter media using Fourier transform infrared spectrophotometry; 1989. Report No.: PB-90-130105/XAB United StatesTue Feb 12 14:18:47 EST 2008NTIS, PC A04/MF A01GRA; GRA-90-01599; EDB-90-049275; ERA-15-022510English.
49. Lorberau CD. Investigation of the determination of respirable quartz on filter media using Fourier Transform Infrared spectrophotometry. *Applied Occupational and Environmental Hygiene* 1990;5(6):348-350.
50. Ojima J. Determining of crystalline silica in respirable dust samples by infrared spectrophotometry in the presence of interferences. *Journal of Occupational Health* 2003;45:94-103.
51. Otvos JW, Stone H, Harp Jr WR. Theory of radiant-energy absorption by randomly dispersed discrete particles. *Spectrochimica Acta* 1957;9(2):148-156.
52. Reut S, Stadnichenko R, Hillis D, Pityn P. Factors affecting the accuracy of airborne quartz determination. *Journal of Occupational and Environmental Hygiene* 2007;4(2):80-86.
53. Salisbury JW, Eastes JW. The effect of particle size and porosity on spectral contrast in the mid-infrared. *Icarus* 1985;64(3):586-588.

54. Toffolo D, Lockington JN. Direct infrared spectrophotometric analysis of free crystalline silica in respirable dust from a steel foundry. *American Industrial Hygiene Association Journal* 1981;42(8):579-585.
55. Tuddenham WM, Lyon RJP. Infrared techniques in the identification and measurement of minerals. *Analytical Chemistry* 1960;32(12):1630-1634.
56. National Institute for Occupational Safety and Health (NIOSH). Silica, crystalline, by XRD (filter redeposition) - Method No. NIOSH 7500. *NIOSH Manual of Analytical Methods*, Fourth Edition 2003.
57. National Institute for Occupational Safety and Health (NIOSH). Quartz in coal mine dust, by IR (filter redeposition) - Method No. NIOSH 7603. *NIOSH Manual of Analytical Methods*, Fourth Edition 2003.
58. Verma D, Sebestyen A, Julian J, Muir D, Schmidt H, Bernholz C, et al. Silica exposure and silicosis among Ontario hardrock miners: II. Exposure estimates. *American Journal of Industrial Medicine* 1989;16:13-18.
59. Tomb T, Haney R. Comparison of number and respirable mass concentration determinations. In: VIIth International Pneumoconioses Conference; 1988; Pittsburgh, PA; 1988. p. 1106-1110.
60. Federal Mine Safety and Health Act (Mine Act) of 1977, as amended by the Mine Improvement and New Emergency Response Act (MINER Act) of 2006. In. United States; 1977.
61. 30 CFR 56.5001. Safety and health standards. Underground metal and nonmetal mines. Exposure limits for airborne contaminants. Code of Federal Regulations. Washington, DC: U.S. Government Printing Office, Office of the Federal Register.
62. 30 CFR 57.5001. Safety and health standards. Underground metal and nonmetal mines. Exposure limits for airborne contaminants. Code of Federal Regulations. Washington, DC: U.S. Government Printing Office, Office of the Federal Register.
63. 30 CFR 70.101. Mandatory health standards - underground coal mines. Respirable dust standard when quartz is present. Code of Federal Regulations. Washington, DC: U.S. Government Printing Office, Office of the Federal Register.
64. 30 CFR 71.101. Mandatory health standards - surface coal mines. Respirable dust standard when quartz is present. Code of Federal Regulations. Washington, DC: U.S. Government Printing Office, Office of the Federal Register.
65. Kumari S, Kumar R, Mishra KK, Pandey JK, Udayabhanu GN, Bandopadhyay AK. Determination of quartz and its abundance in respirable airborne dust in both coal and metal mines in India. *Procedia Engineering* 2011;26:1810-1819.
66. Hunt JM, Wisherd MP, Bonham LC. Infrared absorption spectra of minerals and other inorganic compounds. *Analytical Chemistry* 1950;22(12):1478-1497.

67. Mine Safety Health Administration (MSHA). Infrared determination of quartz in respirable coal mine dust - Method no. MSHA P7. US Dept of Labor-MSHA-Pittsburgh Safety and Health Technology Center 2008.
68. Lorberau CD, Abell MT. Methods used by the United States National Institute for Occupational Safety and Health to monitor crystalline silica. *Scandinavian Journal of Work, Environment & Health* 1995;21(Suppl 2):35-38.
69. Ferg EE, Loyson P, Gromer G. The influence of particle size and composition on the quantification of airborne quartz analysis on filter paper. *Industrial Health* 2008;46(2):144-151.
70. Mine Safety Health Administration (MSHA). X-ray diffraction determination of quartz and cristobalite in respirable mine dust - Method no. MSHA P2. US Dept of Labor-MSHA-Pittsburgh Safety and Health Technology Center 2013.
71. Clark GL, Reynolds DH. Quantitative analysis of mine dusts: An X-ray diffraction method. *Industrial & Engineering Chemistry Analytical Edition* 1936;8(1):36-40.
72. U.S. Geological Survey (USGS). A laboratory manual for X-ray powder diffraction. In.
73. Eller P, Feng H, Song R, Key-Schwartz R, Esche C, Groff J. Proficiency Analytical Testing (PAT) silica variability, 1990-1998. *American Industrial Hygiene Association Journal* 1999;60:533-539.
74. Harper M, Sarkisian K, Andrew M. Assessment of respirable crystalline silica analysis using Proficiency Analytical Testing results from 2003-2013. *Journal of Occupational and Environmental Hygiene* 2014;11:D157-D163.
75. Madsen FA, Rose MC, Cee R. Review of quartz analytical methodologies: Present and future needs. *Applied Occupational and Environmental Hygiene* 1995;10(12):991-1002.
76. Sirianni G, Hosgood HD, Slade MD, Borak J. Particle size distribution and particle size-related crystalline silica content in granite quarry dust. *Journal of Occupational and Environmental Hygiene* 2008;5(5):279-285.
77. Page SJ. Comparison of coal mine dust size distributions and calibration standards for crystalline silica analysis. *AIHA Journal* 2003;64:30-39.
78. Hinds WC. *Aerosol Technology: Properties, Behavior, and Measurement of Airborne Particles*. 2nd ed: John Wiley & Sons, Inc.; 1999.
79. CEN European Committee for Standardization. Size fraction definition for measurement of airborne particles. In. Brussels, Belgium; 1993.
80. Warheit DB, Webb TR, Colvin VL, Reed KL, Sayes CM. Pulmonary bioassay studies with nanoscale and fine-quartz particles in rats: Toxicity is not dependent upon particle size but on surface characteristics. *Toxicological Sciences* 2007;95(1):270-280.
81. Kajiwara T, Ogami A, Yamato H, Oyabu T, Morimoto Y, Tanaka I. Effect of particle size of intratracheally instilled crystalline silica on pulmonary inflammation. *Journal of Occupational Health* 2007;49(2):88-94.

82. Colinet J, National Institute for Occupational S, Health. Office for Mine S, Health R. Best practices for dust control in metal/nonmetal mining. Pittsburgh, Pa.: U.S. Department of Health and Human Services, CDC/NIOSH Office of Mine Safety and Health Research; 2010.
83. Stacey P, Mecchia M, Verpaele S, Pretorius C, Key-Schwartz R, Mattenklott M, et al. Differences between samplers for respirable dust and the analysis of quartz - an international study. In: Harper M, Lee T, editors. ASTM International; 2013; West Conshohocken, PA; 2013.
84. NIOSH Policy Statement: Respiratory protection recommendations for airborne exposures to crystalline silica, DHHS (NIOSH) Publication no. 2008-140. In: Services DoHaH, editor.; 2008.
85. Martin SB, Moyer ES. Electrostatic respirator filter media: Filter efficiency and most penetrating particle size effects. *Applied Occupational and Environmental Hygiene* 2000;15(8):609-617.
86. Vo E, Zhuang Z, Horvatin M, Liu Y, He X, Rengasamy S. Respirator performance against nanoparticles under simulated workplace activities. *Annals of Occupational Hygiene* 2015;59(8):1012-1021.
87. Duyckaerts G. The infra-red analysis of solid substances: A review. *The Analyst* 1959;84:201-214.
88. Nagelschmidt G, Gordon RL, Griffin OG. Surface of finely-ground silica. *Nature* 1952;169(4300):539-540.
89. Dempster PB, Ritchie PD. Surface of finely-ground silica. *Nature* 1952;169(4300):538-539.
90. Page S. Crystalline silica analysis: A comparison of calibration materials and recent coal mine dust size distributions. *J ASTM Int* 2006;3(1):1-14.
91. Huggins CW, Snyder JG, Segreti JM, Johnson SN. Determination of alpha quartz particle distribution in respirable coal mine dust samples and reference standards; 1985.
92. Pickard KJ, Walker RF, West NG. A comparison of X-ray diffraction and infrared spectrophotometric methods for the analysis of alpha-quartz in airborne dusts. *Annals of Occupational Hygiene* 1985;29(2):149-167.
93. Bhaskar R, Li JL, Xu LJ. A comparative study of particle size dependency of IR and XRD methods for quartz analysis. *American Industrial Hygiene Association Journal* 1994;55(7):605-609.
94. Freedman RW, Toma SZ, Lang HW. On-filter analysis of quartz in respirable coal dust by infrared absorption and X-ray diffraction. *American Industrial Hygiene Association Journal* 1974;35(7):411-418.
95. National Institute for Occupational Safety and Health (NIOSH). Determination of airborne crystalline silica. *NIOSH Manual of Analytical Methods*, Fourth Edition 2003:260-280.

96. Dixon K, Fretwell T. The determination of quartz in the airborne dust of coal mines and in coal measure minerals by infra-red spectroscopy. South Nottinghamshire Area: National Coal Board; 1968.
97. DeNee PB. Mine dust characterization using the scanning electron microscope. American Industrial Hygiene Association Journal 1972;33(10):654-660.
98. Sellaro R, Sarver E, Baxter D. A standard characterization methodology for respirable coal mine dust using SEM-EDX. Resources 2015;4(4):939.
99. Sellaro RM. Development of a standard methodology for respirable mine dust characterization using SEM-EDX. Blacksburg, VA: Virginia Polytechnic Institute and State University; 2014.
100. Qi C, Echt A, Gressel MG. On the characterization of the generation rate and size-dependent crystalline silica content of the dust from cutting fiber cement siding. Annals of Occupational Hygiene 2015.
101. Marple VA, Rubow KL. An aerosol chamber for instrument evaluation and calibration. American Industrial Hygiene Association Journal 1983;44(5):361-367.
102. Volkwein JC, Vinson RP, McWilliams LJ, Tuchman DP, Mischler SE. Performance of a new personal respirable dust monitor for mine use. In: US Department of Health and Human Services PHS, Centers for Disease Control and Prevention, National Institute for Occupational Safety and Health, DHHS (NIOSH) Publication No. 2004-151, Report of Investigations 9663, 2004 Jun :1-25., editor.; 2004.
103. Volkwein JC, Vinson RP, Page SJ, McWilliams LJ, Joy GJ, Mischler SE, et al. Laboratory and field performance of a continuously measuring personal respirable dust monitor. In: US Department of Health and Human Services PHS, Centers for Disease Control and Prevention, National Institute for Occupational Safety and Health, DHHS (NIOSH) Publication No. 2006-145, Report of Investigations 9669, 2006 Sept:1-55., editor.; 2006.
104. Kaaden N, Massling A, Schladitz A, Müller T, Kandler K, Schütz L, et al. State of mixing, shape factor, number size distribution, and hygroscopic growth of the Saharan anthropogenic and mineral dust aerosol at Tinfou, Morocco. Tellus B 2009;61(1):51-63.
105. Reid JS, Jonsson HH, Maring HB, Smirnov A, Savoie DL, Cliff SS, et al. Comparison of size and morphological measurements of coarse mode dust particles from Africa. Journal of geophysical research 2003;108(d19).
106. Roberts GC, Artaxo P, Zhou J, Swietlicki E. Sensitivity of CCN spectra on the chemical and physical properties of aerosol: A case study from the Amazon Basin. Journal of Geophysical Research 2002;107(D20).
107. Marple VA, Rubow KL, Behm SM. A microorifice uniform deposit impactor (MOUDI): Description, calibration, and use. Aerosol Science and Technology 1991;14(4):434-446.
108. O'Shaughnessy PT, Raabe OG. A comparison of cascade impactor data reduction methods. Aerosol Science and Technology 2003;37(2):187-200.

109. Farcas D, Lee T, Chisholm WP, Soo J-C, Harper M. Replacement of filters for respirable quartz measurement in coal mine dust by infrared spectroscopy. *Journal of Occupational and Environmental Hygiene* 2016;13(2):D16-D22.
110. Meyer-Jacob C, Vogel H, Boxberg F, Rosén P, Weber ME, Bindler R. Independent measurement of biogenic silica in sediments by FTIR spectroscopy and PLS regression. *Journal of Paleolimnology* 2014;52(3):245-255.
111. Rosén P, Vogel H, Cunningham L, Hahn A, Hausmann S, Pienitz R, et al. Universally applicable model for the quantitative determination of lake sediment composition using fourier transform infrared spectroscopy. *Environmental Science and Technology* 2011;45(20):8858-8865.
112. Weakley AT, Miller AL, Griffiths PR, Bayman SJ. Quantifying silica in filter-deposited mine dusts using infrared spectra and partial least squares regression. *Analytical and Bioanalytical Chemistry* 2014;406(19):4715-4724.
113. Elias Z, Poirot O, Danière MC, Terzetti F, Marande AM, Dzwigaj S, et al. Cytotoxic and transforming effects of silica particles with different surface properties in Syrian hamster embryo (SHE) cells. *Toxicology in Vitro* 2000;14(5):409-422.
114. Carpenter MA, Lifshin E, Gauvin R. SEM-EDS quantitative analysis of aerosols > 80 nm: Impacts on atmospheric aerosol characterizations campaigns. *Microscopy and Microanalysis* 2002;8(Suppl 2).
115. Chou C, Formenti P, Maille M, Ausset P, Helas G, Harrison M, et al. Size distribution, shape, and composition of mineral dust aerosols collected during the African Monsoon Multidisciplinary Analysis Special Observation Period 0: Dust and Biomass-Burning Experiment field campaign in Niger, January 2006. *Journal of Geophysical Research* 2008;113.
116. Fujiwara F, Rebagliati RJ, Dawidowski L, Gómez D, Polla G, Pereyra V, et al. Spatial and chemical patterns of size fractionated road dust collected in a megacity. *Atmospheric Environment* 2011;45:1497-1505.
117. McMurry PH. A review of atmospheric aerosol measurements. *Atmospheric Environment* 2000;34(12-14):1959-1999.
118. Anderson JR, Aggett FJ, Buseck PR, Germani MS, Shattuck TW. Chemistry of individual aerosol particles from Chandler, Arizona, an arid urban environment. *Environmental Science & Technology* 1988;22(7):811-818.
119. Casuccio GS, Janocko PB, Lee RJ, Kelly JF, Dattner SL, Mgebroff JS. The use of computer controlled scanning electron microscopy in environmental studies. *Journal of the Air Pollution Control Association* 1983;33(10):937-943.
120. Schwoeble AJ, Dalley AM, Henderson BC, Casuccio GS. Computer-controlled SEM and micro-imaging of fine particles. *Metals* 1988;40:11.
121. Rietveld H. A profile refinement method for nuclear and magnetic structures. *Journal of Applied Crystallography* 1969;2(65-71).

122. Laskin A, Cowin JP. Automated single-particle SEM/EDX analysis of submicrometer particles down to 0.1 μm . *Analytical Chemistry* 2001;73(5):1023-1029.
123. Kittelson DB. Engines and nanoparticles: a review. *Journal of Aerosol Science* 1998;29(5–6):575-588.
124. Shi JP, Mark D, Harrison RM. Characterization of particles from a current technology heavy-duty diesel engine. *Environmental Science & Technology* 2000;34(5):748-755.
125. Vedula G. An investigation of diesel PM particle morphology using TEM and SEM [M.S.]. Ann Arbor: West Virginia University; 2011.
126. Wang Y, Liang X, Shu G, Wang X, Sun X, Liu C. Effect of lubricant oil additive on size distribution, morphology, and nanostructure of diesel particulate matter. *Applied Energy* 2014;130:33-40.
127. Cauda E, Miller A, Drake P. Promoting early exposure monitoring for respirable crystalline silica: Taking the laboratory to the mine site. *Journal of Occupational and Environmental Hygiene* 2016;13(3):D39-D45.
128. Shepherd S, Woskie SR, Holcroft C, Ellenbecker M. Reducing silica and dust exposures in construction during use of powered concrete-cutting hand tools: efficacy of local exhaust ventilation on hammer drills. *Journal of Occupational and Environmental Hygiene* 2008;6(1):42-51.
129. Hicks J, Yager J. Airborne crystalline silica concentrations at coal-fired power plants associated with coal fly ash. *Journal of Occupational and Environmental Hygiene* 2006;3(8):448-455.
130. Singh M, Misra C, Sioutas C. Field evaluation of a personal cascade impactor sampler (PCIS). *Atmospheric Environment* 2003;37(34):4781-4793.
131. Demokritou P, Gupta T, Ferguson S, Koutrakis P. Development and laboratory performance evaluation of a personal cascade impactor. *Journal of the Air & Waste Management Association* 2002;52(10):1230-1237.
132. Rubow KL, Marple VA, Olin J, McCawley MA. A personal cascade impactor: Design, evaluation and calibration. *American Industrial Hygiene Association Journal* 1987;48(6):532-538.
133. Anderson PL. Free silica analysis of environmental samples - a critical literature review. *American Industrial Hygiene Association Journal* 1975;36(10):767-778.